Investigating Weather Forecasts for Hydropower Maximization in Small and
Medium Storage Dams

Shahryar Khalique Ahmad

A thesis

submitted in partial fulfillment of the

requirements for the degree of

Master of Science in Civil Engineering

University of Washington

2017

Committee:

Faisal Hossain

Bart Nijssen

Program Authorized to Offer Degree:

Civil and Environmental Engineering

University of Washington

Abstract

Investigating Weather Forecasts for Hydropower Maximization in Small and Medium Storage
Dams

Shahryar Khalique Ahmad

Chair of the Supervisory Committee:
Professor Faisal Hossain
Civil and Environmental Engineering

The study explores the optimization of reservoir operations based on weather forecasts to

maximize hydropower production, without compromising other competing objectives. Two dam

sites with small to medium storage receiving unregulated inflow were selected. Short-term weather

forecasts from the Global Forecast System (GFS) and dynamically downscaled by the Weather

Research Forecasting (WRF) Model were used to forecast reservoir inflow. The resulting forecast

inflow information was used to optimize reservoir operations aimed at maximizing hydropower

with flood control, environmental flow and dam safety as key constraints. Three strategies of

optimization were tested to study the effect of lead time and forecasting skill on derived benefits.

Results suggest that significant hydropower benefits can be obtained by forecasting the inflow

peak early and maintaining the reservoir levels accordingly. Despite reduced forecasting skill at

longer lead times, hydropower maximization is found to be greater when the dam operator optimizes storage and releases earlier based on forecasted inflow. The reservoir state at the end of a flood event is found to be closer to the historical rule-curve of the dams, thereby leaving sufficient pool to handle future and unexpected flood events. The study clearly highlights the added value of weather forecasts for hydropower maximization when compared with conventional operations using the rigid rule curves for medium and small storage dams that represent 98% of US dams. Because of the significant amount of additional hydropower that is generated, the use of weather forecasts is a clear source of additional economic benefits for society that should be scaled up across the nation to further reduce dependence on fossil-fuel based energy production in the long run.

TABLE OF CONTENTS

LIST OF FIGURES

LIST OF TABLES

ACKNOWLEDGEMENTS

DEDICATION

This thesis is dedicated to my parents, Dr. Shakeel Ahmad and Mrs. Shameema Khatoon, and my sister, Dr. Shazia Durdana.

Chapter 1. INTRODUCTION

1.1 MOTIVATION

The hydropower infrastructure, over the last several decades, has proven to be a stable and low-cost source of energy around the world [Hamlet et al., 2002]. Being able to turn-on and –off quickly, it serves as an instant source of power generation and a backup for power outages. Unlike the non-hydropower energy sector that has experienced periods of fluctuations and fundamental shifts in the past, hydropower has effectively supported the development of the power grid and industrial growth [DOE Report, 2016]. The significant operational flexibility, low operating and maintenance costs, and the capability of integration with intermittent renewables like solar and wind make hydropower a robust power generation source.

Recently, a clever initiative was undertaken by a German firm, called the "wind-hydro combination" by developing the first wind farm with an integrated hydropower plant [Grumet, 2016]. As storing excess energy in wind farms has not yet been practical, excess energy harvested (during periods of favorable weather conditions) directly goes to the grid leading sometimes to negative energy prices, as observed on May 8, 2016 in Germany where commercial consumers were being paid to consume the excess electricity produced [Coren, 2016]. This "wind-hydro combination", also termed as four-turbine project (due to the proposed four wind turbine sites), is aimed to create an affordable way to store excess energy in a natural reservoir, integrating the source of energy (wind, water) and storage (water) into one system. The proposed plan is to store energy from the spinning blades by pumping water about 100 feet up inside the turbine structure itself. Basins around each base will store another 9 million gallons. When the wind stops, water flows downhill to generate hydroelectric power and a man-made lake in the valley below collects

1

water until turbines pump the water back up again. Figure 1.1 shows an illustration of the concept from the German firm Max Boegl Wind AG.
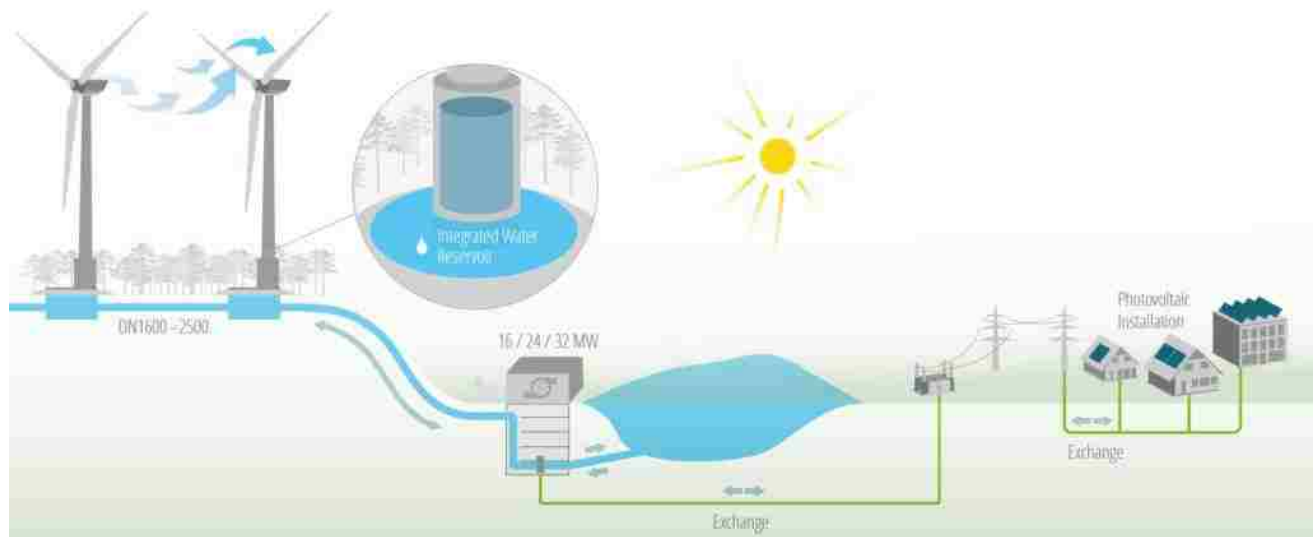
Figure 1.1. Illustration of the wind-hydro combination. The turbines will stand 584 feet high when the blade is pointing straight up with the bottom serving as a water reservoir.

(Source: Coren, 2016)

Although, hydropower is not considered fully renewable because of the drastic impact of dams on fisheries and natural river flows [Lessard et al., 2003], the overwhelming societal benefits of hydropower cannot be overlooked. As reported by World Energy Council (WEC) in its 2016 report [WEC, 2016], the contribution of hydropower to the world's electricity generation from all sources reached 16.4% with an installed capacity of 1,064 GW (excluding pumped storage capacities) in 2016. The recent years have witnessed a major surge in the global installation of hydropower capacity. Statistics show an average growth rate of nearly 4% per year with a total capacity rise of 39% during 2005-2015 [WEC, 2016]. Its drivers include the increased demand for

2

electricity, easy energy storage, flexibility of generation, freshwater management, and climate change mitigation solutions. However, most of the newer installed capacity is concentrated in the developing world that includes the markets of Asia (particularly China), Latin America and Africa, offering an opportunity to supply electricity to under-served populations and a growing industrial base, while at the same time providing a range of complementary benefits associated with multi-purpose projects [WEC, 2016]. As per the report, China has been at the forefront for hydropower capacity, accounting for 26% of global installed capacity in 2015, far ahead of USA (8.4%), Brazil (7.6%) and Canada (6.5%). China has strengthened its hydropower reserve by adding 19 GW in 2015, almost three times the new capacity of the next five countries combined. The statistics for installed and total hydropower capacity for top 6 countries are summarized in Table 1.1. Further, Figure 1.2 plots the newly installed hydropower capacity in 2015 for the respective countries.

Table 1.1. Statistics for countries with top hydropower capacity as of 2015

Country	Total Capacity at the end of 2015 (GW)	% of global installed capacity	Production (TWh)
China	319	26%	1,126
USA	102	8.4%	250
Brazil	92	7.6%	382
Canada	79	6.5%	376
India	52	4.3%	120

[Data from WEC, 2016]
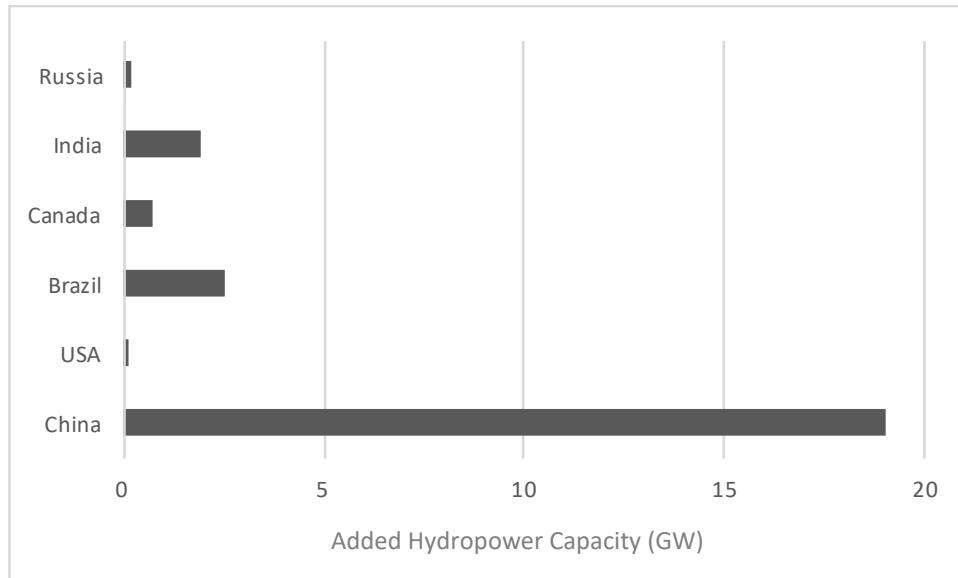
Figure 1.2. Installed hydropower capacity (GW) in 2015

As can be observed from Figure 1.2 there is hardly any new installation in the year 2015 in the US and the trend has been the same over the past decade. In more mature hydropower markets such as that of Western Europe and the U.S., the most economical sites have already been explored and any further expansion is usually hindered by environmental concerns [Labadie, 2004]. This can also be observed from the global scenario of hydropower dam construction, where the under-construction and planned dams in the developed nations are almost non-existent, while the number is much higher in the developing part of the world [Zarfl et al., 2014]. This is illustrated in Figure 1.3 which plots the dams with a capacity of >1000 MW that are planned and under construction.

Figure 1.3. Distribution of under construction and planned dams (>1000 MW) over the world

(From Zarfl et al., 2014)

Furthermore, the hydroelectricity consumption has seen a significant increase in the past decade especially in the regions where the dam construction is on the rise, while the trend is towards saturation in the nations otherwise. Figure 1.4 plots the yearly consumption (TWh) at the continental scale over the world from which the trend is quite apparent.
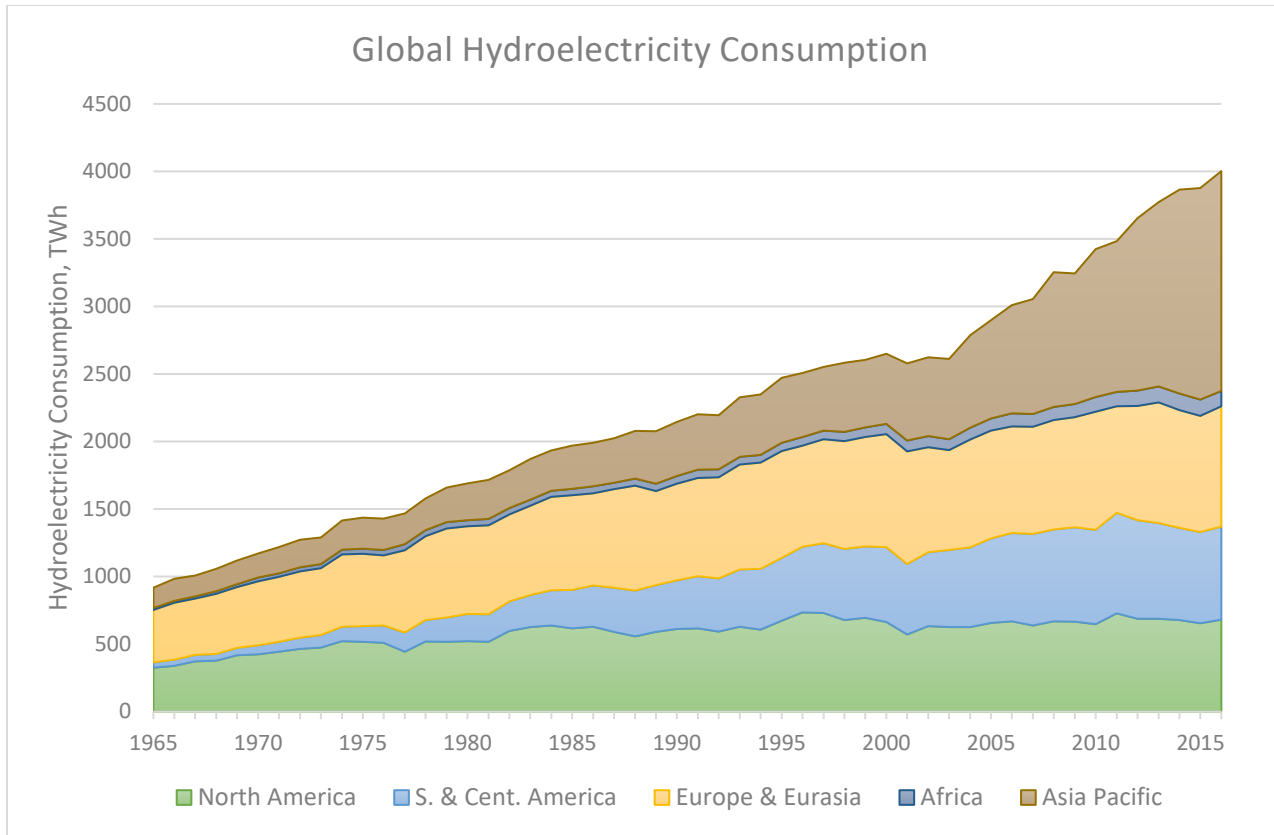
Figure 1.4. Yearly consumption of hydroelectricity (TWh) from 1965-2016

(Data: BP Statistical Review of World Energy, 2017)

1.2   HYDROPOWER SCENARIO IN THE U.S.

The installation of hydropower in the U.S. started in the late 19th century, after which it actively grew with large projects built mostly between 1930 and 1970, according to the US Department of Energy Report of 2016. Various small to medium-sized projects were also completed in the 1980s. However, these did not represent large capacity increases similar to previous decades. Cumulatively, over the past 65 years (1950-2015), hydropower has contributed 10% to the total U.S. electricity generation, and 85% to the total U.S. renewable power generation over the same period. This has efficiently supported the power grid development and its industrial growth. By the end of 2015, the U.S. hydropower generation fleet included 2,198 active power plants with a

total capacity of 79.6 GW and 42 Pumped Storage Hydropower (PSH) plants totaling 21.6 GW, for a total installed hydropower capacity of 101 GW [DOE Report, 2016]. Among the U.S. states, only a handful, those bestowed with abundant water resources and climatological conditions, have been able to harness hydropower for producing a significant share of electricity. The states of Washington, California, and Oregon possess the most installed capacity (around 40 GW in 565 power plants), and within these, the Columbia River basin plants in the Pacific Northwest produce more than 40% of total U.S. hydropower generation [DOE Report, 2016]. Interestingly, Mississippi and Delaware are the two states that have not used hydropower for electricity yet, although hydropower project construction is expected to kick off between 2017 and 2018 in Mississippi. The distribution of existing hydropower generation capacity in the United States as of 2016 is shown in Figure 1.5.
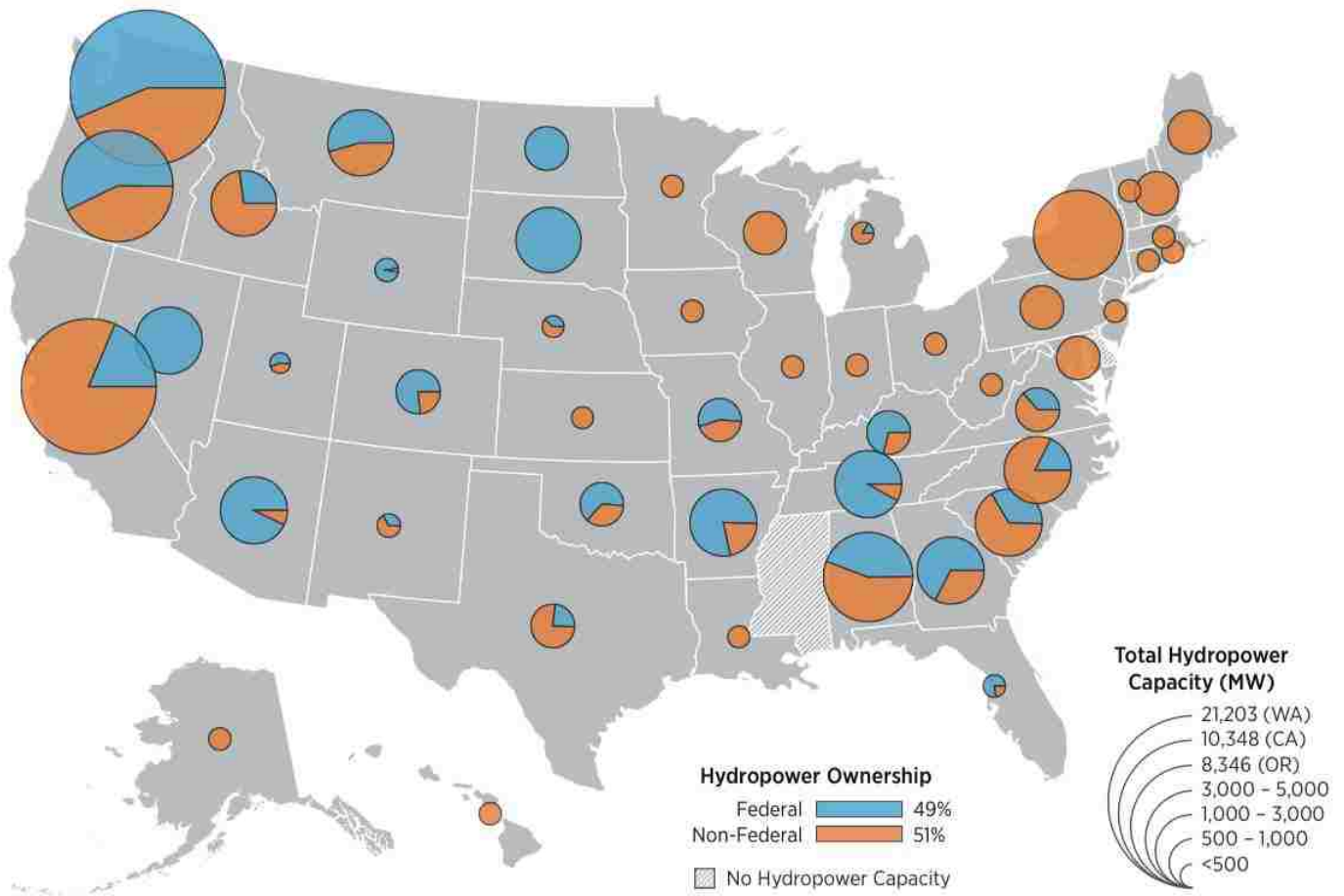
Figure 1.5. Existing hydropower generation capacity in the United States as of 2016 (79.6 GW)

(Source: DOE Report, 2016)

According to DOE, the amount of nation's net total electricity generation contributed by hydropower has decreased, from 30% in 1950 to 7% in 2013, as nuclear power, coal, natural gas, and other sources were added to the nation's energy portfolio to meet rising demands. In the last decade, no large-scale (> 500 MW) hydropower dam project has been constructed in the United States. Factors such as lower economic growth, concerns related to environmental impacts, stagnant energy market, uncertainties owing to climate change and recent breakthroughs in the shale gas and oil industries [Miao et al., 2016] have contributed to the stagnation in the U.S. Figure

1.6 illustrates this stagnation observed with the decrease in annual hydropower capacity additions [DOE Report, 2016].
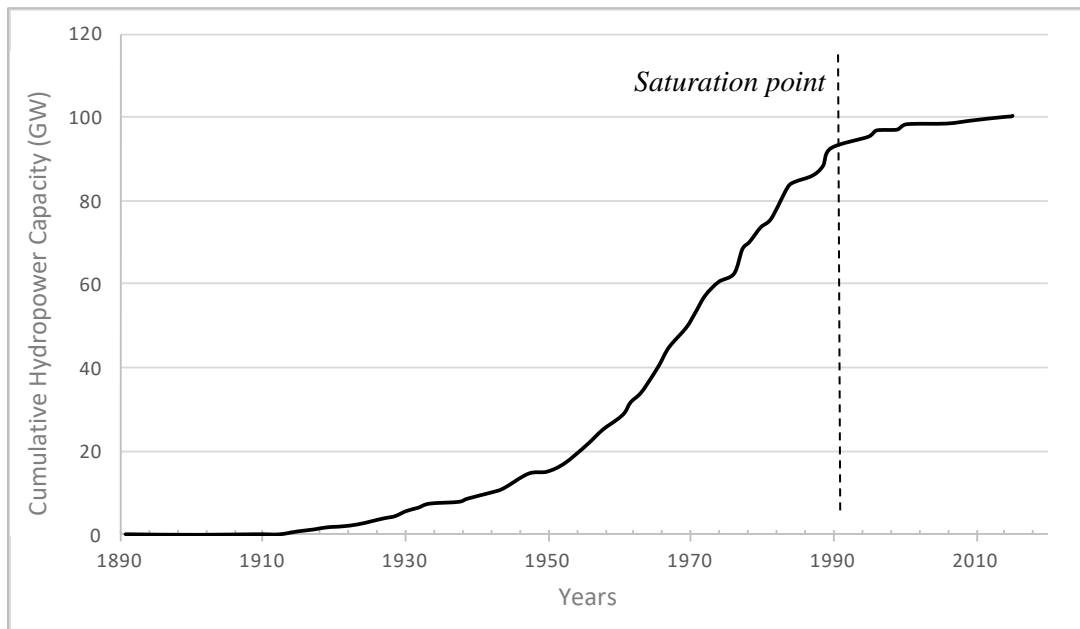
Figure 1.6. Cumulative installed hydropower capacity from 1890-2015 over the United States (Reproduced from DOE Report, 2016)

As most economical hydropower sites have already been explored over the previous century, no significant rise in the trend of hydropower capacity can be expected [Labadie, 2004]. The changing climate [Voisin et al., 2017] and the drastic impacts of the dams over aquatic ecosystems will likely limit new hydropower projects in the US. Thus, building new dams to harvest power is unrealistic considering the present constraints in the US. This calls for the energy community in the developed world such as the United States to explore the maximization of operational effectiveness of existing hydropower infrastructure and make use of the state-of-the-art advancements in the fields of atmospheric sciences, optimization and numerical modeling. Such an exploration can potentially improve energy security of a region, maximize benefits and

9

avoid financial losses of current hydropower infrastructure that are here to stay in the foreseeable future.

1.3 CURRENT STATE OF RESERVOIR OPERATIONS

The operation for almost all dams in US is guided by water control manuals which were developed when the dams and reservoirs were constructed. The three major federal agencies - U.S. Army Corps of Engineers, Bureau of Reclamation, and the Tennessee Valley Authority operate about 10% of the total number of hydropower facilities in the US, representing 49% of the installed capacity [DOE Report, 2016]. Each federally operated reservoir has congressionally mandated purposes, and the rationale is to use the control manuals to balance those purposes. The manuals provide details on the reservoir's history, authorizations, watershed characteristics, data collection networks, forecasting methods, and stakeholder coordination [US Army Corps of Engineers]. The most critical of them is the reservoir operating policy, outlining the operational plan designed to benefit each of the downstream stakeholder needs involving water supply, recreation, hydropower, environment and flood control in the most reliable and effective manner. Reservoir operating policies are often defined in terms of 'Rule Curves,' also termed as 'Standard Operating Procedures.' They specify the storage targets that the reservoir needs to meet at specific time intervals of the year. The dam operator has to release the water as necessary and as close to the recommended levels in the manual to achieve the respective targets for each stakeholder need [Loucks et al., 2005]. However, the actual releases vary depending on the storage and dynamic inflows that actually occur. An example rule curve is shown in Figure 1.7 for the Detroit dam in Oregon, specifying the monthly elevations that the reservoir operator is supposed to follow.

10
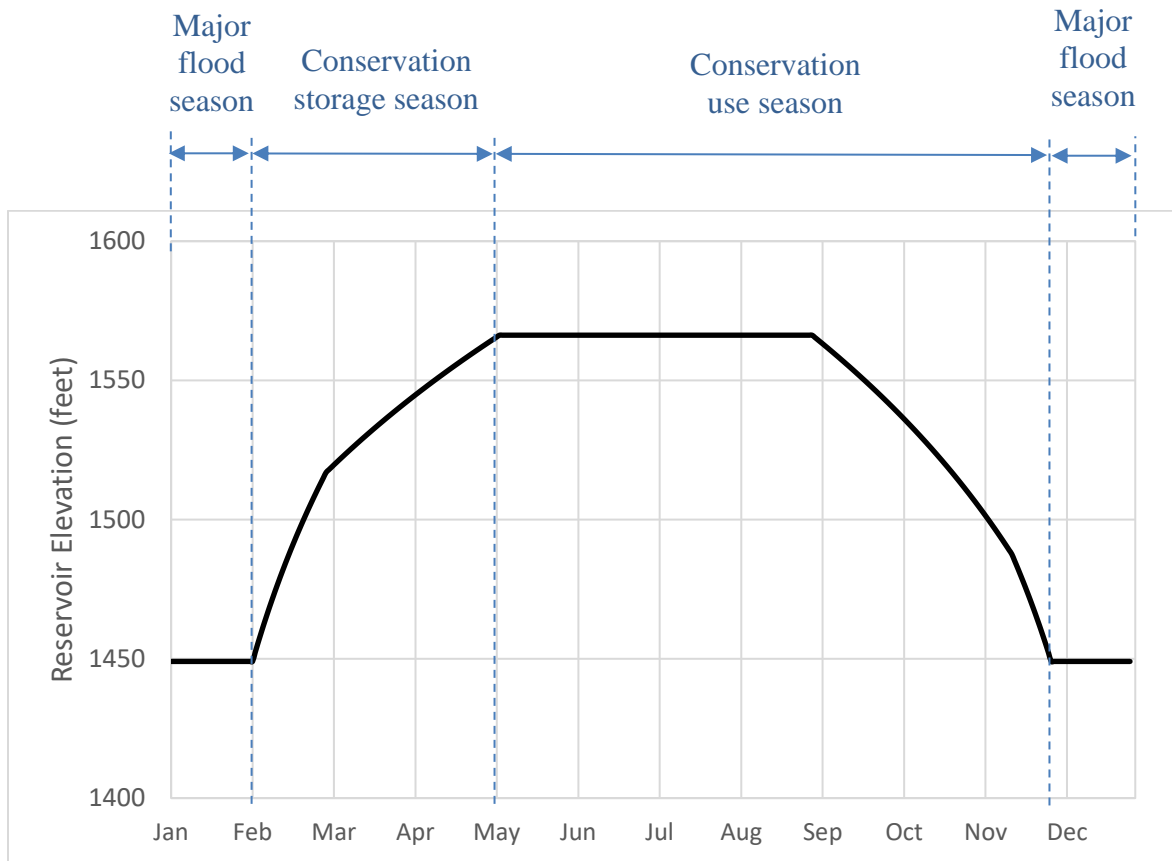
Figure 1.7. Operating Rule Curve for Detroit Dam, Oregon, specifying the monthly reservoir elevations (w.r.t mean sea level) to be maintained as closely as possible by the dam operator

Although the rule curves, specified in the control manuals, were developed using the best information available at the time of dam construction, they have not been adjusted/modified to reflect the changing climatological conditions over the course of the last several decades [Lee et al., 2009; "FIRO Overview", 2016]. Consequently, the manuals cannot account for the change in inflow patterns that has resulted over the long span of time with change in climate and land cover conditions [Hossain et al., 2012; Woldemichael et al., 2012]. Furthermore, releases in the standard operating procedures were specified independently of future inflow forecasts. Rather, they are typically based only on existing storage volumes and within-year periods using a climatology of

historical flow observations [Jordan et al., 2012]. This makes the rule curves prone to misrepresentation of an impending situation at the weather scale and can lead to sacrificing the benefits to downstream stakeholders. For instance, in a weaker-than-average flood-prone month during the flood season, lowering the pool to rule-curve recommended level will result in significant loss in hydropower generation, which otherwise could have been avoided if the inflow forecasts were made ahead of time [Miao et al., 2016]. This is just one of the many scenarios where the static and traditional rule curves could be made more adaptive for real-time operations to harvest more hydropower.

As the scientific community began tapping the potential of satellites in the previous decade, the vast information associated with the most remote locations of land and oceans started getting unveiled [Knudby et al., 2016]. Further, with advancements in the field of atmospheric sciences and numerical modeling over the last few decades, weather forecasting skill has improved considerably with a reasonable accuracy [Block, 2011]. The advanced numerical weather forecasting models have made it possible to forecast the future and obtain inflow information into the reservoir that was unavailable when the manuals were developed during dam construction. This information has the potential to tweak the static reservoir operating policies and adjust it according to the real-time and near-future scenario [Block, 2011]. As concluded by Bauer et al. [2015], the skill in forecasts from numerical weather prediction model at a lead time of 10-days has improved by around 40% since 1995, which can be sufficient in many cases to forecast, for instance, a peak flood event and adjust the dam operations accordingly. Not only can the weather forecasts provide an emergency flood warning, but incorporating that forecast information to adjust reservoir operations can often result in two-fold benefit of maximizing hydropower production without sacrificing downstream flood safety. This study presents a timely exploration

12

for the hydropower infrastructure community to leverage numerical weather forecasting tools at short-term and make the reservoir operations more dynamic in order to generate additional hydropower without compromising flood safety.

1.4 RESEARCH QUESTIONS

The focus of this study is on the small and medium storage dams that typically receive unregulated flow. The goal is to explore the optimization of reservoir operations to maximize the hydropower production, especially during short-term peak events, without compromising other competing objectives of flood security, water supply and environmental flow constraints. Specifically, this study tries to answer the following question: *Can the short-term reservoir inflow forecast from numerical weather prediction improve the existing hydropower generation scenario for small and medium storage dams, without compromising other competing objectives?*

The broader impacts of this study are threefold: 1) contribution towards the integration of operational short-term weather forecasts and management activities by federal and state agencies (in the US and in the developing world) to increase efficiency of existing water resource and hydropower infrastructure, 2) re-evaluation of the potential decision policies (i.e., rule curves) pertaining to the real-time operations for maximized hydropower production and enhanced flood protection, and 3) pilot demonstration for more global scale replication over other reservoirs in the U.S. and developing nations. An overview of the methodology is shown in the schematic below in Figure 1.8, where the red arrows signify the fluxes in and out of the reservoir system, with one of the end objectives being hydropower electricity generation.
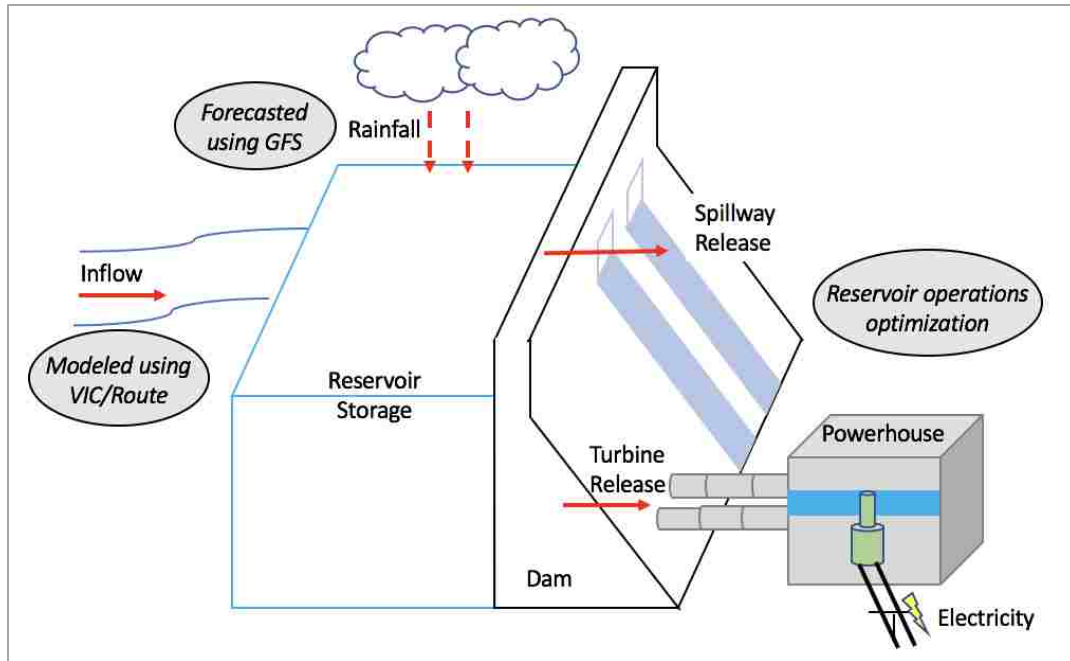
(a)
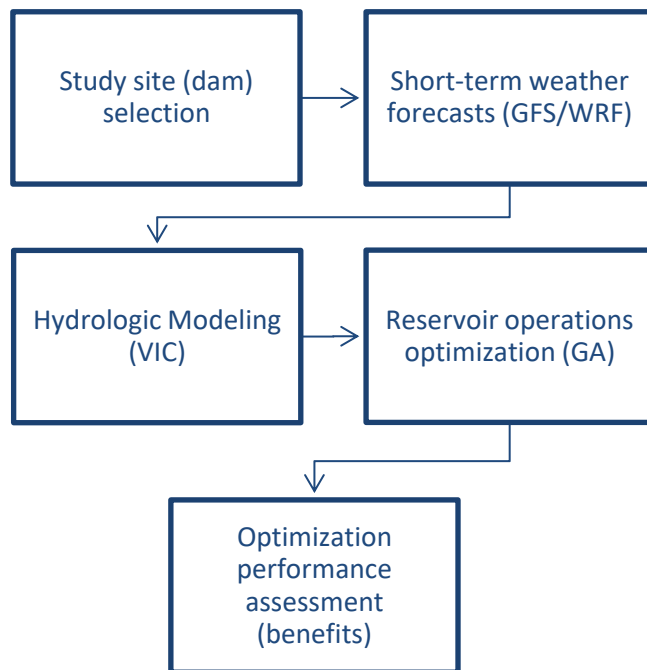
GFS - Global Forecasting System for
          weather forecasts from NOAA
WRF - Weather Research Forecasting
          Model for dynamic downscaling
VIC   - Hydrologic model for predicting
          inflows
GA   - Genetic Algorithm used for the
          optimization

(b)

Figure 1.8. (a) Illustration of the major steps of modeling the meteorological parameters/

reservoir operations (b) Overview of the major components used in the hydropower study.

14

The study starts with the selection of two dam sites that satisfy the criteria of being small/medium storage dam receiving unregulated inflow. Next, the short-term forecast forcing data are obtained from the Global Forecast System (GFS) data, dynamically downscaled by Weather Research Forecasting (WRF) Model. These forecast forcings are used along with the hindcast data to run the hydrological model, resulting into forecasted streamflow into the reservoir. This forecast inflow information is subsequently used to optimize the operations maximizing the hydropower generated, considering pertinent constraints associated with flood control and dam safety. These steps are illustrated in Figure 1.9. Hereafter, we shall use 'dams' and 'reservoirs' interchangeably for the dam-reservoir management system.
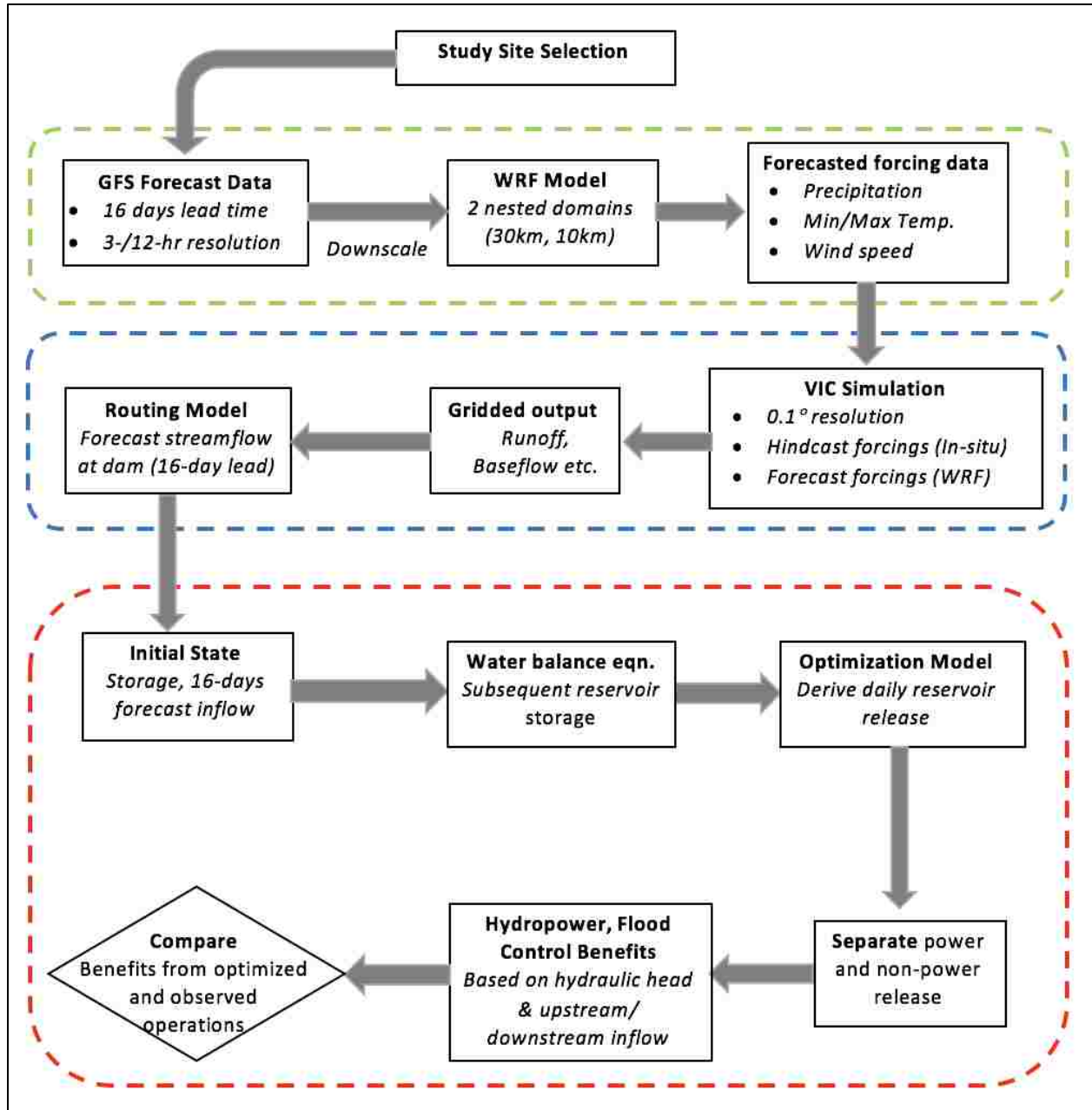
Figure 1.9. Detailed illustration of the involved methodology. Green box – forecasting; Blue box – hydrologic modeling; Red box – reservoir operations modeling and optimization component.

1.5 THESIS OUTLINE

The thesis has been organized as follows. Chapter 2 gives an overview of the relevant work done in the past or is in progress on reservoir operations optimization and hydropower maximization.

Chapter 3 describes the methodology that was implemented to approach the problem. Essentially, it elaborates on the site selection criteria, details of weather forecasting model and its downscaling and steps of hydrological modeling along with its calibration and validation procedures applied on the selected dam sites. The chapter ends with the section on reservoir operations modeling which provides details on the optimization model, the strategy of optimization, optimization technique used and different components involved therein. In Chapter 4, a case study is presented applying the steps described in Chapter 3 over the selected dam sites to demonstrate the effectiveness of the present study and its real-world application. The chapter applies the optimization strategies which the dam operator will use for operational purposes. The performance of the optimization model has also been assessed considering the competing objectives of downstream stakeholder benefits. A discussion on the obtained results and findings is presented in Chapter 5 along with concluding remarks and recommendations on further study.

Chapter 2. BACKGROUND

The current lack of the use of weather forecasts for reservoir operations, especially for water resources management can be pinned on the risk averse nature of water managers, difficulty in integrating operational forecasts into existing water management decision processes, and lack of focus on specific stakeholder benefits [Block 2011; Hamlet et al., 2002; Broad et al., 2007]. As reported in Block [2011], the abundant literature produced over the previous years should motivate more and more case studies to evaluate and outline the potential benefits and reliability through inclusion of forecast information.

In order to embody the uncertainty that is brought in by the forecast model, several studies have used an ensemble of forecasts [Demargne et al., 2010] resulting in various possible realizations of the streamflow. For instance, Zhao et al. [2011] synthetically generates ensemble streamflow forecast to study its effect on real-time reservoir operations. Xu et al. [2016] used multistage stochastic programming to represent the uncertain long-term streamflow forecasts by limited number of discretized scenarios to form a scenario-tree. Seguin et al. [2017] investigates the complexity required in such scenario trees to obtain a good operational solution to the stochastic short-term hydropower problem. Another study by Fan et al. [2016] explores the deterministic and probabilistic forecasts, in combination with the stochastic optimization to force short-term optimization model over a Brazilian reservoir. Considering studies on reservoir systems within US, Stedinger et al. [2014] focuses on stochastic short-term scheduling models for 10-project subsystem of the federal reservoirs on the Columbia and Snake River systems, while Yao et al. [2001] used ensemble forecasts for daily and hourly optimization at Folsom Lake. Other studies incorporating ensemble forecasts for short term optimization include Wang et al. [2012], Ficchi et al. [2015], Fan et al. [2016], and Schwanenberg et al. [2015].

The optimization objective is the key towards optimizing the operations, and most of the studies have focused on single user benefits. These include optimizations for downstream aquatic resources [Sale et al., 1982], flood control and security [Lee et al., 2009; Hsu et al., 2007; Windsor, 1973], hydropower production [Barros et al., 2003; Yasar, 2016; Jothiprakash et al., 2014], water supply [Ji, 2016; Neelakantan, 1999], irrigation and crop planning [Georgiou et al., 2008; Sadati et al., 2014] and environmental concerns [Mao et al., 2016]. However, due to the wide-ranging diversity of property rights and stakeholders, optimizing for a single stakeholder is practically unfeasible. This calls for an objective function balancing the major competing benefits of the downstream users for harnessing the maximum and equitable benefit out of the existing infrastructure.

Some of the multi-objective optimization studies include Ding et al. (2015), Jordan et al. (2012), and Ahmadi et al. (2013), but the considered dams have significantly large catchment areas. There are a few ongoing projects that have addressed this issue of optimizing the reservoir operations for more than one objective in specific river basins. The Integrated Forecast and Reservoir Management (INFORM) project (currently in its second phase) attempts to demonstrate integrated operational methodologies of climate and hydrologic forecasting and reservoir management in Northern California for several downstream user benefits, for individual reservoirs as well as for the river system [Georgakakos et al., 2015]. Its foci include the Folsom, Oroville, Shasta, and Trinity reservoirs and their associated water resources. The hydrologic model of INFORM II closely follows the operational hydrologic forecast models used by the California Nevada River Forecast Center (CNRFC). It includes snow and soil water models adapted from the National Weather Service River Forecast System (NWSRFS), where the hydrologic segments within INFORM are based on CNRFC-defined watershed areas for operational forecasting. Inputs

19

to the hydrologic model components are basin mean areal precipitation (MAP) and mean areal temperature (MAT). The MAP and MAT estimates are derived from the INFORM forecast system downscaling of large-scale atmospheric forecasts from the Global Forecast System (GFS, 0-16 days with 6 hourly resolution) and the Climate Forecast System (CFS, 0-41 days with 6-hourly resolution and from 1 to 9 months with daily resolution). INFORM forecast system produces an ensemble of MAP and MAT forecasts over the forecast horizon, and, through the hydrologic and routing models, an ensemble of reservoir inflow forecasts. This ensemble of reservoir inflow forecasts then provides the input to the INFORM decision support system (DSS) component [HRC-GWRI, 2013].

Another project called Forecast Informed Reservoir Operations (FIRO) uses long-term forecasts to tweak the rule curves, optimizing operations of the Lake Mendocino reservoir in Mendocino County, California for improving water supply with enhanced flood risk reduction ["FIRO Overview", 2016]. This project is in the assessment phase at the time of this writing. The major objectives are the identification, assessment and enhancement of the best science available to improve operations to maximize flood control, water supply and ecosystem benefits. The evaluation will identify realistic, short-term steps to provide more accurate and timely information about weather and watershed conditions. A study with similar objectives in Africa is currently exploring seasonal (30-180 day) climate forecasts and remote sensing data to achieve optimum operation planning for improving the hydropower production [Gebremichael et al., 2016]. The anticipated results from this study are schematically shown in Figure 2.1.

20
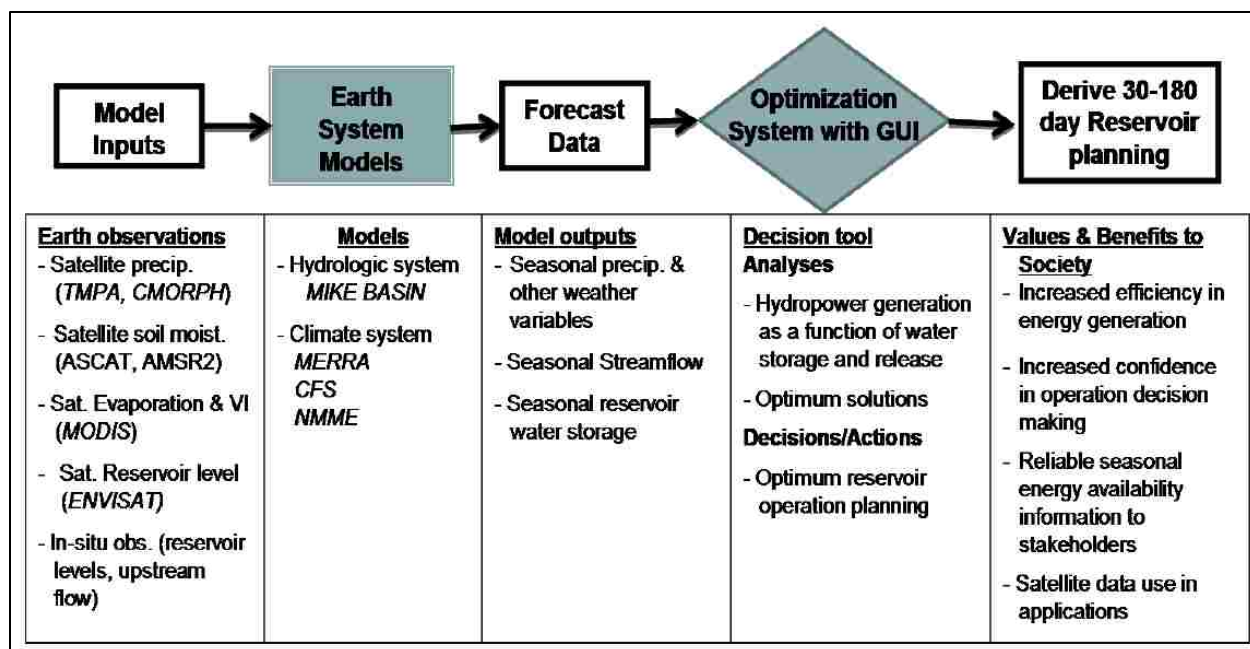
Figure 2.1. Schematic showing Integrated System Solution diagram for the proposed hydropower reservoir operation in Africa (Source: Gebremichael et al., 2016)

Further, the efforts to incorporate seasonal forecasts for optimizing reservoir operations at seasonal/monthly scale are only suitable for large and multi-reservoir systems that possess a large storage buffer. The response time of such systems is quite long and storage does not change significantly at shorter time periods and over short-term extreme events. While the dams with huge storage contribute a major portion to the hydropower production, small and medium-storage dams with modest power generation capacity constitute major chunk of US dams and will continue to be developed in the foreseeable future in the developing world. Such dams often receive unregulated flow due to their location in the upstream and lower order river locations of a river system. For such dams, the response to a peak flood or extreme drought event is appreciably quicker due to limited storage capacity. The short-term forecasts are more valuable when the dams with reservoir capacity smaller than its annual volume and those operated for short-term operation

purposes including flood protection [Anghileri et al., 2016]. An effort has been made here to specifically study such dams, which have hardly been given attention in the existing literature, optimizing the operations by forecasting weather-scale flow events. With the need of ensemble forecasts to fully capture the uncertainty, as emphasized by the works cited above, we view the present research, using deterministic forecasts, to be an exploratory study on small to medium dams exploring informed sensitivity analysis, rather than a prediction of future events.

22

Chapter 3. METHODOLOGY

3.1   SITE SELECTION

As reservoirs operate differently across the U.S. with different climates, topography, dam size, and other pertinent meteorological factors, the study of a single dam or a single river basin is insufficient for generalizing the results over other wide ranging hydrologic conditions. We first explored multiple dam sites representing varying climates, capacities, and upstream drainage areas in the U.S while satisfying the constraints of having small to moderate storage receiving unregulated inflow.

While the International Commission on Large Dams (ICOLD) has characterized dams based on the dam height ["ICOLD: Definition", 2017], the dam storage capacity also plays a significant role on the temporal scale of optimization. A dam with substantially high storage possesses large storage buffer and cannot always respond dynamically in operations to a short-term peak inflow event. On the other hand, small/medium storage capacity dam has little storage buffer necessitating short-term optimization for reservoir operations. We define dams with surface area of less than 200 km^2 to have small to medium storage. This threshold represents about 98% for the dams according to the distribution of surface areas of US dams (see Figure 3.1). In Figure 3.1, the dams are ranked in order of decreasing area and using the Weibull plotting position given by $\frac{i}{n+1}$, where i is the rank and n is the total number of dams ($n = 1647$) obtained from the Global Reservoir and Dams (GRanD) database [Lehner et al., 2011]. The Weibull plotting position is selected as it represents unbiased exceedance probability for distributions [Stedinger et al., 1993].

23
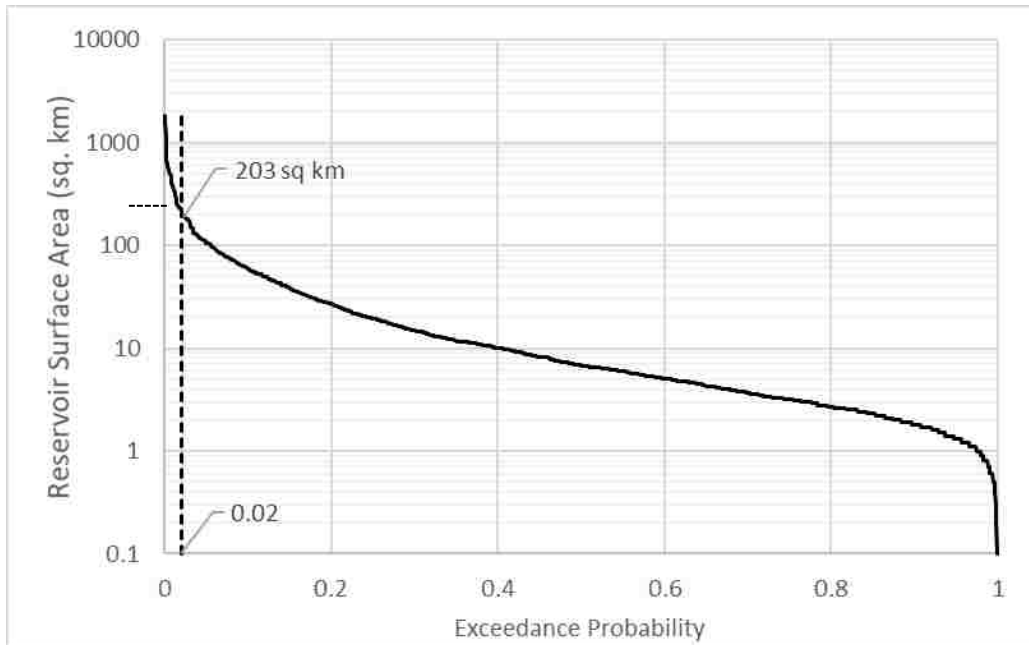
Figure 3.1. Distribution of the surface area of dams in US, with y-axis representing the dam surface area plotted on log-scale

A preliminary search was therefore made for dams satisfying the following criteria: (i) having a reservoir surface area of less than 200km^2, (ii) located upstream in the dam network (in case of a multi-reservoir system) to receive unregulated inflow, in order to facilitate VIC hydrological modeling, (iii) operated for hydropower generation or flood control as the primary and secondary purpose, and (iv) reservoir with storage capacity smaller than the annual inflow volume for the short-term forecasts to be valuable. Out of several potential locations, two dams were selected to be within the study's scope based on the data availability and processing time constraints for an exploratory study. Both dams are considered to be operated mainly for hydropower production with flood control being the other major use. There are, no doubt, many more dams that fit the above criteria for a more comprehensive national study in future.

24

The first dam chosen for this study is the Detroit dam, which is situated in Oregon on the North Santiam River, forming Detroit Lake (see Figure 3.2). The reservoir's surface area is 14.1 km^2, being categorized as one of the small reservoirs [Lehner et al., 2011]. The dam lies upstream amongst other dams in the network and receives mostly unregulated natural flow. Located in the Cascades, the climate of the region is temperate with a warm summer, as per the Köppen-Geiger climate classification [Kottek et al., 2006]. The dam is operated and managed by United States Army Corps of Engineers.

The second site is the Pensacola dam, also called Grand River Dam, on the Grand River in Oklahoma. The dam creates Grand Lake o' the Cherokees with a medium surface area of 188.2 km^2, in contrast to the Detroit dam's smaller sized reservoir. It is Oklahoma's first hydroelectric power plant, operated by Grand River Dam Authority [Pensacola Project, 2008], with other operational purposes including flood control and recreation. The region is classified as temperate with hot summer Köppen-Geiger class. The locations of the selected dams along with the relevant information are shown below in Figure 3.2. The storage-elevation relations and further details for both the dams can be found in Appendix A. Additionally, the respective values of reservoirs' storage capacity for the two dams are shown in Table 3.1, being smaller than the annual inflow volume for the short-term forecasts to be valuable [Anghileri et al., 2016].

Table 3.1. Statistics Comparison of Storage Capacity with Annual Inflow for the two dams

Dam	Storage Capacity (ac-ft)	Annual Inflow (ac-ft)	Capacity < Annual Inflow
Detroit	455,000	1,420,360	Yes
Pensacola	1,672,000	5,996,482	Yes

25
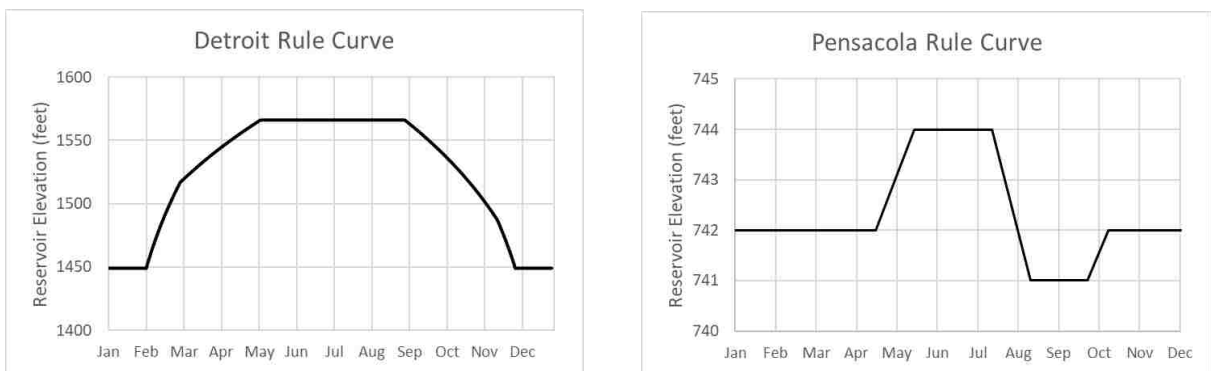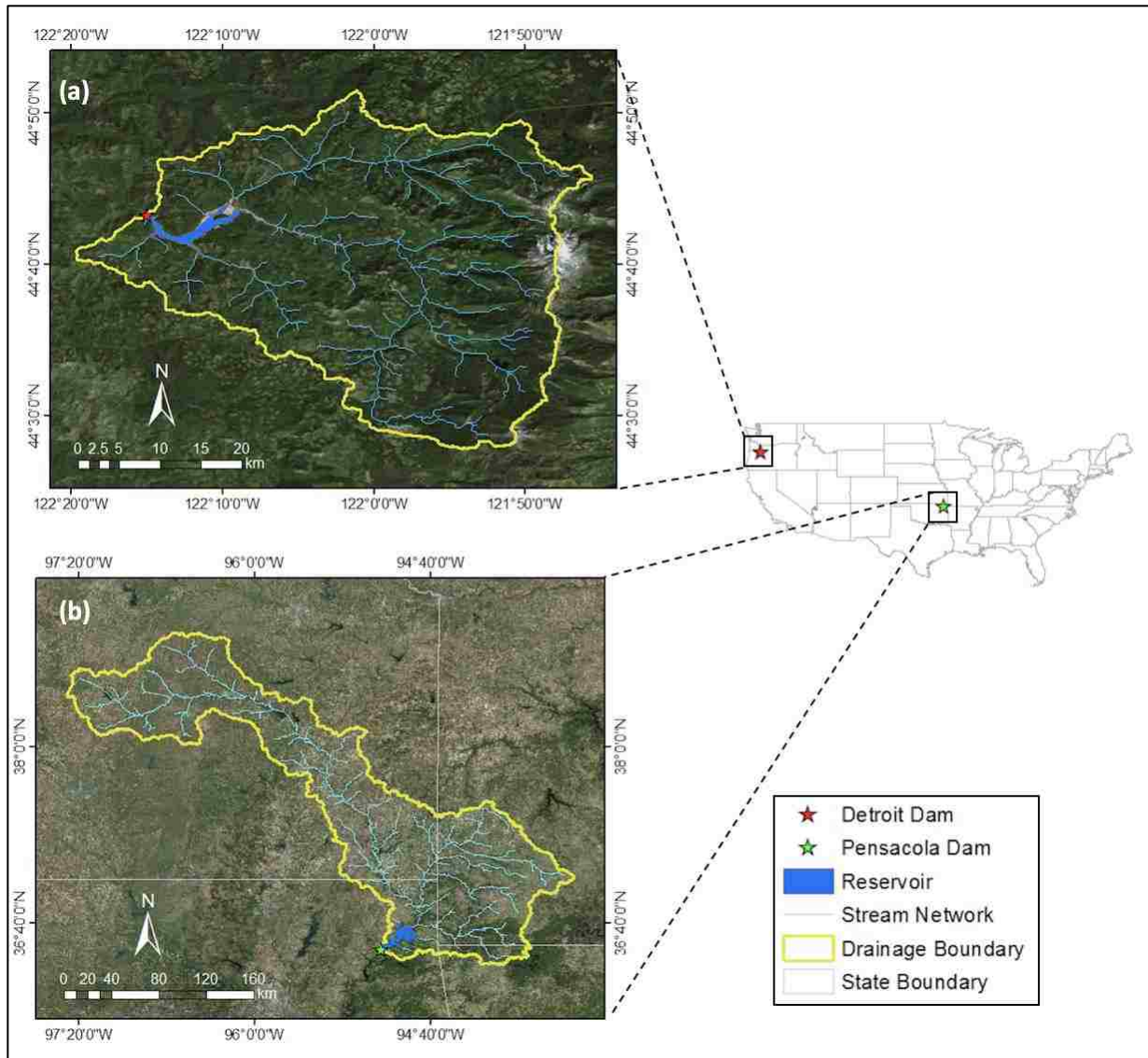
Figure 3.2. Location of selected dams along with drainage boundaries and stream networks (a)

Detroit Dam (b) Pensacola Dam (c) Respective Rule Curves of the two dams

26

3.2   DATASETS USED

The study uses several satellite-based, in-situ and post-processed datasets for application in the forecasting model, hydrologic model and for reservoir operations optimization. These are described in detail in the following sections.

3.2.1   *Global Forecast System forecast data*

The Global Forecast System (GFS) is a weather forecast model developed by the National Centers for Environmental Prediction (NCEP) at NOAA. The GFS model is a coupled model, composed of four separate models (an atmosphere model, an ocean model, a land/soil model, and a sea ice model), which work together to provide an accurate picture of weather conditions. The forecast model outputs a variety of atmospheric and land-soil variables including temperature, wind speed, precipitation soil moisture, atmospheric ozone concentration and so on. The model has a base resolution of 18 miles (28 km) between grid points, which is used by the operational forecasters. This drops to 44 miles (70 km) between grid point for forecasts between one week and two weeks ["Global Forecast System", 2017].

Although this resolution is suitable for a global scale analysis, the data turns out to be much coarser when used for application over a short-scale basin. Hence, some sort of downscaling needs to be done beforehand to be able to use the forecast data meaningfully. For this particular study, the GFS forecast data was used for lead time up to 16 days, for the period revolving around the considered peak inflow event. The GFS analysis/re-analysis data are also available, but the forecast data was used to assess the performance of optimization under real-time operational scenario where the dam operator will use the forecast data. The grib-2 files were downloaded by requesting the required files from Archive Information Request System managed by NOAA ["Order data -

27

NCDC"]. The forecasts are at 3-hourly resolution for the first 8-days lead time following which the resolution drops down to 12-hours, the spatial resolution being 0.5˚. The forecast data at 0.25˚ till 2015 are also archived. Further, this data was dynamically downscaled using Weather Research Forecasting (WRF) model (see section 3.3). An example of the GFS forecast precipitation at 0.5˚ resolution of Sept 3, 2017 at a lead time of 1-day is shown in Figure 3.3.
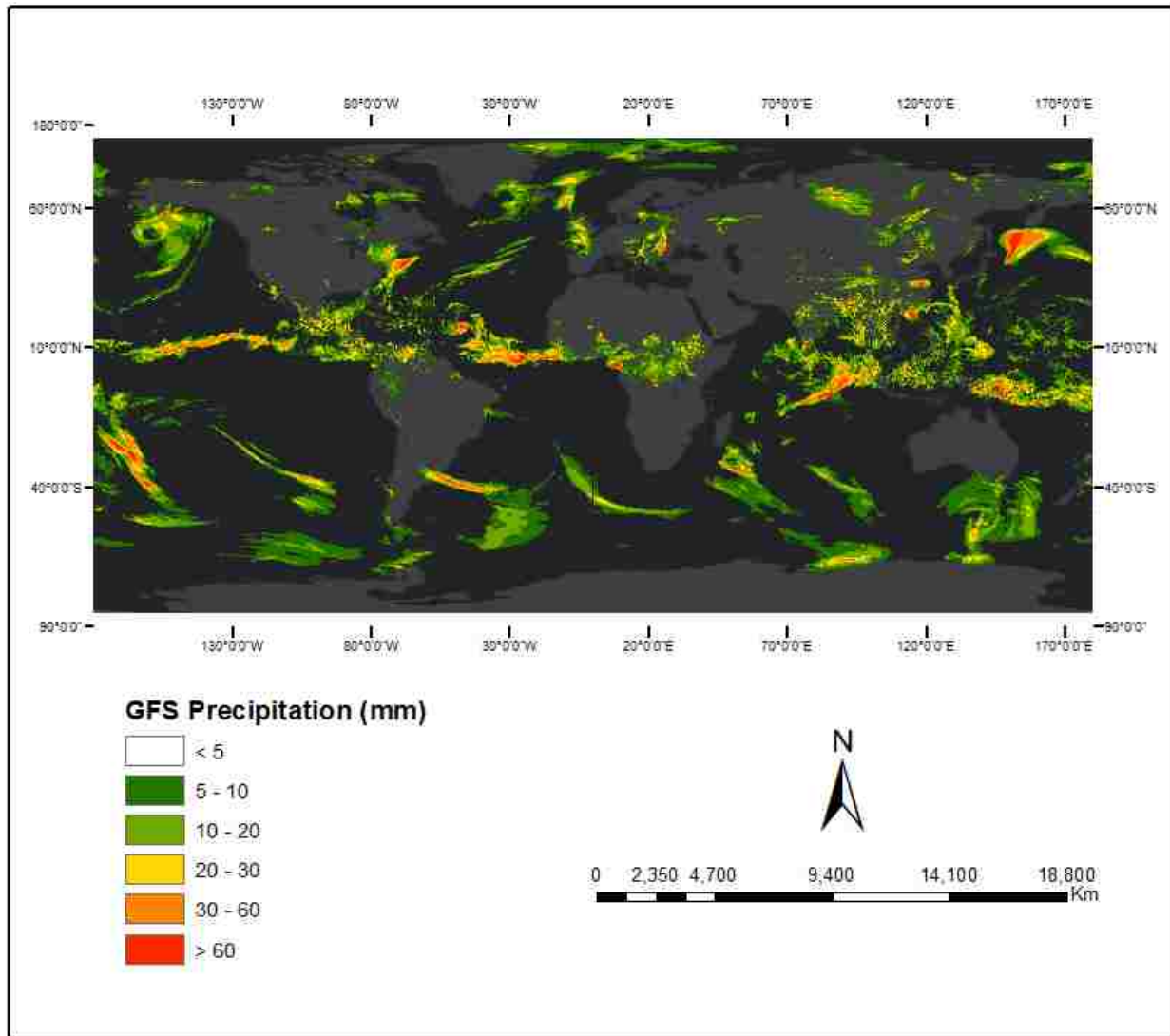
Figure 3.3. GFS forecast precipitation (mm) at 0.5˚ resolution of Sept 3, 2017 at 1-day lead time

28

3.2.2 *NCDC-GSOD Dataset*

While the forecast forcings were provided by the GFS forecast data, in order to run the hydrologic model, hindcast forcings are also required for a period of at least two years to account for the model spin-up period and facilitate the model calibration and validation. Global Surface Summary of the Day (GSOD) is an in-situ observational data from National Climatic Data Center (NCDC), derived from the Integrated Surface Hourly (ISH) dataset. The ISH dataset includes global data obtained from the USAF Climatology Center. Historical data are generally available for 1929 to the present, with data from 1973 to the present being the most complete. The latency of latest summary data is 1-2 days and incorporates data typically over 9000 stations over the globe ["GSOD", 2017]. The data are reported and summarized based on Greenwich Mean Time (GMT) after going through a quality control assessment. For instance, the precipitation will only appear if the stations report enough data to result in a valid value, and a minimum of 4 observations for the day need to be present. The dataset encompasses several hydrological parameters, and the ones required as forcing data to the VIC hydrologic model were extracted and processed into ASCII files. These include the precipitation amount, mean wind speed, minimum and maximum temperature. These are downloaded from the ftp site managed by NCDC (ftp://ftp.ncdc.noaa.gov/pub/data/gsod) for the stations that lie within or around the drainage basin of the selected dam sites. The stations found in NCDC-GSOD Server over the drainage basins of Detroit and Pensacola dam and their spatial distribution are shown in Figure 3.4. The interpolation was performed using the Inverse Distance Weighted (IDW) technique to result in a gridded raster of 0.1˚ resolution of the required forcings to be consistent with that obtained from post-processing of the WRF output.

29
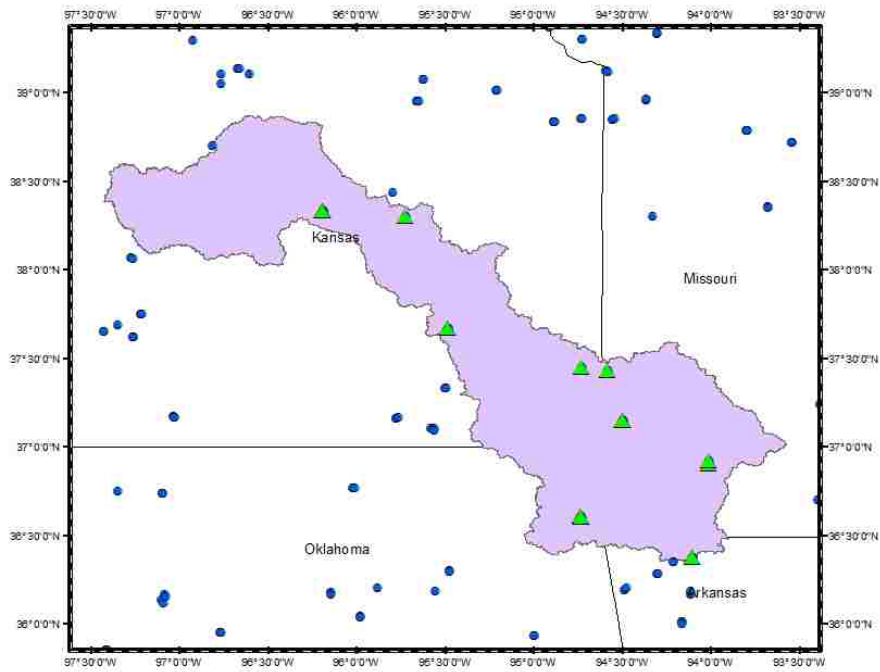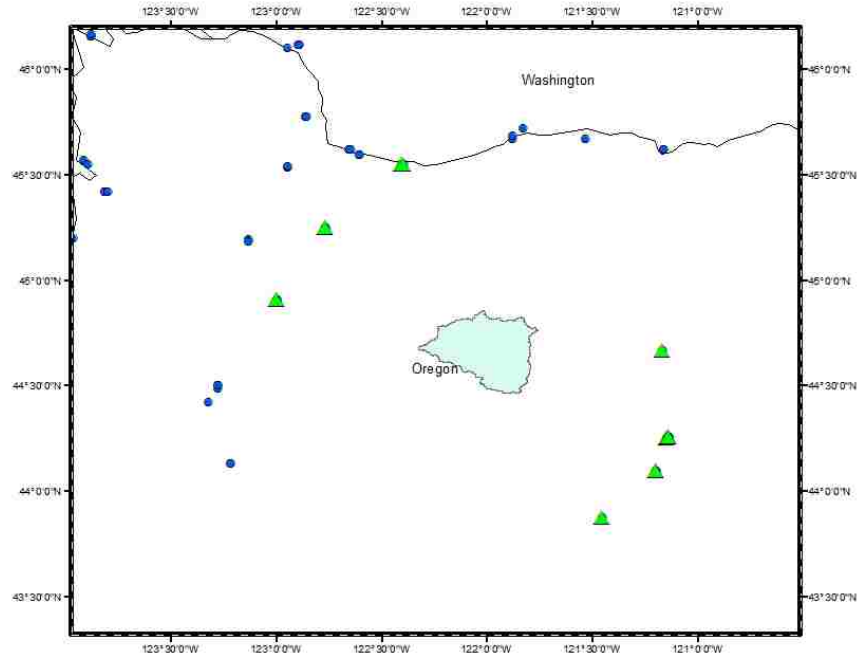
Legend

▲ Selected NCDC stations

● World NCDC stations

Pensacola Drainage Basin

Detroit Drainage Basin

State Boundary

N

0 15 30   60   90   120
Kilometers
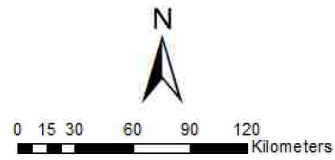
Figure 3.4. Spatial distribution of the stations found in NCDC-GSOD Server over the drainage basins of Detroit and Pensacola Dams

3.3   SHORT-TERM FORECAST MODEL

In order to optimize the reservoir operations, the short-term numerical forecasts of the weather need to be incorporated into the hydrologic model to obtain the daily forecast of inflow over short lead times (see Figure 3, green box). Real-time ensemble forecasts for short-term (1-16 days) lead time are provided by the Global Forecast System (GFS) global-scale Numerical Weather Prediction model developed by the NOAA. The 16-day forecast data are available at 0.25˚, 0.5˚, 1˚, and 2.5˚ resolution through the National Center for Environmental Prediction (NCEP). However, the resolution of forecast data is too coarse to be used for hydrological modeling over a reservoir with small to moderate surface area, which necessitates downscaling before application. There are essentially two kinds of downscaling techniques - the statistical/probabilistic downscaling methods use archived forecasts to downscale the information, while dynamical downscaling techniques involve dynamical models of the atmosphere and physics [Murphy, 2000; Chen et al., 2016; Sikder et al., 2016]. The present study uses the dynamical downscaling of GFS forecast data using the numerical Weather Research Forecasting (WRF) model.

WRF, being a mesoscale atmospheric numerical modeling system, is widely used in operations and research. WRF has demonstrated its capability for constructing the atmospheric conditions, at both local and regional scales [Chen et al., 2016; Skamarock et al., 2005]. The GFS forecast data was acquired at 0.5-degree resolution for 1-16 days' (384 hours) lead time with a 3-hourly temporal resolution for first 192 hours (8 days) and 12-hourly for the remaining period. Two nested domains of 10 km and 30 km were used for both the dams as shown in Figure 3.5. The

31

resolution of child domain was kept as 10 km to match the resolution of hydrologic model used for reservoir inflow prediction. The outputs from WRF are $100 \ km^2$ (0.1×0.1-degree resolution) gridded forcing datasets of minimum and maximum temperature, precipitation and wind speed, which subsequently are the input to hydrological model for forecasting inflow.
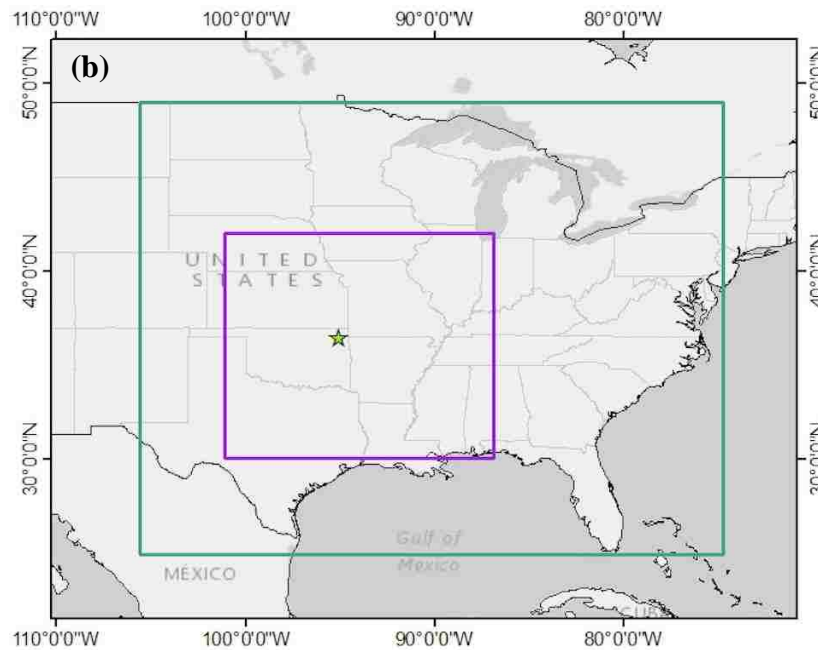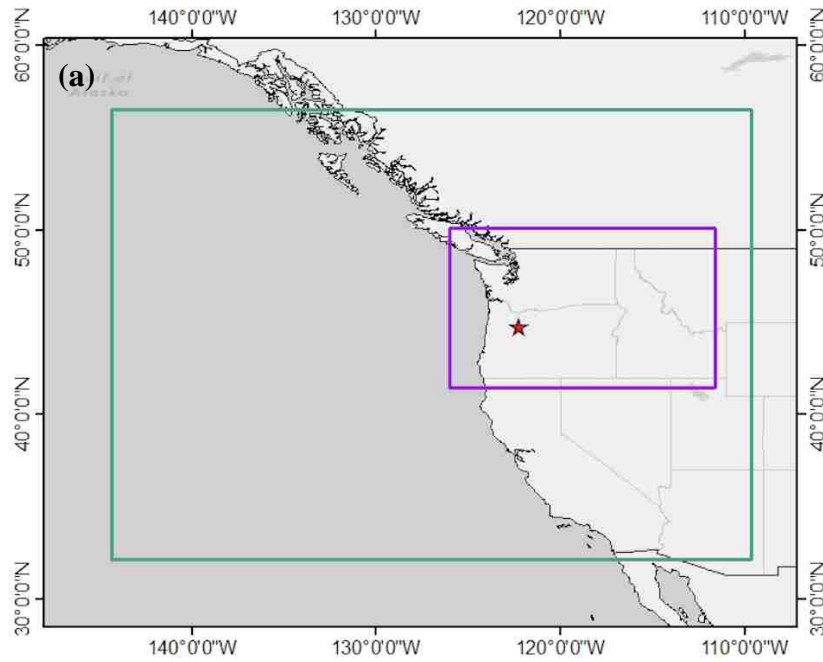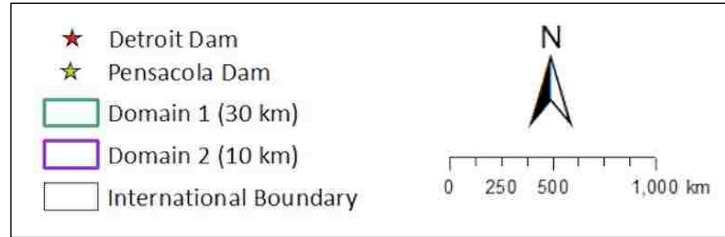
Figure 3.5. The nested domains for WRF simulation at 30km and 10km, for (a) Detroit Dam, OR and (b) Pensacola Dam, OK

In a numerical model like WRF, the Microphysics (MP) and Cumulus Parameterization (CP) schemes are the controlling factors for precipitation as reported in existing literature [Stensrud, 2007; Kumar et al., 2008; Chen et al., 2016]. The water vapor, cloud, and precipitation process are explicitly resolved by the microphysics schemes, while the subgrid-scale convective process and shallow clouds are managed by the cumulus parameterization [Sikder et al., 2016]. As the Detroit dam is in Pacific Northwest region, the model configurations are inherited from the forecast model runs of the Department of Atmospheric Sciences at the University of Washington ["Pacific Northwest Mesoscale Model", 2016]. At the department, forecasts are run twice a day to produce high resolution meteorological guidance for the Pacific Northwest. Specifically, the Thompson scheme with graupel was considered for the microphysics (MP) scheme and Grell–Freitas Ensemble scheme for the cumulus physics (CP) for Detroit Dam. For the Pensacola dam in Oklahoma, the Morrison microphysics scheme was used as recommended by Chen et al. [2016] as starting option for extreme storm simulation, while CP is kept the same as for Detroit dam. The detailed configurations of the WRF model for both the dams can be found in Appendix C, showing the *namelist.input* file (required input for running the WRF model).

The evaluation of WRF forecasted precipitation was performed using Livneh daily CONUS near-surface gridded meteorological dataset [Livneh et al., 2013]. The dataset provides

33

long-term precipitation record over the CONUS, and was generated from rain gauge records since 1915. The spatial coverage of daily rainfall was evaluated under various metrics (Probability of Detection, POD; False Alert Ratio, FAR; and Frequency Bias) [Chen et al., 2016]. For Pensacola dam, the WRF model was set up for the peak inflow event of 19-20 March 2012, for which the control and actual forecast runs were performed (see section 3.5.1). The GFS forecast data for 15 March was downloaded for lead time of 16 days up to 30 March, and subsequently downscaled with WRF. The forecast precipitation forcing was compared with the Livneh dataset for the 16-day period and the respective peak event was found to be captured reasonably well by the WRF downscaled output. In case of Detroit dam, although the control run was performed for December 2014 event, but due to the absence of Livneh dataset after 2014, WRF model was set up for a peak inflow event of 18-19 December 2007. The GFS forecasts of 17 December for 16-day lead time were downscaled using WRF. For both the dams, the WRF setup revealed that performance of the forecast model deteriorates with the lead time with higher number of misses (true negatives) and false positives as compared to the true positives, while the event was better captured (most true positives) for smaller lead times.

3.4 HYDROLOGIC MODEL

The hydrologic model chosen for this study to model the forecasted reservoir inflows is the macroscale semi-distributed Variable Infiltration Capacity (VIC) hydrologic model [Liang et al., 1994, 1996]. The VIC model is driven by gridded precipitation, minimum and maximum temperature, and wind time series. The model simulates snow accumulation and melt, soil moisture dynamics and evapotranspiration, as well as surface runoff and baseflow, which are subsequently routed through a grid-based flow network to simulate streamflow at select points within the basin [Christensen et al., 2004]. Details and examples of VIC model applications, calibration approach,

34

and streamflow routing can be found in Nijssen et al. [1997] and Hamlet et al. [1999]. Figure 3.6 represents a schematic view of VIC Land cover tiles along with the soil column and major fluxes.

The VIC model was run with 0.1-degree spatial resolution at daily time scale to obtain the gridded outputs over the upstream drainage area of the respective reservoirs. These gridded outputs include soil moisture, baseflow, runoff and evaporation. The forcings of precipitation, minimum and maximum temperature, and wind time series were obtained from NOAA's NCDC-GSOD data (see section 3.2.2 for details). In order to obtain the inflow at the most downstream station of basin (the dam location), routing of streamflow was performed separately using the routing model of Lohmann et al. [1996; 1998]. Model calibration was performed by adjusting the parameters of VIC model that govern baseflow recession, infiltration, and soil layer depths to match the simulated streamflow with reference dataset, maximizing the Nash-Sutcliffe efficiency and minimizing RMSE. The Nash-Sutcliffe efficiency, described by Nash and Sutcliffe [1970] is based on the deviation variance, expressed as,

$$NSE = 1 - \frac{\sigma_e^2}{\sigma_o^2} \tag{3.1}$$

where,

NSE = Nash-Sutcliffe efficiency

σ_e^2 = variance of the deviation between observation and simulation, and

σ_o^2 = variance of the observations

The variance of deviation is defined as:

$$\sigma_e^2 = \frac{1}{N-1} \sum_{i=1}^{N} \left(Q_{observed,i} - Q_{simulated,i} \right)^2 \tag{3.2}$$

The efficiency is similar to the statistical parameter coefficient of determination, R^2, with a value of 1 for a perfect fit, and can be negative as well for poor fits.

35

The parameters of stream flow routing model have also been fine-tuned to obtain the best matching streamflow [Hossain et al., 2017]. The details of the model simulation and calibration for the two dams are provided in the following sections.
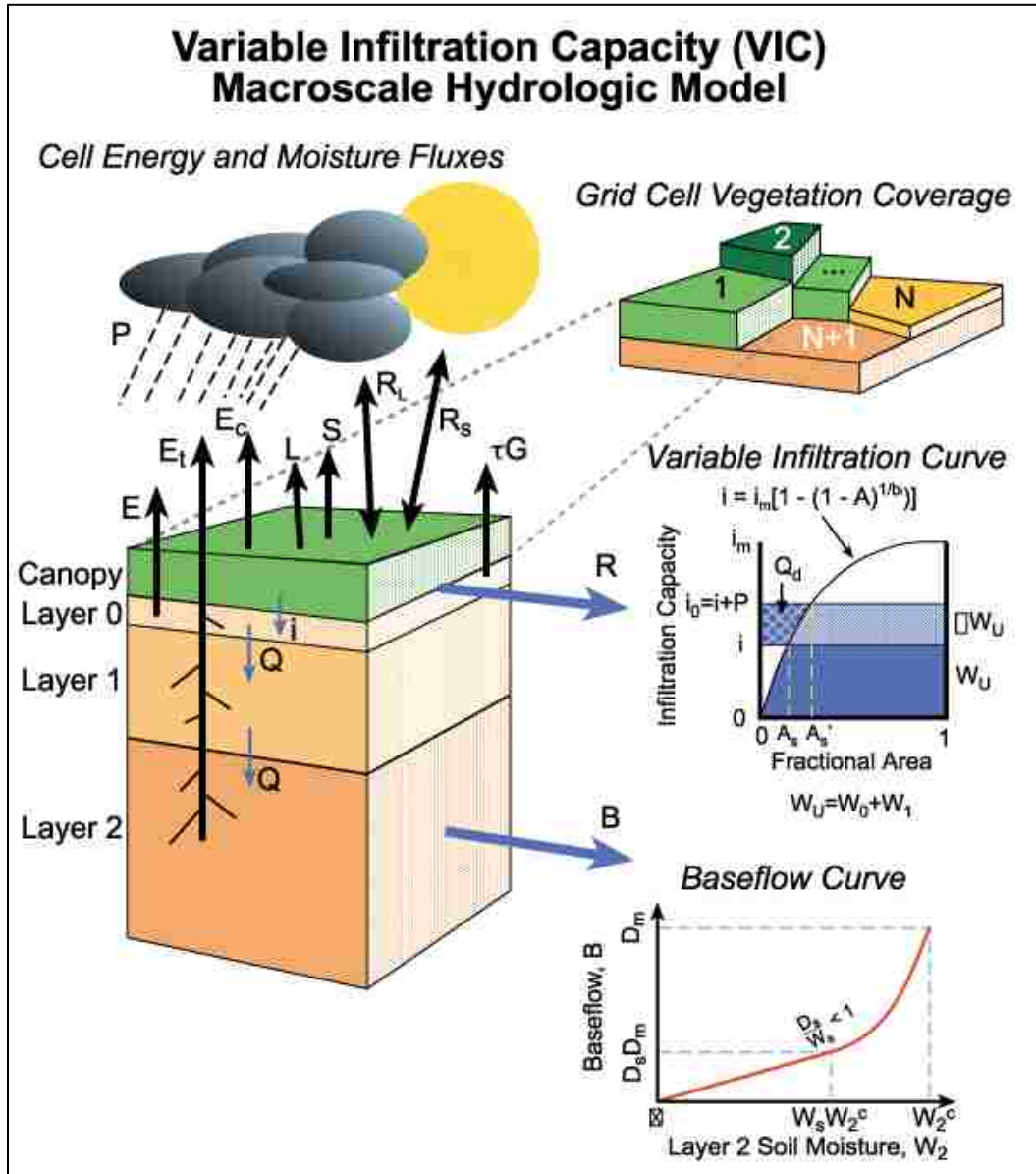
Figure 3.6. Schematic of VIC land cover tiles and soil column, with major water and energy fluxes. (Source: http://vic.readthedocs.io/en/master/Overview/ModelOverview/)

3.4.1 *Detroit Dam*

The Northwestern Division of US Army Corps of Engineers provides the daily streamflow data for Detroit dam on the Dataquery portal ["Dataquery 2.0", USACE]. Considering this to be unregulated inflow into the dam, the modeled VIC inflow was compared with USACE's daily streamflow in order to perform the calibration and validation of the model. Calibration was performed on the period from 2012-15, and the validation performed over 2009-11. The first few months were ignored for calculating metrics, taking into account the model run's spin-up period. Normalized RMSE is calculated as $\frac{RMSE}{\sigma_{obs}}$ (where σ_{obs} is standard deviation of the observed streamflow). The results for calibration and validation are shown in Figure 3.7.
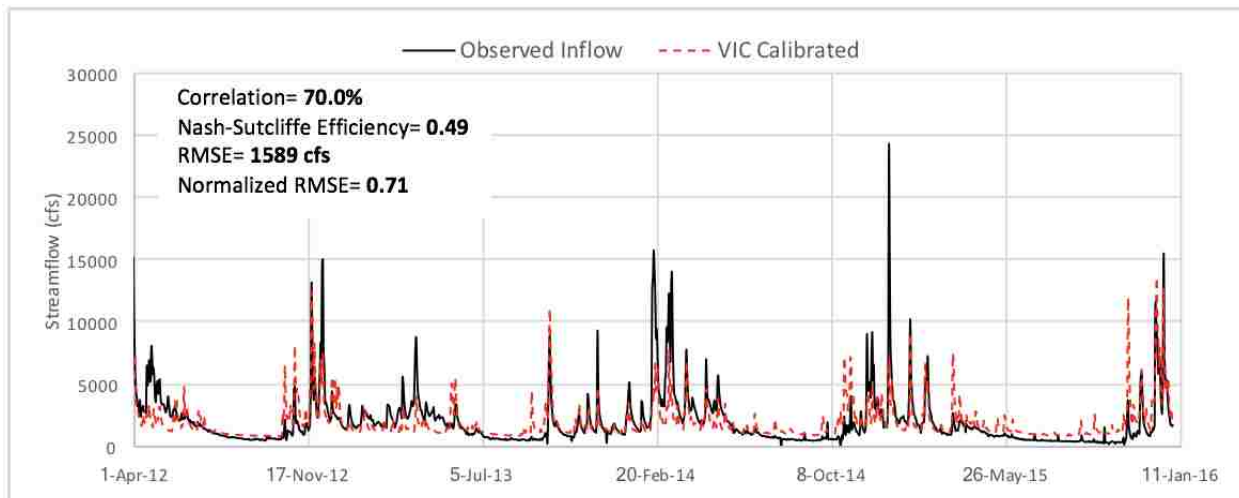
(a)
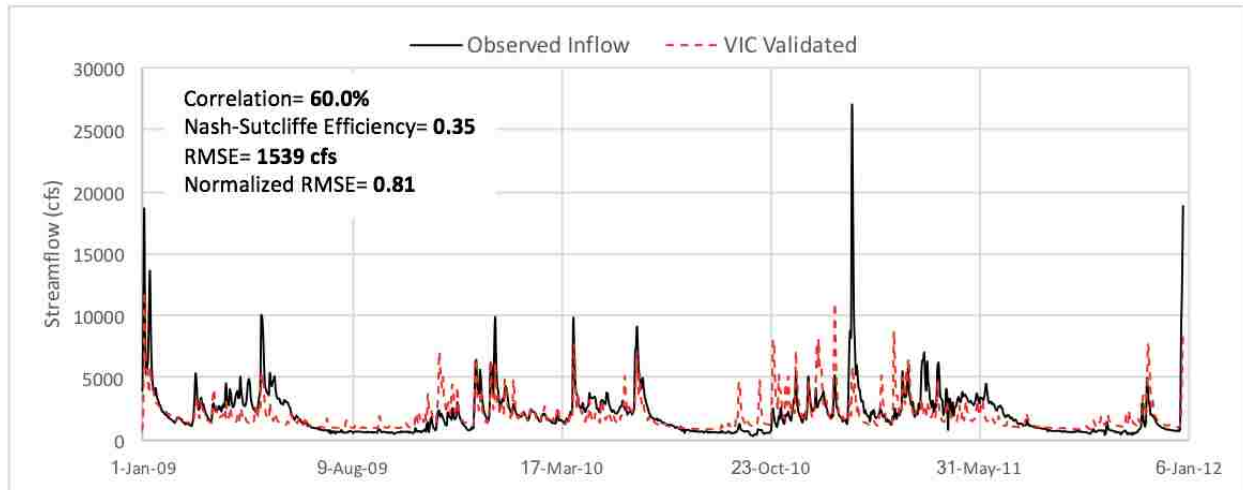
(b)

Figure 3.7. (a) VIC calibrated and (b) validated streamflow, along with the observed values at

Detroit Dam, OR

3.4.2   *Pensacola Dam*

The daily streamflow data for Pensacola dam was obtained from the Water Control Data Portal managed by the Southwestern Division of US Army Corps of Engineers ["Monthly Charts", USACE]. The website provides monthly reports of the Grand Lake, formed by Pensacola Dam that includes daily pool elevation, storage, releases, inflow into dam and other pertinent variables. As the dam is located in the most upstream point in the river network, this inflow is assumed to be natural and unregulated with no effect of water management. These monthly reports were processed over 2010-16 to extract the daily inflow data for calibration. The validation was performed over the period of 2001-05. The calibration and validation results are shown below in Figure 3.8.

38
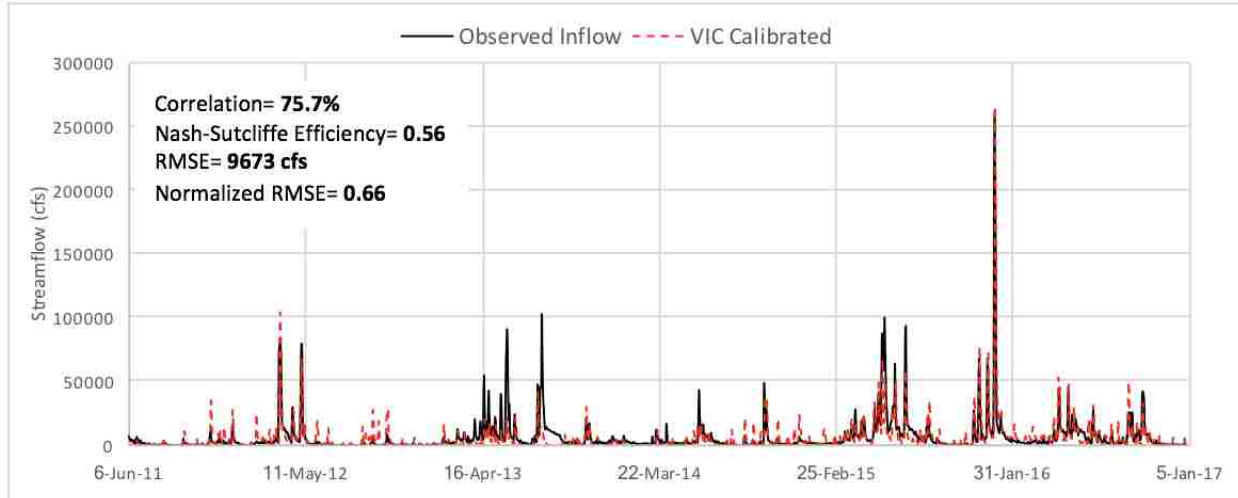
(a)
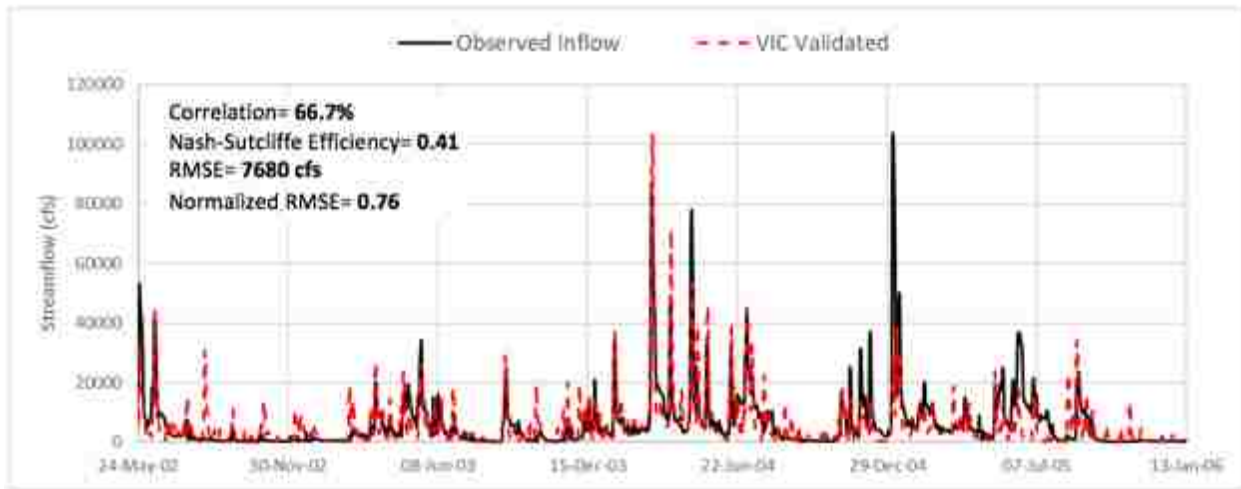
(b)

Figure 3.8. (a) VIC calibrated and (b) validated streamflow, along with the observed values at

Pensacola Dam, OK.

The calibrated parameters for VIC model for both the dams are summarized in Table 3.2.

Table 3.2. Calibrated parameters for VIC model simulation

Parameter	Units	Detroit Dam	Pensacola Dam
b_{infilt}	n/a	0.23	0.23
Ws	fraction	0.0028	0.001
Ds	fraction	0.39	0.99
Layer 1 depth, D_1	meters	0.25	0.90
Layer 2 depth, D_2	meters	0.28	0.10

39

The performance of VIC model in case of Pensacola dam is better as compared to that of Detroit dam, which essentially is the consequence of the smaller sized catchment in the latter case. Running VIC model at 0.1˚ resolution leads to inconsistencies in the modeled streamflow for smaller domains that other higher resolution models may be able to address. Yet, based on the performance metrics, the model is able to capture the peaks and pattern of observed inflow reasonably well and therefore is suited for forecasting inflow.

3.5 RESERVOIR OPERATION MODELING

The forecasting and hydrologic modeling components (Figure 1.9) result in the forecasted inflow into the reservoir for lead times of up to 16 days. The next step (see Figure 1.9, red box) is to model the reservoir operations using this forecast inflow information and optimizing the releases that need to be made from the reservoir to maximize hydropower generation. Optimizing at the daily time step is most suitable when it comes to real-time operations of small and medium-storage dams. A small dam operator is very unlikely to be making decisions on reservoir releases for such dams at frequencies higher than every 24 hours, while time steps larger than 1 day may miss a short term intense rainfall event leading to high inflow into the reservoir. Optimization can significantly add value to the use of forecast information, avoiding sub-optimal decisions and low efficiency operations concerning downstream stakeholder benefits. For instance, a study conducted on the economic value of long-term streamflow forecast for hydropower production in the Columbia River system, USA, found that an average increase of about US$ 150 million in annual revenue could be obtained [Hamlet et al., 2002]. Although a long-term forecast is different from the short-term forecasts from Numerical Weather Prediction (NWP) models, these figures reveal that the optimization of operations on short-term basis, an area still relatively untapped, also has the potential to maximize the economic benefits.

3.5.1 *Optimization Strategy*

In general, setting up an optimization framework involves three components – 1) advanced scheduling of water releases through the turbines, 2) accurate inflow forecasts that serve as input data, and 3) an optimization model that utilizes forecast information to the best advantage [Yeh 1985]. An extensive literature review and evaluation of different state-of-the-art optimization techniques is provided by Yeh [1985], ReVelle [1997] and Labadie [2004]. The optimization requires setting up the objective function to be maximized/minimized, imposing several constraints taking into consideration the interests of downstream stakeholders, dam safety and other environmental concerns.

A major limitation in operating the reservoirs for multiple downstream demands occurs during the flood/peak streamflow season when the high uncertainty in predicting a flood peak leaves the dam operator uncertain as to how much water needs to be released to balance the conflicting objectives. The static rule curves do not help much in handling this uncertainty. Hence, the short-term forecasts provide a way to overcome this limitation (as mentioned earlier in section 1.2) by including flood control as a constraint in the optimization model. However, as the forecasting models can never be perfectly accurate, optimizing based on these forecasts over the short-term period can result in an operation strategy that might not be the most optimum when operated according to the forecast inflow.

In order to assess the effect of uncertainty in forecasts as well as the impact of lead times on the resulting optimization scheme, the following schemes for optimization were employed:

1.   *Control Run*: This scheme assumes that the forecast inflow information obtained from the numerical weather prediction model is perfectly accurate and mimics the actual inflow over the course of 16-days of optimization. We use a retrospective observed streamflow dataset as one-

41

time perfect forecasts to optimize for the 16-days lead time, which is expected to approximate the use of a sophisticated forecasting system and free of possible modeling biases in the construction of forecasts [Denaro et al., 2017]. This essentially represents the best-case scenario for the optimization revealing the theoretical benefit (*perfect forecast benefits*) that could be obtained from optimized operation procedure on top of what the operations without any optimization result in. So, this strategy substitutes the GFS forecast data with the actual inflow data over the 16-day period.

2.   *Actual Forecast Run*: The potential of actual WRF simulated forecasts for the optimization of reservoir operations is assessed by the actual forecast runs. The 16-day deterministic forecast inflow obtained from one-time actual forecasts followed by hydrological modeling (see Figure 1.9, blue box) is used for the optimization instead of the actual inflow. The resulting optimized release policy is evaluated by calculating the hydropower benefits (a) using the WRF forecast inflow (*actual forecast benefits*), and (b) using the actual observed inflow as input to the reservoir system (*realized benefits*). This scheme is employed for exploring the effectiveness of forecasts with varying lead times on the benefits that could be obtained out of optimization.

3.   *Real-time sequential run:* Once the potential of the WRF simulated forecasts is realized and the effect of lead time of forecasts on the resulting optimized elevations and stakeholder benefits is investigated through actual forecast runs, another scheme for investigating the efficiency of forecasts is tested. This scheme sequentially updates the inflow into reservoir with actual WRF forecasts being updated every alternate day, running the optimization for 16-day period. This is closer to the real-time reservoir operations and what a dam operator will most likely be using for operational purpose, as updates on the forecast of reservoir inflow will be sought as frequently as possible. The scheme outputs a single net benefit (*net sequential benefit*) over the

course of the optimization run, obtained by passing the actual inflow downstream and using the sequentially updated releases.

The methods of obtaining the various benefits are summarized in Table 3.3. The benefits refer to the hydropower energy production (MWh) as a product of hydraulic head and power release, considering the turbine efficiency, operating hours and the capacity factor.

Table 3.3. Summary of various benefits for the evaluation of the control, actual forecast and real-time sequential runs

	Perfect Forecast Benefits	Actual Forecast Benefits	Realized Benefits	Net Sequential Benefit	No Optimization Benefits
Optimized based on	AI	FI	FI	UFI	-
Benefits based on	AI	FI	AI	AI	AI

AI: Actual Inflows; FI: Forecasted Inflows; UFI: Forecasted Inflows updated every alternate day

For all the three schemes, the strategy to optimize operations over a short-term peak inflow event involves the following: (1) As soon as high inflow (defined as any value greater than the turbine capacity, requiring water to be released over the spillways) is forecasted within the confidence bounds of WRF model, water is released through the penstocks ahead of the event to the maximum of turbine capacity, so that the spillage can be minimized when the peak inflow hits the reservoir. This maximizes hydropower over the release period, leaving more reservoir space for the future peak inflow to occur. (2) At the end of the high flow period (as estimated with the forecast data), the system is brought back to the rule curve specified stage, to ensure normal state of the reservoir after the peak event.

The Genetic Algorithm was employed as the optimization technique interfacing the other components of weather forecasting and hydrological modeling to determine the actual gate operations during the real-time operations of the reservoir. It is described in detail in the following section. To quantify the hydropower benefits, the hydroelectric energy produced (MWh) using the

43

observed release procedures (from data provided by USACE, or modeling the hydropower) without any optimization and that produced using the optimized release procedures was compared. Further, the optimization was performed individually for one peak inflow event for each dam. The events were chosen to represent yearly-scale peaks, and peak event of such a magnitude usually occurs once or twice a year over both the dams.

3.5.2 *Optimization Technique – Genetic Algorithm*

Amongst the plethora of metaheuristic techniques, Evolutionary Algorithms (EA's) are the most influential ones and are becoming more popular for optimization. EA's are a class of general-purpose stochastic global optimization algorithms simulating the natural evolution of biological systems. Genetic Algorithm (GA) is the most popular form of EA. The study of genetic algorithms (GAs) originated in the mid-1970s [Holland 1975], after which, GAs have developed into a powerful technique used in a diverse range of fields. An excellent overview of GAs can be found in the literature by Goldberg [1989] and Michalewicz [1992]. Goldberg [1989] identifies the following as the significant differences between GAs and more traditional optimization methods:

1. GAs work with a coding of the parameter set, not with the parameters themselves.

2. GAs search from a population of points, not a single point.

3. GAs use objective function information, not derivatives/other auxiliary knowledge.

4. GAs use probabilistic transition rules, not deterministic rules.

For a particular optimization problem, the possible solutions are coded into a series of substrings, or genes, representing components or variables that either form or can be used to evaluate the objective function of the problem. The series of substrings is termed as a chromosome. For instance, in the problem of single-reservoir operation optimization over 16-days in which the objective function is composed of reservoir releases over 16 days, the chromosome would

44

comprise of 16 genes, each representing 1 day of reservoir release. The GA starts with a population of chromosomes and tries to produce successive populations that are fitter. This reproduction process involves three genetic operators: selection, crossover and mutation. The chromosomes from the population with a high fitness value have a higher probability of being selected for combination with the other highly fit chromosomes. This combination takes place by crossover of the pieces of genetic material between the selected chromosomes. Mutation is required for the random mutations of bits of information in the individual genes. This process, through successive iterations, results in a progressively improved population of chromosomes.

MS Excel's in-built Evolutionary Solver was used for the purpose, to generate the optimum release/storage values in a user-friendly environment accompanied with a strong visualization capability. A screenshot of the interface for Evolutionary solver window is shown in Figure 3.9, along with the required options to run the genetic algorithm in Figure 3.10.
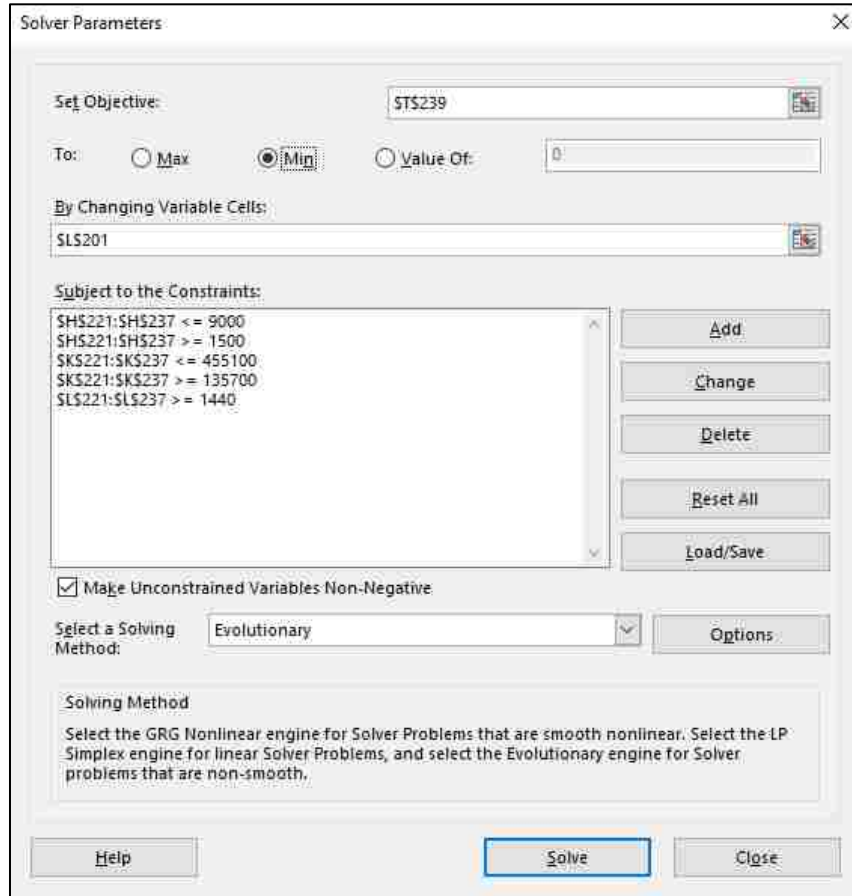
Figure 3.9. Evolutionary solver window in MS Excel
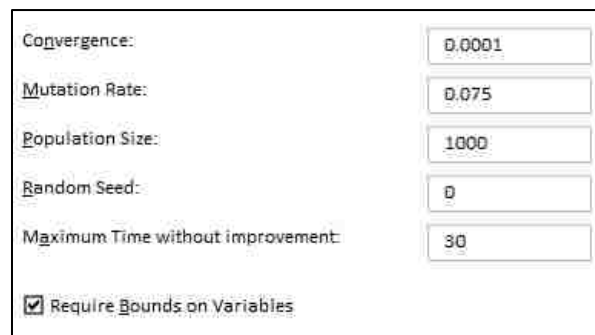
Figure 3.10. Specified options for the Evolutionary Solver

For setting up the optimization problem, an objective cell needs to be specified, which for

this study, comprises of the additional hydropower benefits over the optimization period (16-days)

and the deviation of the reservoir level from the rule curve specified level for a particular number

of days at the end of peak inflow event (depends on the length of event) to bring the reservoir back to normal state of operation after the event. As the optimization was formulated to minimize the objective, the hydropower benefit comes with a negative sign while the deviation of reservoir level is in positive. The default parameters of population size of 1000, convergence rate of 0.0001 and mutation rate of 0.075 were used for implementing the optimization strategy. Population size is the number of different potential values for the decision variables that the GA maintains at any given time in its population of candidate solutions. Convergence rate represents the maximum percentage difference in objective values for the top 99% of the population that Solver allows before stopping to iterate. Smaller rates of convergence consume more time but will stop at a point closer to the optimal solution. Mutation rate takes values between 0 and 1, and signify the relative frequency with which some members of the population will be mutated to create a new trial solution during each "generation" or sub-problem considered by the Evolutionary method. A higher mutation rate usually increases the diversity of the population and probability of arriving at better solution, although this may increase total computational time ["Excel Solver", 2017].

3.5.3   *Optimization Components*

3.5.3.1   Decision Variables

The variables needed to be optimized for the operational purpose are (a) the release made from the reservoir $R_{tot,t}$ at daily time step t, and (b) reservoir storage S_t at time step t. The daily release can be further categorized as (i) power release, R_p and (ii) non-power release, R_{np}. Power release is the effective water released through the penstocks, contributing to the hydropower generation, while non-power release is the water released via spillways or regulating outlets and includes water discharged for a purpose other than electricity generation.

47

3.5.3.2 Objective Functions

Over the period of flood event, the proposed optimization model involves the following objectives:

1. Maximize the hydroelectric energy produced (MWh) [Barros et al., 2003],

$$\max f_1 = \sum_t \epsilon \cdot (HF_t - HT_t) \cdot R_{p,t} \cdot \Delta t_{turb} \qquad (3.3)$$

2. Minimize the sum of the absolute value of storage deviations from the rule curve-specified value at the end of flood event to bring the system back to normal operations after the peak inflow event ends. The function is represented as,

$$\min f_2 = \sum_{t'} |S_t - T_t| \qquad (3.4)$$

3. Minimize total spilled ('missed') energy from non-power release,

$$\min f_3 = \sum_t R_{np,t} \qquad (3.5)$$

where:

HF – Reservoir forebay water level, obtained from area-elevation curve

HT – Reservoir tailrace water level,

$R_{p,t}$ – Power-release from penstocks

$R_{np,t}$ – Non-power release from spillways leading to missed energy

ϵ – Turbine efficiency

Δt_{turb} – Turbine operating hours

S_t – Reservoir storage

T_t – Target (rule curve specified) storage

t' – Number of days at the end of peak inflow event, depends on the length of event

t – Time step over the period of optimization

Thus, considering the appropriate sign for each objective, the composite objective function to be minimized can be written as,

48

$$\min F = -f_1 + f_2 + f_3 \tag{3.6}$$

Together, these objectives ensure that over the course of peak inflow event, the hydropower production is maximized and once the event ends (within the predictive ability of inflow forecasts), the reservoir system returns to the rule-curve stated levels to prevent the extremely high/low storage scenarios.

3.4.2.3 Constraints

The constraints comprise limiting values of the decision variables and other controlling parameters derived to ensure the dam safety, address environmental concerns, and satisfy multiple downstream stakeholders' demands. We define following constraints for our optimization model:

1. The maximum release through the turbines is constrained by the turbine capacity for each time step t,

$$R_{p,t} \leq R_{turb} , \forall t \tag{3.7}$$

(R_{turb} - Turbine capacity, MW)

2. The system must follow the storage volume continuity (water-balance equation) which requires that in each period t, initial active storage S_t plus the inflow I_t, less the losses L_t and release $(R_{p,t} + R_{np,t})$, equals the final storage, or equivalently the initial storage, S_{t+1}, in the following period $t + 1$.

$$S_{t+1} = S_t + [I_t - L_t - (R_{p,t} + R_{np,t})] \cdot \Delta t, \ \forall t \tag{3.8}$$

However, as the optimization is performed at daily time steps ($\Delta t = 1$), the losses due to evaporation and seepage over a day can be considered to be negligible and hence the loss term, L_t is ignored in the continuity equation above. As the storage is in acre-feet/day while inflow/releases are in cubic feet per second (cfs), a conversion factor of 1.983 was used for inflow and release terms to convert cfs into acre-feet/day.

49

3. The reservoir storage is limited within the bounds considering dam safety and infeasible storage scenarios such as reservoir running empty.

$$S_{min} \leq S_t \leq S_{max}, \quad \forall t \qquad (3.9)$$

Here, S_{min} is set up considering the conservation pool of the reservoir to keep it at a suitable level above the inactive pool, while S_{max} denotes the active storage capacity till the reservoir's full pool.

4. In order to avoid excessive and infeasible rates of non-power release via the spillway, the non-power release rate was limited to the spillway capacity,

$$R_{np,t} \leq Spill_{max}, \quad \forall t \qquad (3.10)$$

5. To prevent the downstream flooding hazards, the total release was constrained to a maximum limit of R_{max} based on the historical records of outflow causing flooding at a downstream control station,

$$R_{p,t} + R_{np,t} \leq R_{max}, \quad \forall t \qquad (3.11)$$

6. Lastly, the releases made from reservoir should comply with the environmental flow limit, Q_{env}, allowing safer fish passage, temperature control and minimum instream flow requirements,

$$R_{np,t} + R_{p,t} \geq Q_{env}, \quad \forall t \qquad (3.12)$$

The optimization model is nonlinearly constrained with a nonlinear objective function, as the energy production function,

$$\sum_t \epsilon \cdot (HF_t - HT_t) \cdot R_{p,t} \cdot \Delta t_{turb} \qquad (3.13)$$

comprises the reservoir head which is based on the nonlinear storage-elevation relation specific to each reservoir.

50

Chapter 4. CASE STUDY AND RESULTS

4.1   CASE 1: DETROIT DAM

4.1.1   *Dam Logistics*

The Detroit dam, as highlighted in section 3.1, is a storage dam located at the North Santiam River in Marion County, Oregon, used for flood control, power generation, irrigation, navigation, and recreation (Figure 3.2). It was constructed as a part of the Willamette Valley Project authorized by the Flood Control Act of 1938. An overview of the Willamette basin along with the dams therein is shown in Figure A.1 (Appendix A). The dam, lying in the North Santiam Sub-basin, is a concrete gravity structure approximately 463 feet tall and 1580 feet long, having six spillway gates. The spillway crest is located at elevation 1541 feet above mean sea level (MSL), and full pool is at 1569.0 feet MSL. The powerhouse contains two Francis turbine units with a hydraulic capacity of 5340 cubic feet per second (cfs) and a total combined nameplate capacity of 100 megawatts (MW) (50MW each). Downstream fish passage is available only through the spillway, turbines, or regulating outlets [Duncan et al., 2011]. The dam lies upstream in the network with inflow into it experiencing no regulations, as can be seen from the schematic in Figure 4.1. Downstream of Detroit dam is the Big Cliff dam which is a re-regulating dam with small reservoir located nearly 3 miles downstream ["Willamette River Basin", 2011]. Big Cliff dam is used to smooth out the power generation water releases from Detroit dam and to control downstream river level fluctuations. Complete details of the dam are shown in Figure 4.2 and the pertinent dam logistics are summarized in Table 4.1.
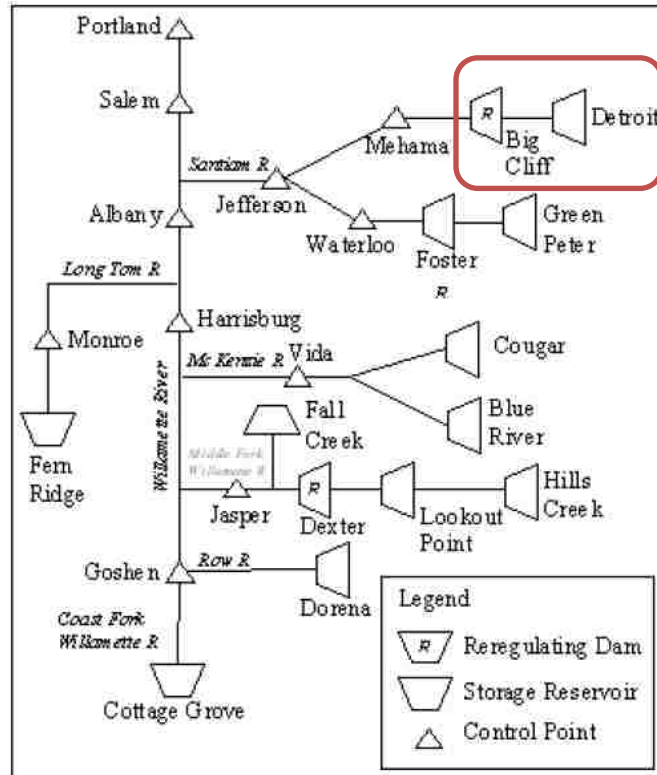
Figure 4.1. Willamette Valley Project schematic (Source: "Willamette River Basin", 2011)

To obtain the relation between storage and elevation of the reservoir to be used in operations modeling (see Figure 1.3, red box), the storage-elevation curve was obtained using the most recent data provided by USACE ["Dataquery 2.0", USACE]. Datasets corresponding to reservoir's storage and forebay elevation (see Figure 4.2 for various pool values) for the last 5 years were fitted with an exponential curve to obtain the relation, as plotted in Figure 4.3 (a) below. Further, as the turbine operating hours and efficiency of operation usually varies over the event and season, a model for hydropower estimation (MWh) based on available historical daily generation data from USACE was developed. The assumption made here is that the turbines will continue to operate in the near future with the same efficiency and average number of operating hours as obtained from the historical operations. As hydropower from a turbine is directly

52

proportional to the discharge and the hydraulic head [Yao et al., 2001], linear regression was performed between the actual production data (in MWh) and the product of hydraulic head ΔH and power release R_p (adjusted for units to be in MW) as plotted in Figure 4.3(b). The constant for converting from MW to MWh is 19.72 hours, which takes into account the turbine efficiency, average number of operating hours and its capacity factor (ratio of the average power generated and nameplate capacity).
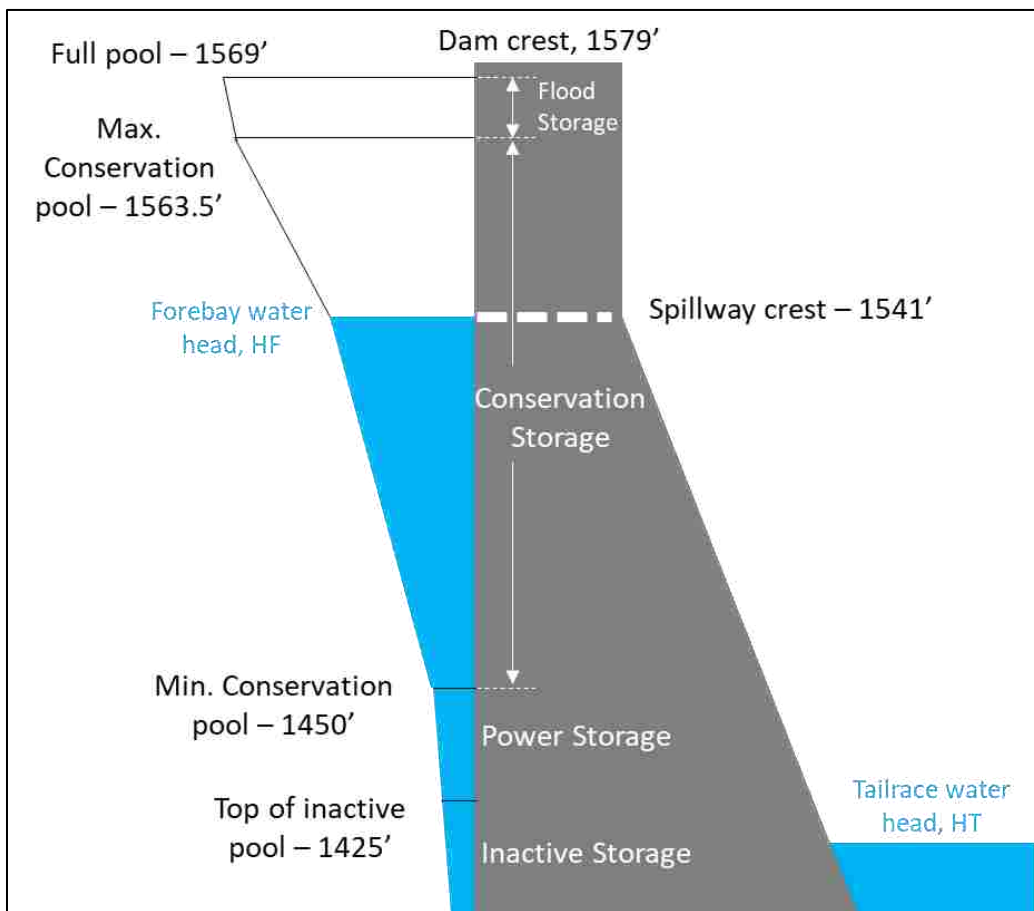
Figure 4.2. Cross-section of Detroit dam (not to scale) showing relevant elevations (from mean sea level, MSL)

53

Table 4.1. Detroit Dam logistics

Year of completion	1953
Drainage Area	438 sq. miles
Dam Height	450 feet
Turbines	Two 50 MW Francis type
Turbine Capacity	5340 cfs
Spillway Gates	6 radial tainter gates
Spillway Capacity	176,000 cfs
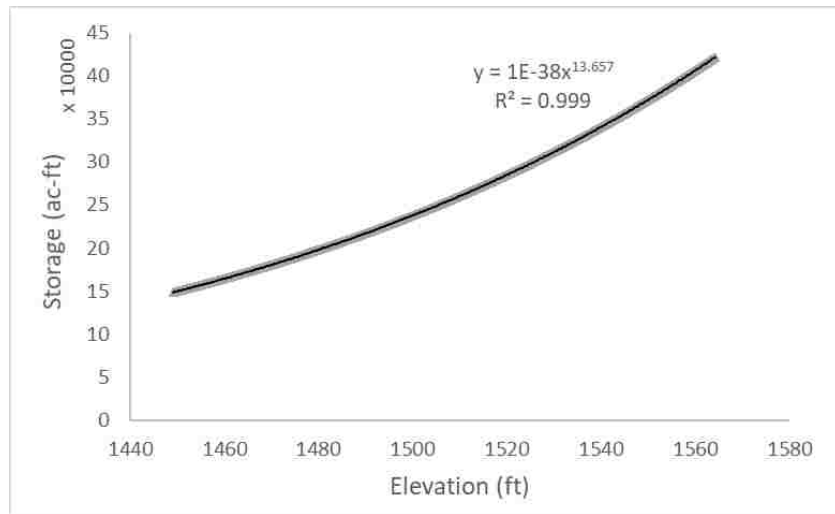
(a)
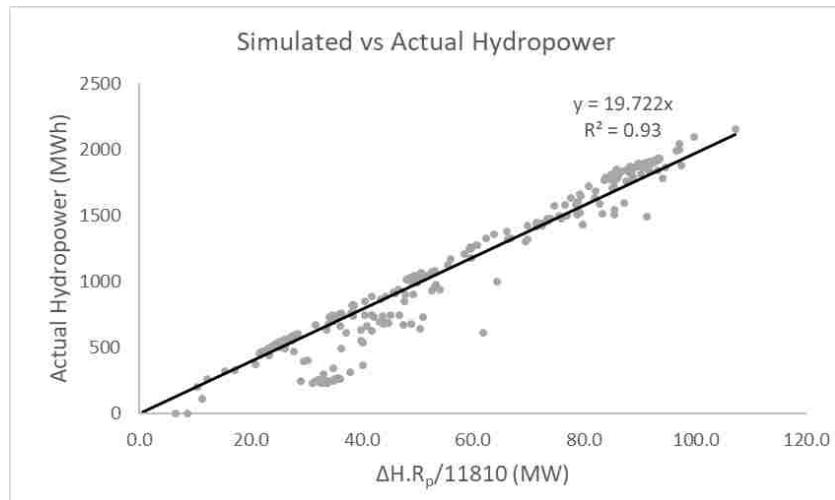
(b)

Figure 4.3. (a) Storage-Elevation curve and corresponding fitted exponential curve for Detroit

dam (b) Linear regression model for simulating the turbine efficiency and operating hours in the

hydropower production equation.

54

4.1.2 *Optimization Model*

The optimization model was set up using the constraints as described in section 3.4.2.3. The values for each of the bounds was obtained from the dam's operational data from USACE. The minimum storage limit was arrived at by obtaining 95% of the 10-year historical minimum of the storage, to keep the reservoir within the conservation pool, while the maximum storage limit was set to the maximum conservation pool of the dam. Minimum environmental flow limit for the release was obtained from a study done on the Detroit dam [Risley et al., 2012]. The maximum total release is usually set to control a downstream point to some threshold value, so that the outflow is set to minimum for peak events. Although the threshold still gets exceeded during the actual peak event, but having the project a minimum helps in shaving the peak to some extent. Detroit has three downstream control points - Mehama, Jefferson and Salem. However, as Jefferson and Salem include regulated inflow from other tributaries making it harder to model, only Mehama was used to obtain the threshold. Detroit dam is operated to keep Mehama at less than 17,000 cfs when possible [Personal communication with Christopher Frans, USACE]. However, as another tributary of Santiam River adds to the inflow at Mehama, an approximate release value of 9000 cfs was chosen considering the factor of safety. The locations of each of the control stations are shown in Figure 4.4. The constraints are summarized in Table 4.2.

Table 4.2. Constraints for Optimization for Detroit dam, OR

Constraint	Value
Turbine Capacity	5340 cfs
Spillway Capacity, $Spill_{max}$	176,000 cfs
Minimum storage limit, S_{min}	135,700 ac-ft (95% of 10-year minimum)
Maximum storage limit, S_{max}	455,100 ac-ft (max conservation pool)
Maximum total release, R_{max}	9000 cfs (avoid flooding at Mehama)
Environmental flow limit, Q_{env}	1500 cfs
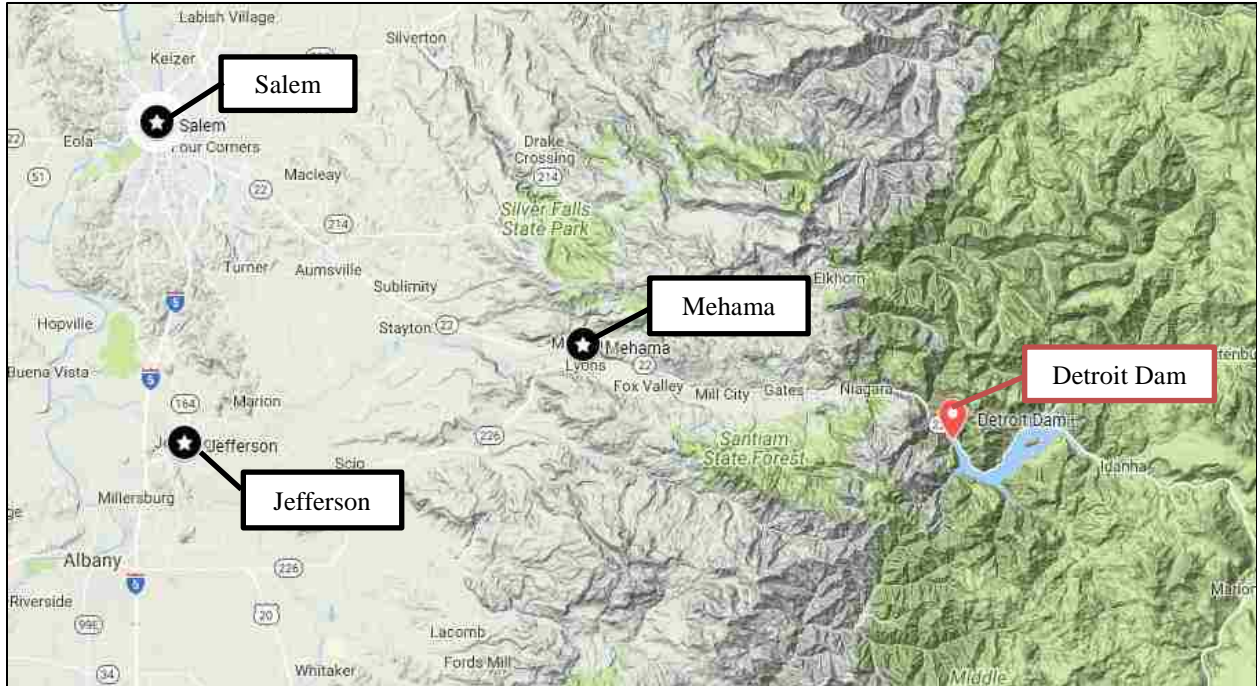
Figure 4.4. Locations of the control stations downstream of Detroit dam, OR

With this optimization model setup, the respective schemes of optimizing the operations (see section 3.4.1) are investigated below.

4.1.2.1   Control Run

The control run was performed over the February 1996 major flood event of Oregon, also termed as Willamette Valley Flood of 1996. The event is considered as a 100-year flood and lasted for around a week with peak inflow occurring on 8 Feb 1996. The flood was triggered by an above average snowpack in lower elevations accompanied with heavy rain and frozen soil. It lasted for a few days only but the effects were long-lasting, causing millions of dollars in damage. Figure 4.5 shows the aerial view of flooded Willamette River.

56

Figure 4.5. Aerial view of flooded Willamette River, over which the Detroit dam is located

(Source: National Weather Service Portland)

When floodwaters were at the peak, dam operations reduced their impact and kept the river level lower than it would have been otherwise, reducing the water levels by 1 – 1.5 feet. Estimates show that these measures saved the region $3.2 billion in catastrophic flood damage to homes and businesses. Although, extreme events like this are rare, but efficient optimization of the operations over such an event can help facilitate the loss prevention and extract additional hydropower, turning the catastrophic event into a future benefit. The actual inflow, releases and storage during the peak inflow event, along with the rule curve, are plotted in Figure 4.6.

57
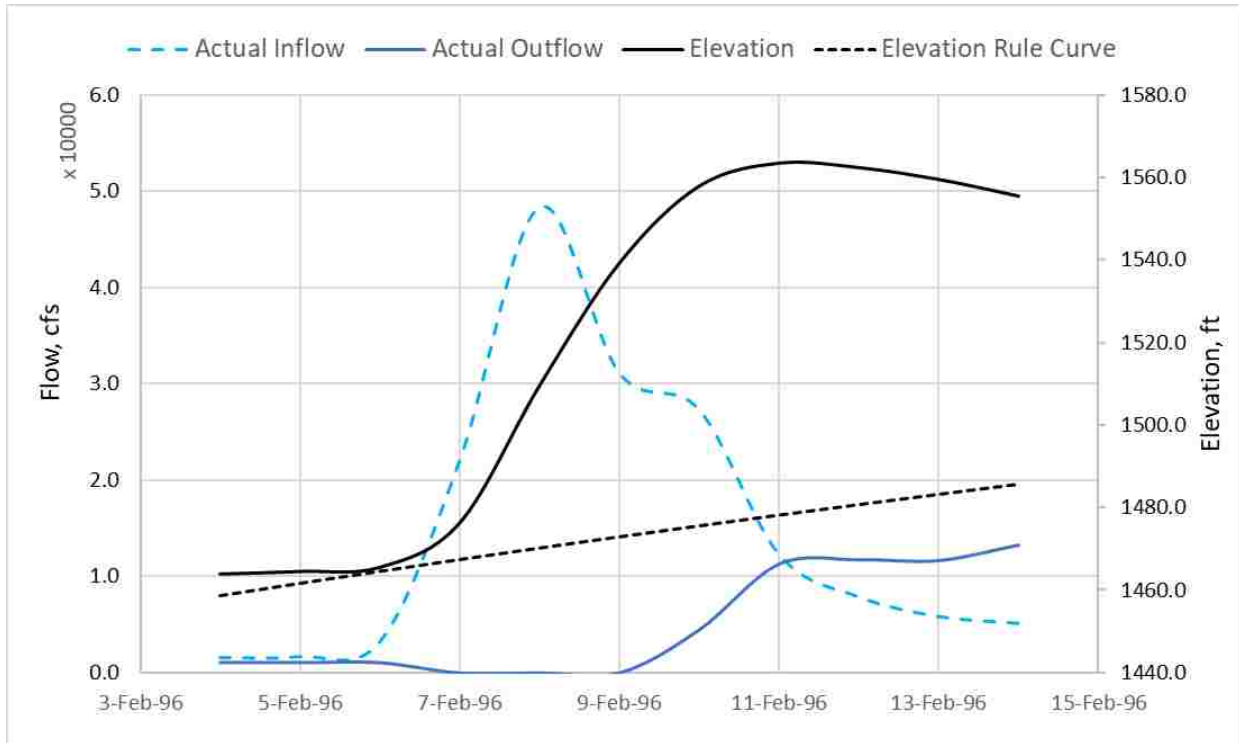
Figure 4.6. Observed inflow, outflow and storage from reservoir operations during Feb 1996

flood event over Detroit dam, OR

The optimization over this extreme event was tested for four scenarios of 1, 4, 7 and 10-days lead depending on when the peak inflow of 8 Feb is forecasted, using the optimization strategy of control run outlined in section 3.5.1. The hydropower benefits (MWh) obtained using the control run optimization at different lead times, along with the respective benefits from observed operations and corresponding difference between the two are plotted in Figure 4.7.

58
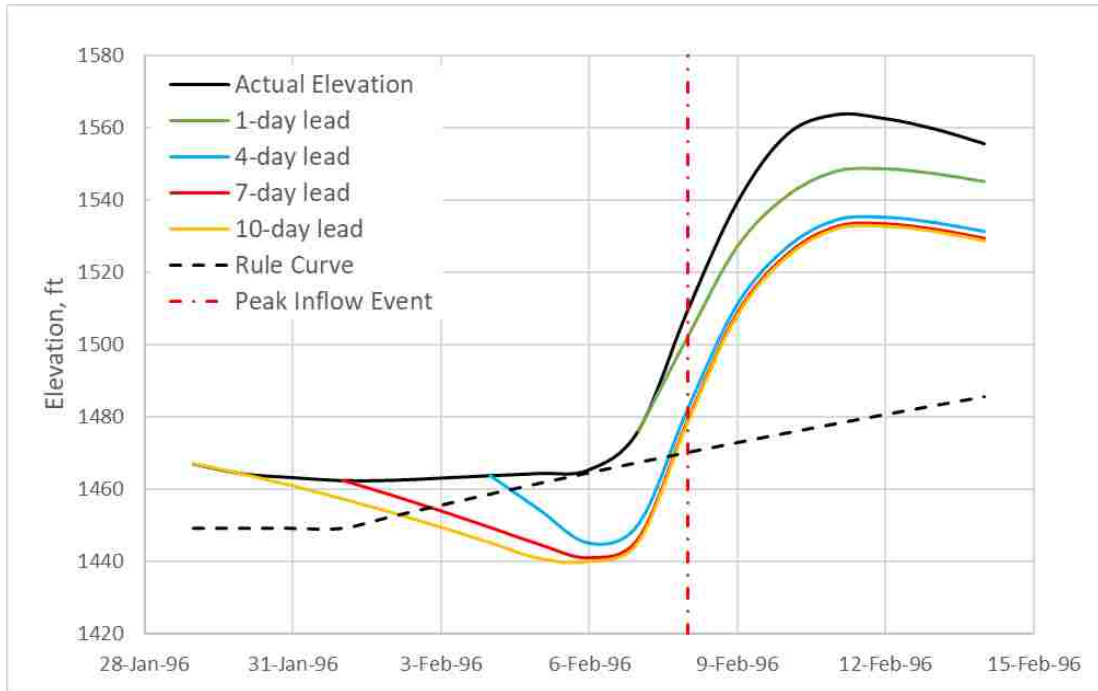
(a)

(b)

Figure 4.7. (a) Optimized elevations at different lead times, (b) Hydropower benefits (MWh)

obtained using the control run optimization at different lead times, along with the respective

benefits from observed operations and corresponding difference (Detroit dam, OR)

59

From Figure 4.7(b), it is apparent that longer lead times of forecasting, a relatively higher additional hydropower benefit can be extracted from the optimization over 16-day period reflected by the larger difference between optimized and no-optimization benefits. Also, considering the competing objective of flood control, a higher lead time brings the reservoir level at the end of flood event closer to the rule curve as suggested by Figure 4.7 (a). However, as longer lead times also come with a loss in forecasting skill, there exists a tradeoff between the longer lead times and the respective benefits that could be harnessed.

To study this tradeoff, actual forecast run (see section 3.5.1) needs to be performed employing the GFS forecast data. However, as the GFS data are unavailable for the year 1996, another peak inflow event with annual scale magnitude was chosen to perform the control run and actual forecast run. This event took place in December 2014, with a peak inflow of 24,170 cfs on 22 December. As Livneh data ends in 2013, NEXRAD Stage IV data from NCEP was used to visualize the heavy precipitation event. The Stage IV data is based on regional multi-sensor (radar and gauges) hourly/6-hourly 'Stage III' precipitation analysis on local 4km polar-stereographic grids produced by the 12 River Forecast Centers (RFCs) in CONUS. NCEP mosaics the Stage III into the national Stage IV product [Lin, 2011]. The precipitation event is shown in Figure 4.7 for 21-23 December. The drainage boundary of Detroit dam is marked in black.

21 December 2014
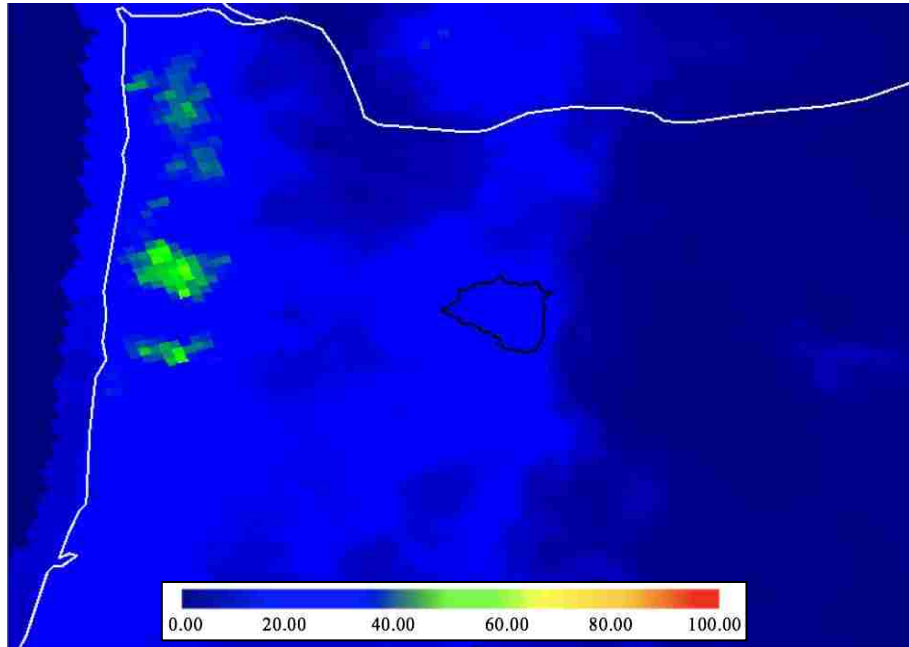
(a)

22 December 2014
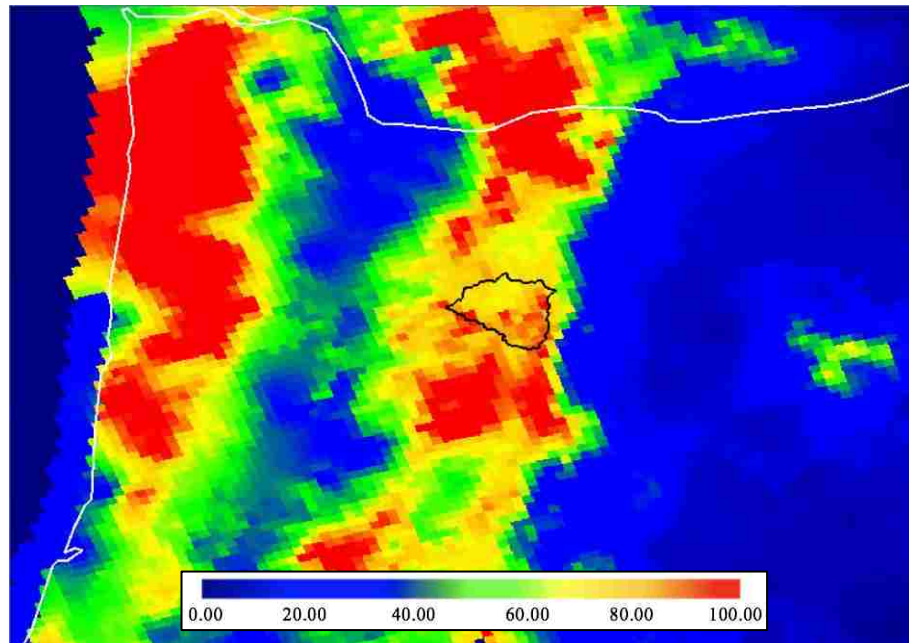
(b)

23 December 2014
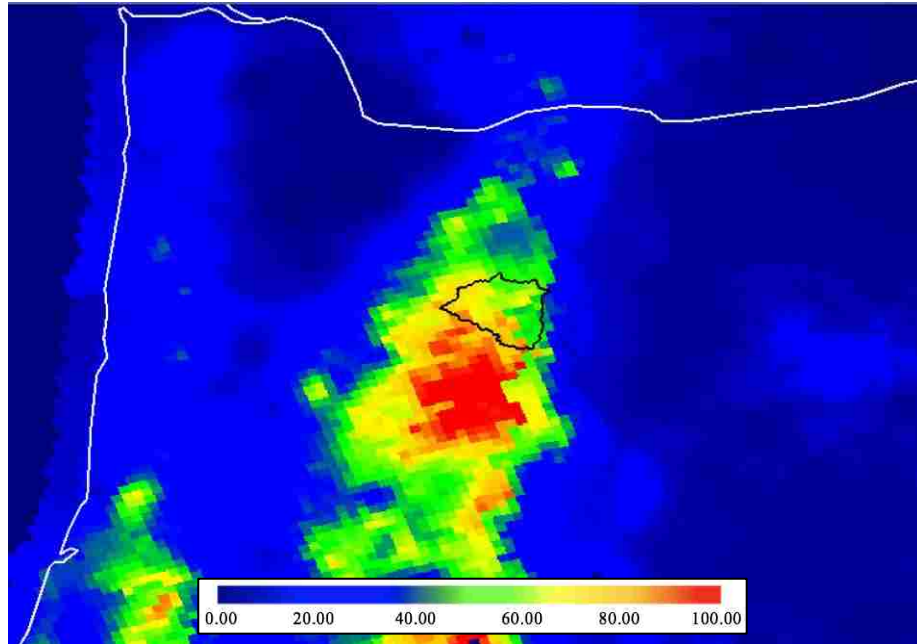
(c)
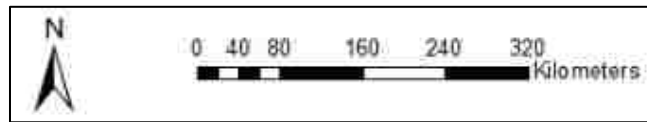
Figure 4.8. Daily 24-hr accumulated surface precipitation (mm) from NEXRAD (Stage

IV) product for 21-23 Dec. 2014, visualized in Weather and Climate Toolkit (WCT) from

NOAA, with Detroit dam's upstream drainage boundary showed in black

An initial control run performed over this event at lead times of 3, 5 and 9 days and over a

16-day period of optimization results into the optimized elevations as shown in Figure 4.9.
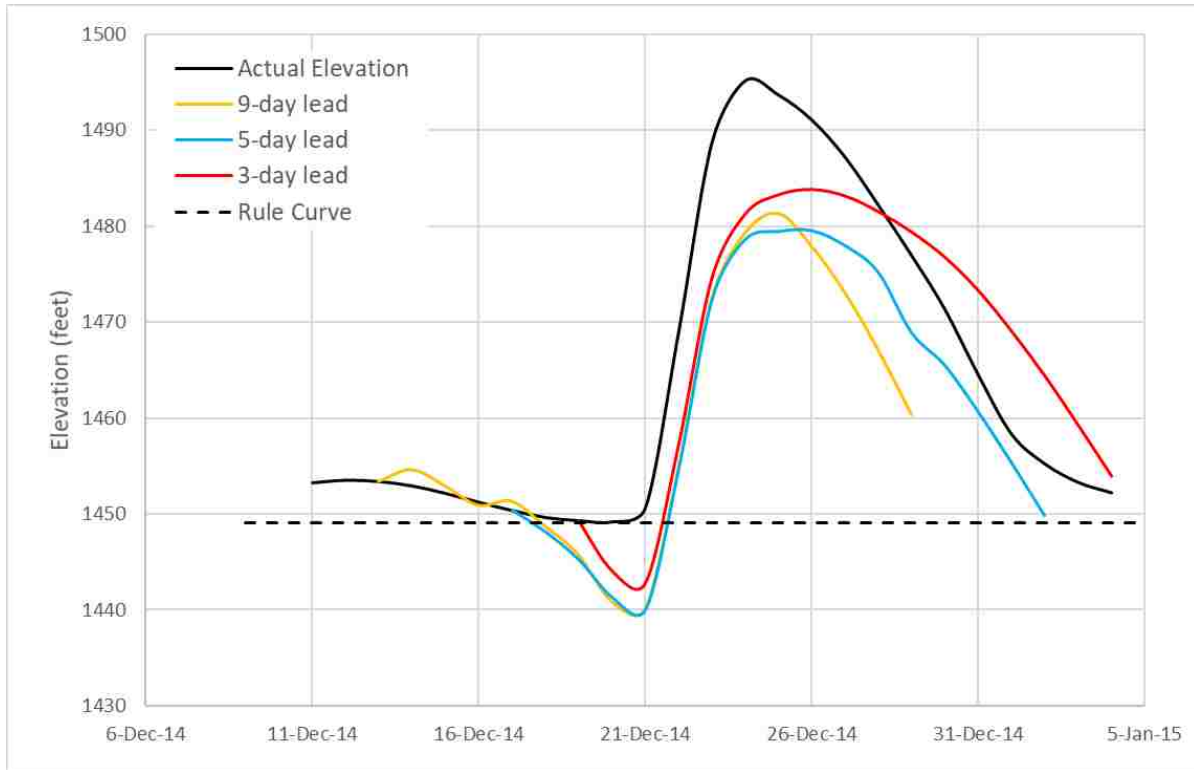
Figure 4.9. Optimized elevations from the control run performed over Dec 2014 peak inflow
event with three different lead time scenarios (Detroit dam, OR)

4.1.2.2 Actual Forecast Run

To assess the tradeoff between the increasing the lead time of forecasts and the respective benefits
that could be reaped from optimization, one-time actual forecast runs were performed over the
December 2014 peak inflow event as described above. The GFS forecasts produced on four
different days corresponding to 3, 5, 7, and 9-day lead times were downscaled using WRF followed
by VIC hydrological modeling, resulting in the forecasted inflow into the dam over 16-day lead
time as plotted in Figure 4.10 (a) (only three lead times shown for clarity). The forecasting skill
increases with shorter lead time, although there are slight overestimations. The respective
optimized elevations using the actual GFS forecast optimization runs are plotted in Figure 4.10
(b).

63
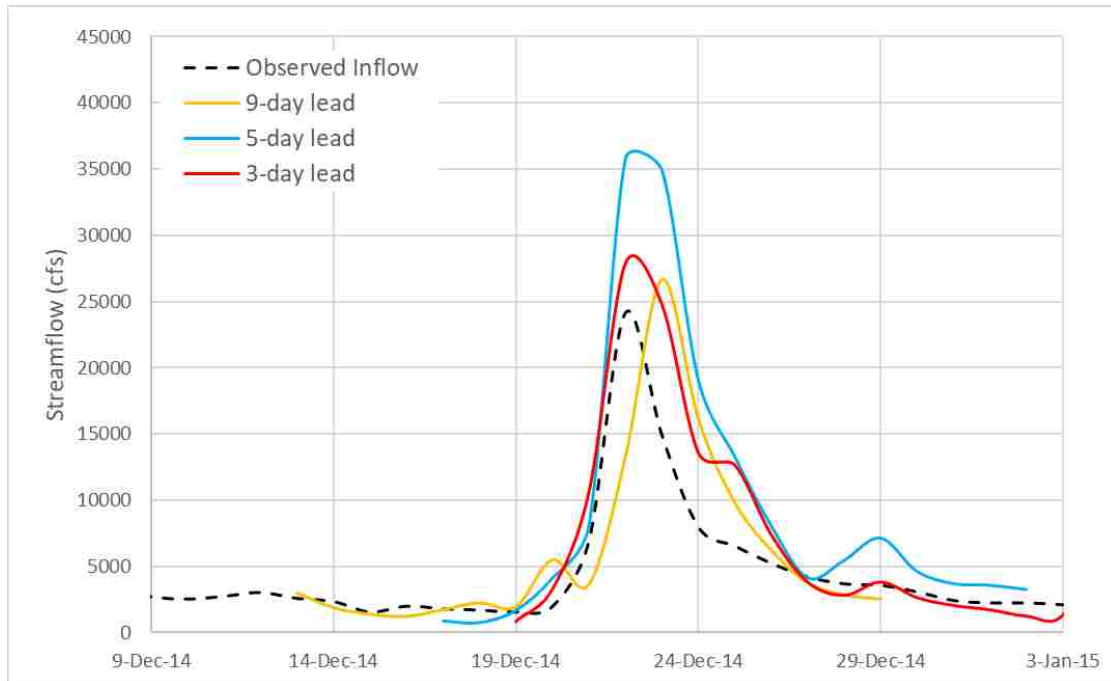
(a)
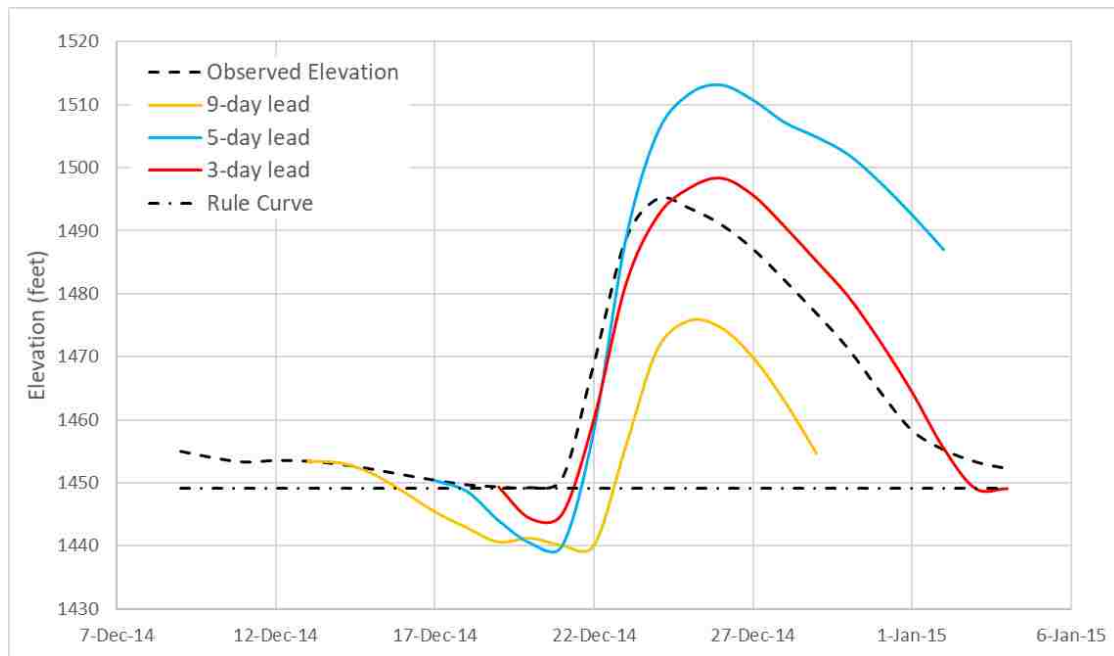
(b)

Figure 4.10. (a) Forecasted inflow at different lead times of forecast; (b) Optimized reservoir

elevations for different lead times, using actual GFS forecasts (Detroit dam, OR)

64

The resulting optimized release policy from one-time actual forecasts was evaluated by calculating the hydropower benefits (a) using the WRF forecast inflow (*actual forecast benefits*), and (b) using the actual observed inflow as input to the reservoir system (*realized benefits*), as plotted in Figure 4.11. The respective benefits from control run (*perfect forecast benefits*) and those from observed operations (*no optimization*) are also shown alongside. The methods of obtaining the various benefits are summarized in Table 3.3.
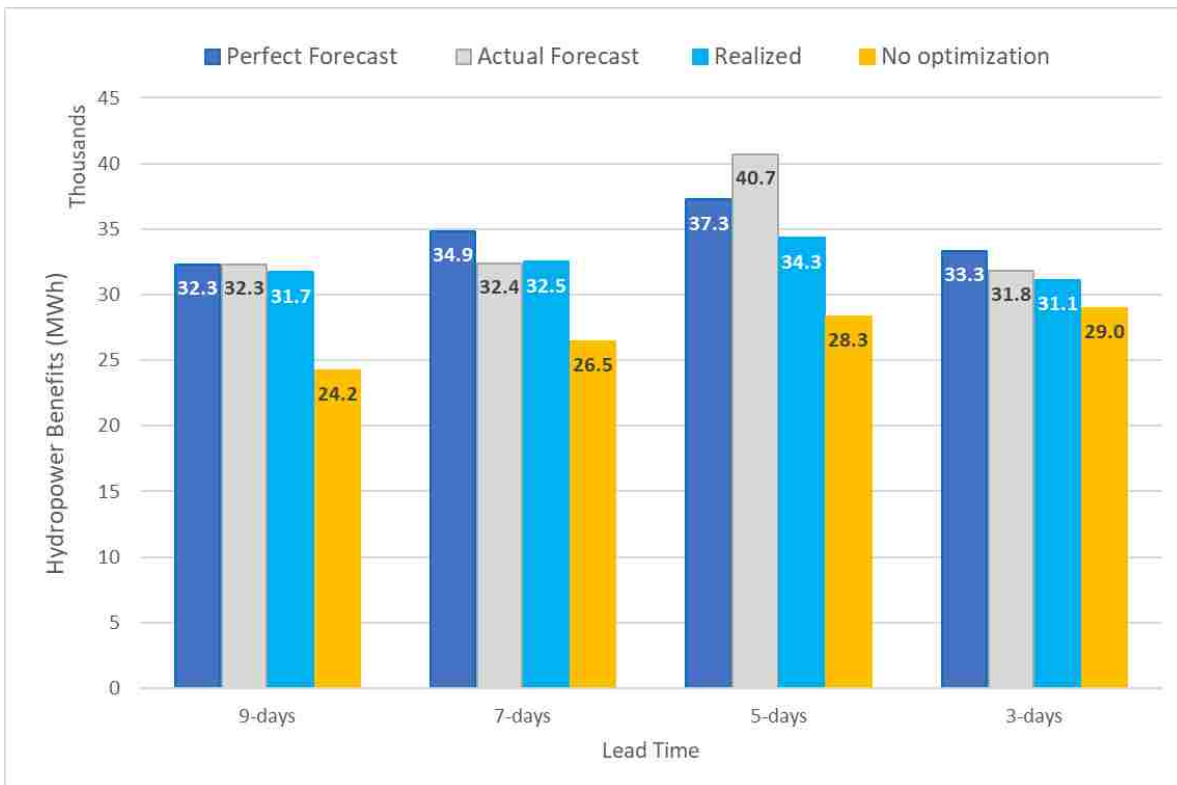
(a)
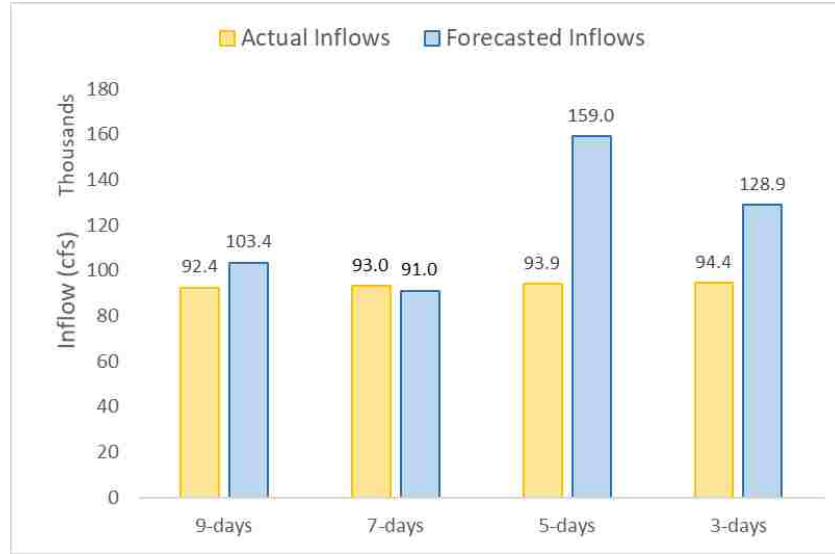
(b)

Figure 4.11. (a) Comparison of the various hydropower benefits obtained using control run and actual forecast run (one-time forecasts) along with those obtained from operations with no optimization (b) Total actual and forecasted inflow over optimization period (Detroit dam, OR).

The benefits from the control run (*perfect forecast benefits*) set the benchmark for the hydropower benefits that cannot be exceeded practically. However, when the actual one-time WRF forecasted inflow is used to estimate the hydropower benefits, the under/overestimation of the forecasted inflow peak due to uncertainties in the forecast cause the benefits (*actual forecast benefits*) to exceed the benchmark. For instance, due to the peak inflow being overestimated with 5-day lead forecast from WRF, the additional hydropower obtained from actual forecast run is higher than what the control run results into. This is certainly not practical and only representative of the effect of uncertainties in forecast over the resulting optimized release policy, where the difference in the *perfect forecast* and *actual forecast benefits* (first two bars) is the measure of the forecast skill. The truer evaluation of the benefits from one-time actual forecasts (*realized benefits*)

66

is achieved by routing the actual inflow instead of the forecasted one, with the reservoir storage calculated accordingly using the actual inflow. The *realized benefits*, as can be observed from Figure 4.11 (a), do not exceed the *perfect forecast benefits*. Further, for the 7-days lead time, where the *realized benefit* is slightly higher than the *actual forecast benefit*, the corresponding total forecasted inflow over the optimization is lower than the actual observed inflow, as shown in Figure 4.11 (b). This generates a higher power (and hence higher realized benefit) when the actual inflow is passed, as compared to when the lower forecasted inflow is used. The effect of lead time on the derived benefits can be assessed by comparing with those obtained from operations without any optimization (*no-optimization benefits*). The difference between the *realized* and *no-optimization benefits* are 7469, 6031, 5970, and 2132 MWh for lead times of 9, 7, 5 and 3-days, respectively. This suggests that the additional benefits go down with smaller lead times, owing to the lesser flexibility in operating the reservoir on approaching the peak inflow event. Also, the tradeoff in lead time needs to be mentioned, where with the increase in the realized benefits obtained with higher lead times, the corresponding forecast skill goes down (higher difference between first two bars). The daily optimization plots for observed and optimized release and elevations for each lead time for control and actual forecast runs are shown in Appendix B.

4.1.2.3   Real-time Sequential Run

Instead of doing multiple runs for different lead times, this scheme sequentially updates the inflow into reservoir with WRF-downscaled GFS forecasts every alternate day, running the optimization every day for 16-day period. This provides with a more dynamic and close to real-time scheme to be followed by a dam operator for operational purposes. For Detroit dam, this is tested on the same Dec 2014 event, with the optimization starting at 11-days lead on 11 Dec (the peak occurs on 22 Dec). The reservoir release procedure is obtained optimizing for the downstream stakeholder

benefits over 16 days using the corresponding forecast information. The resulting procedure is followed for two days (i.e. 11 and 12 Dec), following which an update to the inflow forecasts is made by running the forecast model again on 13 Dec. The optimization is performed again, this time the initial storage being that obtained from the optimized procedure of 11 Dec. Thus, the second optimization run is done based on new inflow forecasts of 13 Dec making subsequent changes to the optimized release procedure.

The sequential updating of inflow forecasts is continued every alternate day till 19 Dec (3-days lead) to result in the optimized release policy over the course of the event, as shown in Figure 4.12. The actual observed outflow and reservoir elevations were compared with the respective optimized parameters. While the releases and elevations from 11-19 Dec are obtained by sequentially updating the forecasts, the values after 19 Dec are obtained from the optimization performed using the forecasts of 19 Dec. Observed inflow is also plotted alongside to show the timing of peak inflow event.

As can be observed from Figure 4.12, the optimized operations result in higher power release as soon as the peak inflow is forecasted, due to which the reservoir levels drop down within dam's safety limits, and surges as the peak hits the reservoir. The elevation at the end of the optimization period is brought closer to the rule curve specified level, closer than what the observed operations (without optimization) resulted in. A total additional hydropower benefit (*sequential net benefit*) of 9,820 MWh was obtained from 11 Dec to 23 Dec (before and during the peak inflow event) over which the sequential updates to the inflow forecasts were made, as shown in the plot of Figure 4.13, highlighting the daily benefits of sequential optimization over observed operations.
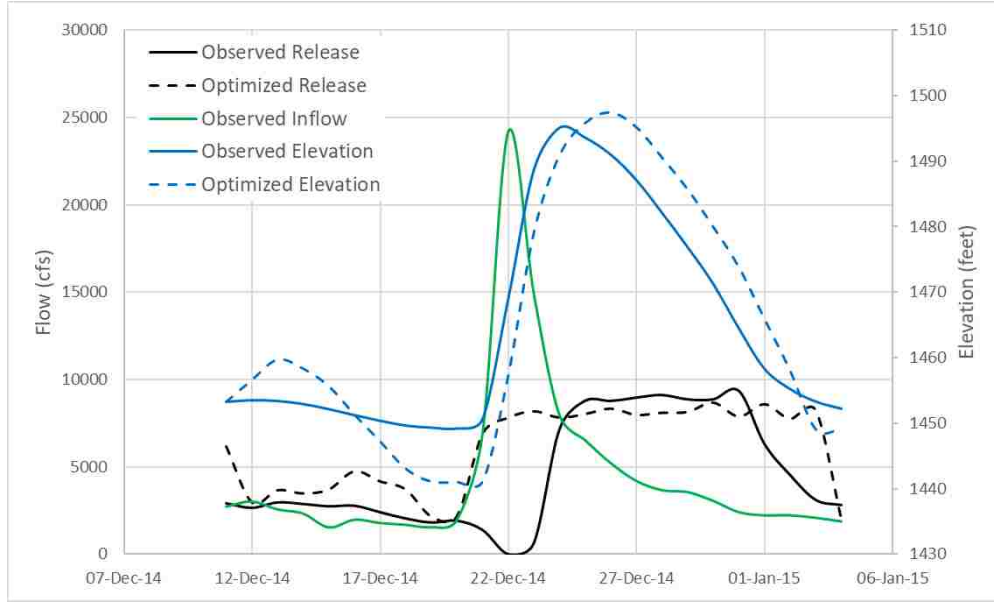
Figure 4.12. Optimized releases and elevations along with the respective observed variables

obtained using real-time sequential run, updating forecasts every alternate day from 11 Dec to 19

Dec, optimized over 16-day period (Detroit dam, OR)
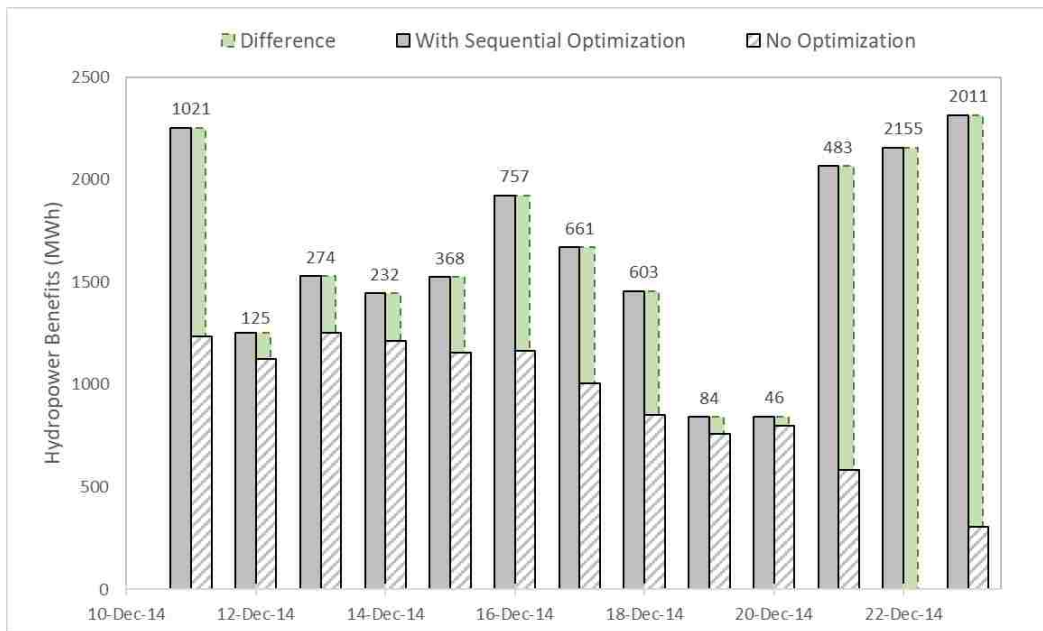
Figure 4.13. Daily comparison of hydropower benefits (MWh) obtained using observed

operations (no-optimization) and from sequential optimization (Detroit dam, OR). Green bars

and the corresponding values show the difference in benefits from the two strategies.

69

Overall, this strategy asserts that the optimization, when performed by sequentially updating the inflow forecasts, can result in significantly higher benefits as compared to what the dam operations would result in when operated without any optimization, and without compromising the flood risk during or after the peak inflow event.

4.2   CASE 2: PENSACOLA DAM

4.2.1   *Dam Logistics*

The Pensacola dam, commissioned in 1941, is a part of the 125-megawatt (MW) Pensacola Hydroelectric Project issued by The Federal Energy Regulatory Commission (FERC) to the Grand River Dam Authority (GRDA). Headquartered in Vinita, GRDA is Oklahoma's state-owned electric utility. The Pensacola project consists of a dam, two auxiliary spillways, an intake structure, and a powerhouse containing six turbine generator units with the nameplate capacity of 120MW [Pensacola Project, 2008]. The main spillway section is controlled by 21 Tainter gates each 36 feet long by 25 feet high. GRDA shares operations with the USACE as part of a basin wide system of flood control and navigation projects. When water levels exceed or are anticipated to exceed 745 feet on Grand Lake O' the Cherokees, the USACE control the amount of water to be released through the floodgates. Once the lake level drops to 745 feet, GRDA once again assumes control over releases. The flood storage is provided between elevations 745 and 755 feet, while the top of the conservation pool varies with seasons. Further details along with the dam logistics are shown in Figure 4.15 and Table 4.3. The storage elevation relation is shown in Figure 4.15, and the corresponding values for storage and elevation are shown in Appendix A.
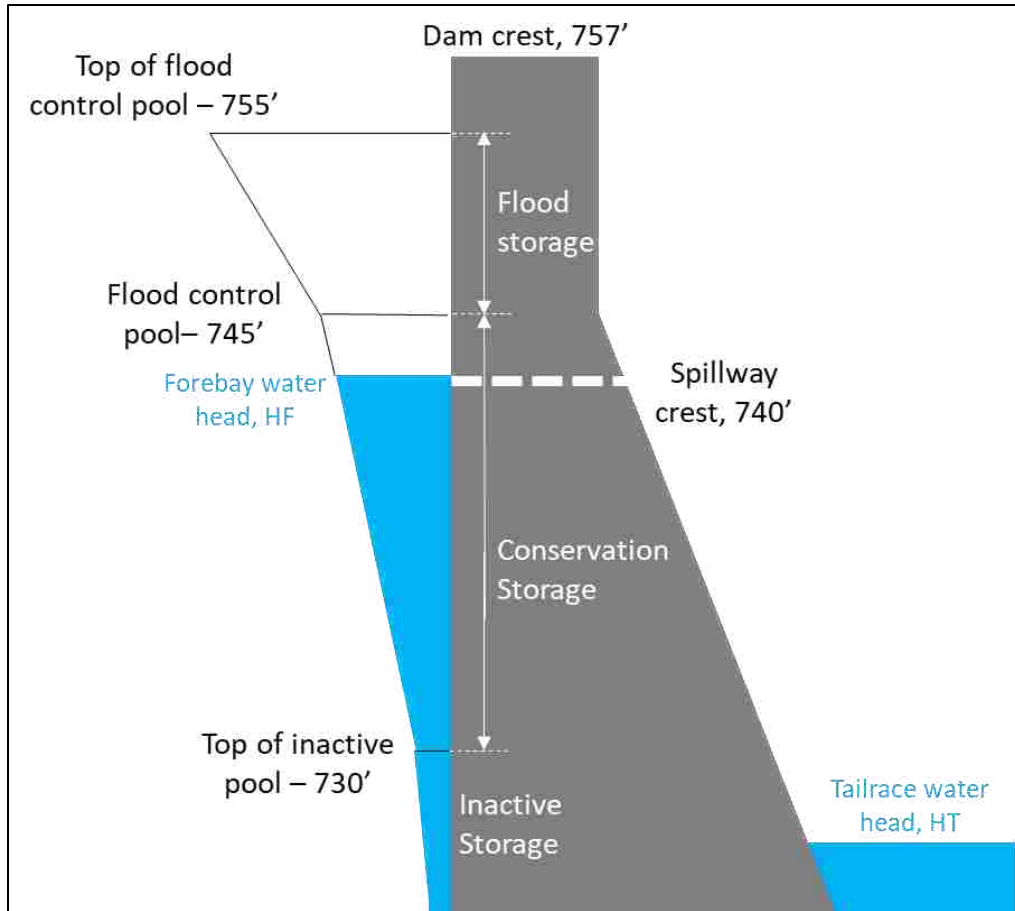
Figure 4.14. Cross-section of Pensacola dam (not to scale) showing relevant elevations (from

mean sea level, MSL)

Table 4.3. Pensacola Dam logistics

Year of completion	1940
Drainage Area	10,293 sq. miles
Dam Height	147 feet
Turbines	Six 20 MW Francis type (total 120MW)
Turbine Capacity	12,000 cfs
Spillway Gates	21 Tainter gates (36' x 25'), 2 auxiliary spillways
Spillway Capacity	525,000 cfs
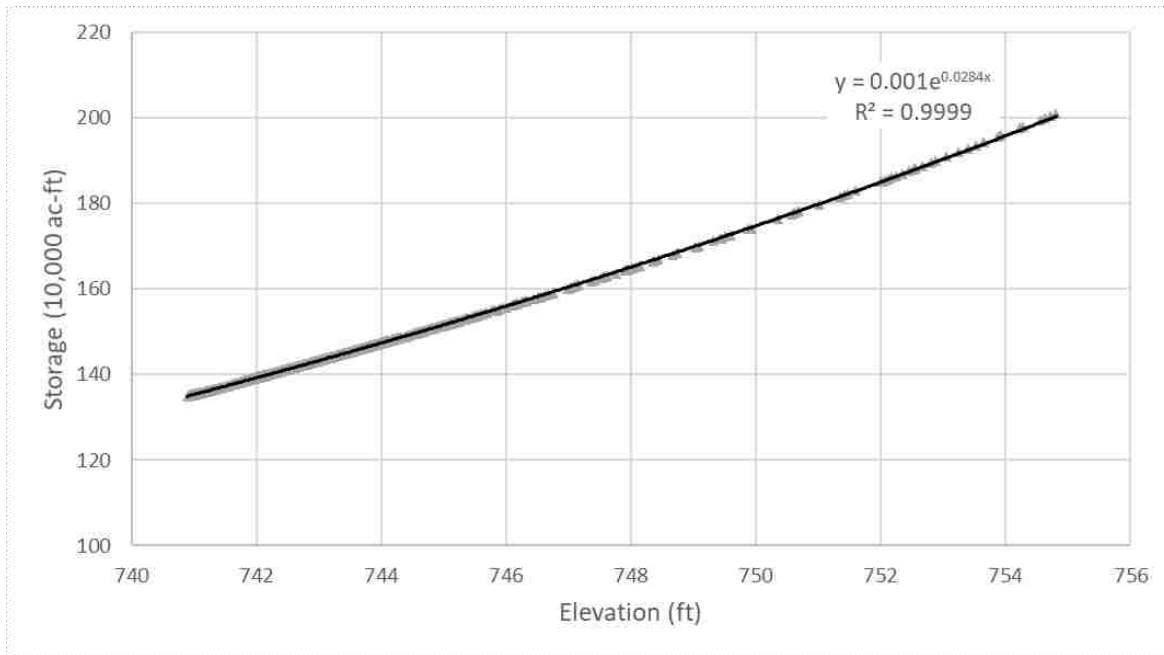
Figure 4.15. Storage-elevation relation for the Pensacola dam using the data from 2000-2015

The original rule curve that the dam was following since the development of control manuals has been recently subjected to a change. The Federal Energy Regulatory Commission (FERC) has approved the GRDA's request for an amendment to the current operating policy for operating Pensacola Dam over the Grand Lake. Under that amendment, GRDA will no longer be required to lower the Grand Lake from 744 feet to 741 feet beginning in mid-August ["GRDA - FERC", 2017], as it was supposed to do until now, as shown in Figure 4.16. As stressed by GRDA, the lowering of the lake by three feet caused recreational safety problems, as well as impacted negatively on the area's economy during a popular summer boating holiday, considering boating and other recreational activities. Instead of lowering the lake from an elevation of 744 feet to 741 feet, the amendment means the lake will only be brought to 743 feet through mid-September, before dropping to 742 feet for the fall and winter months. This amendment will remain in place throughout the remainder of GRDA's existing license, which runs through March 2022.

72
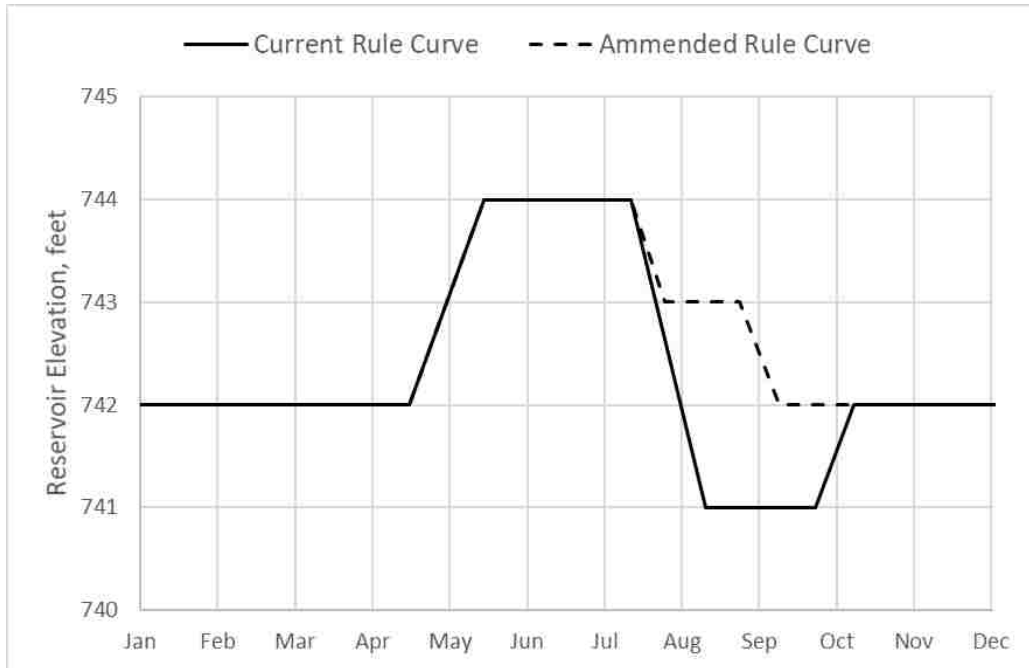
Figure 4.16. Current and amended rule curves (starting Aug 15, 2017) for Pensacola Dam as per
GRDA request for amendment

As the amendment has affected the operations in August and September, while the present
study considered the event that occurred in December, the results of optimization will still be
applicable with the new operational procedure in place. As mentioned by GRDA Chief Executive
Officer, the organization is still seeking a long-term solution to the lake level issue to provide more
operational control over the lake, while balancing all the other stakeholder concerns of
hydroelectric generation, flood control and recreation. This study provides a possible alternative,
delineating the advantages to multiple stakeholders as demanded by the stakeholder agencies.

4.2.2   *Optimization Model*

The optimization constraints for Pensacola dam are summarized in Table 4.4, obtained, similar to
that for Detroit dam, using the actual data from USACE. For the maximum total release, the

73

threshold was obtained by finding the corresponding flood-safe value of streamflow at the downstream USGS station of Neosho River (site ID - 07190500). Also, the spillway capacity was used to limit the rate of the non-power release, thus limiting the speed with which the reservoir levels can go down.

Table 4.4. Constraints for Optimization for Pensacola dam, OK

Constraint	Value
Turbine Capacity	12,000 cfs
Spillway Capacity, $Spill_{max}$	525,000 cfs
Minimum storage limit, S_{min}	126,500 ac-ft (95% of 10-yr minimum)
Maximum storage limit, S_{max}	2,021,679 ac-ft (flood control pool)
Maximum total release, R_{max}	30,000 cfs (avoid flooding at Neosho River downstream)
Environmental flow limit, Q_{env}	4500 cfs

With this optimization model setup, the respective schemes of optimizing the operations (see section 3.5.1) are investigated below.

4.2.2.1   Control Run

The control run was performed over one of the peak inflow events over Pensacola dam in March 2012. This event lasted for 3 weeks and the inflow peak began in 20 March 2012. The peak inflow was 82,350 cfs on 22 March, being the highest in 2012. There was significant precipitation observed over and around the Pensacola dam during this period. The rainfall obtained from Livneh data for 19-21 March is shown in Figure 4.17 below, with the drainage basin of the dam marked in red.

Livneh Prec in mm for Mar 19 2012

Livneh Prec in mm for Mar 20 2012

75
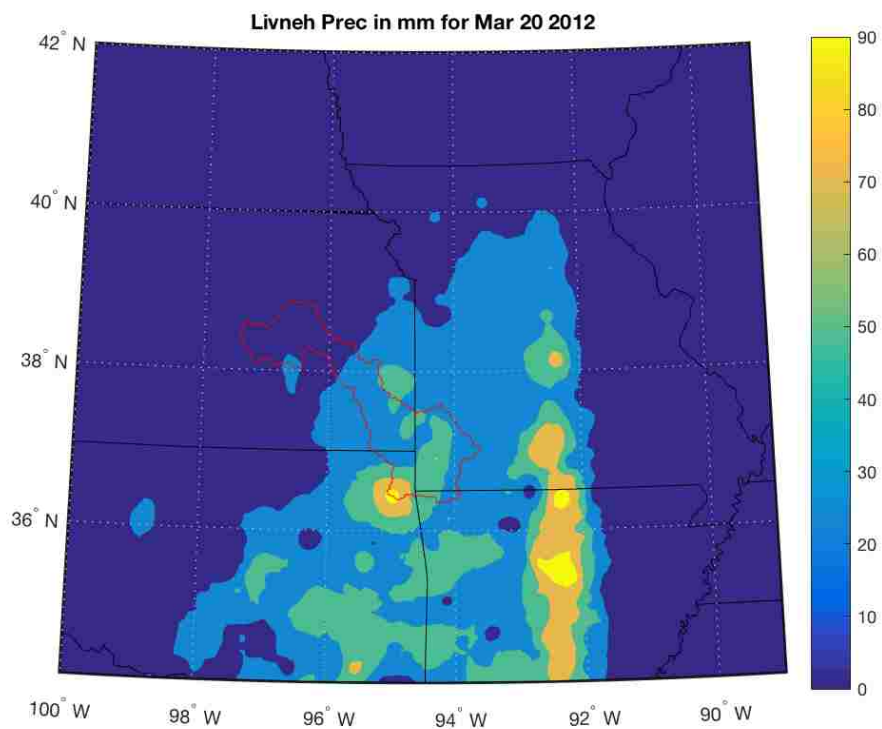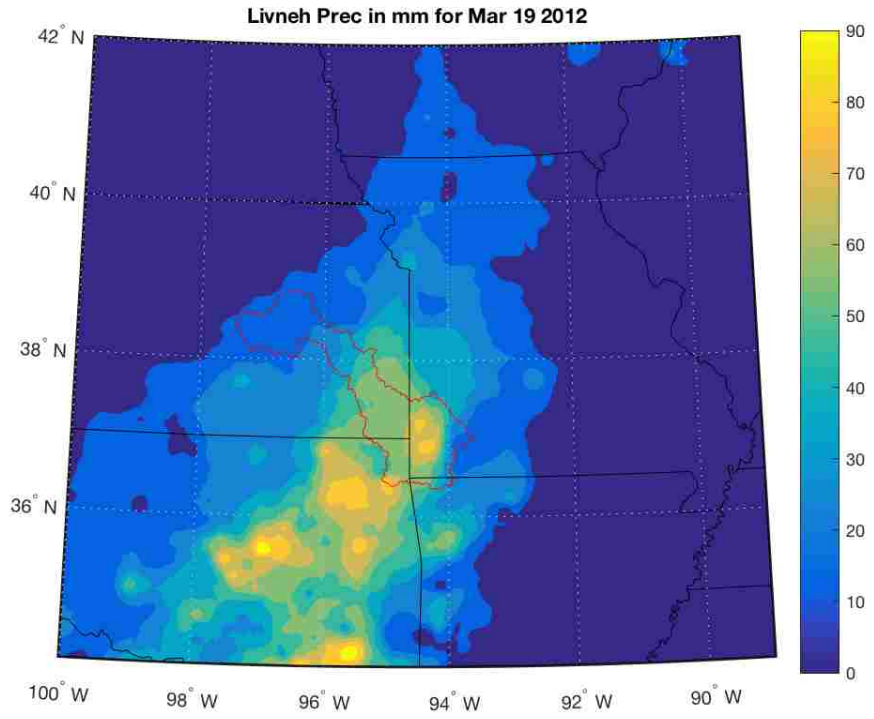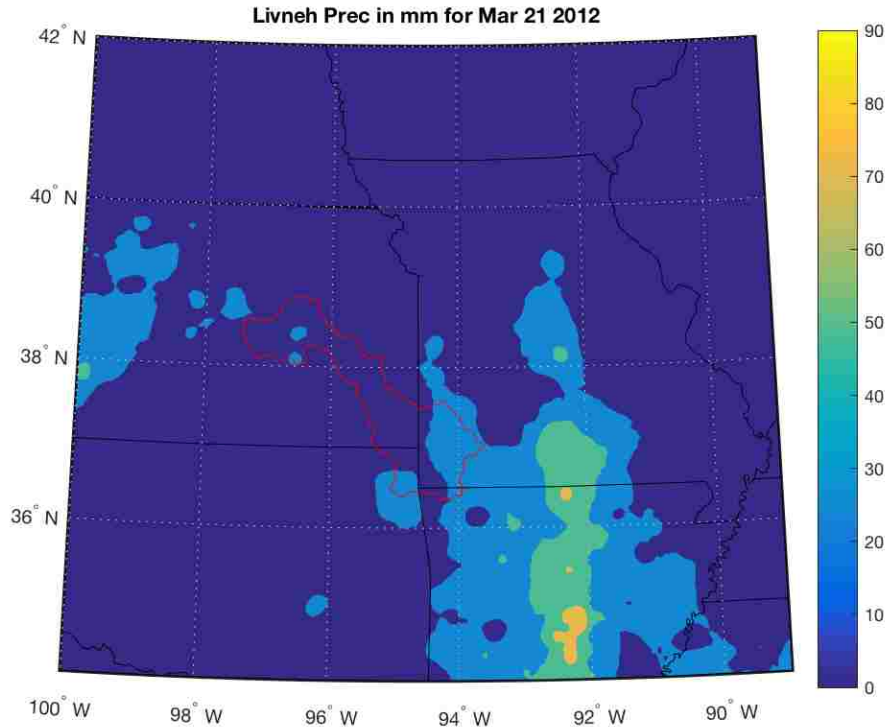
Figure 4.17. Livneh precipitation (mm) plotted over the region surrounding the Pensacola dam. Drainage boundary of dam is shown in red.

Four different scenarios of 3, 5, 7 and 9-days lead were tested for based on when the peak inflow is forecasted to study the effect of lead time. As the actual hydropower data (MWh) is not provided on USACE data portal, a conversion factor from MW to MWh for the hydropower production could not be obtained, in order to take into account the turbine efficiency and average operating hours. Hence, a value of 20 hours was assumed, chosen close to that of Detroit, as both the dams have similar installed hydropower capacities. The respective optimized reservoir elevations are shown in Figure 4.18 (three lead times shown for clarity).

76
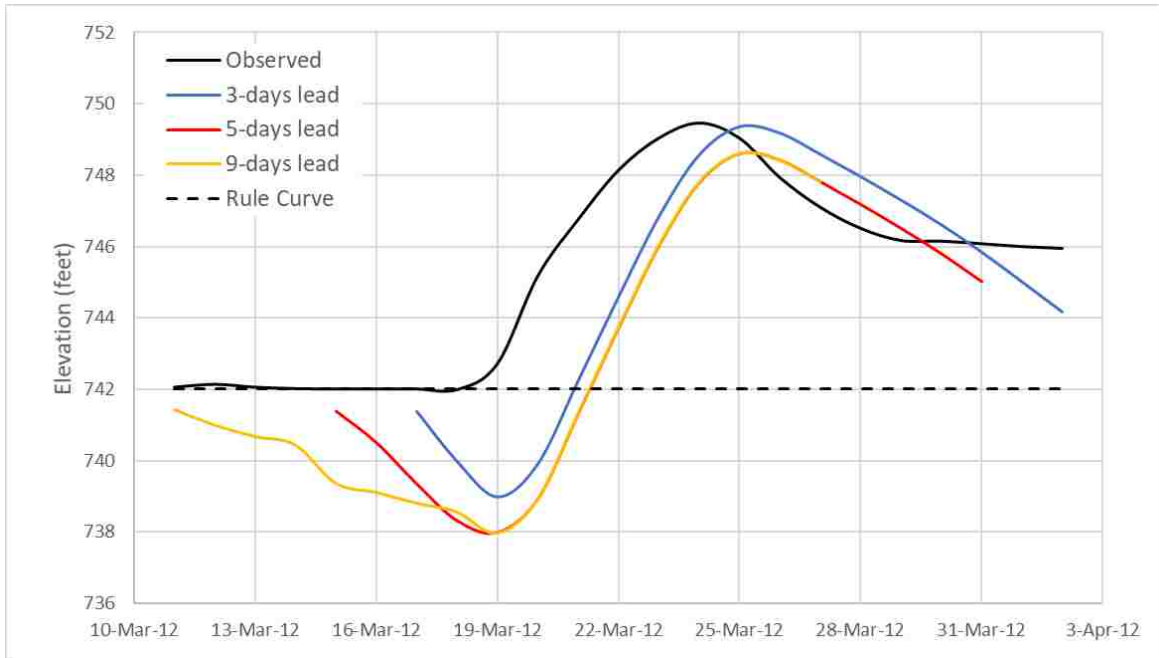
Figure 4.18. Optimized reservoir elevations for different lead times of forecast, under control run

assuming perfectly accurate forecasts (substituting the forecasted inflow with observed inflow)

(Pensacola dam, OK)

4.2.2.2 Actual Forecasts Run

Next, actual GFS forecast runs were tested for each of the four lead time scenarios. GFS forecasts

on four different days corresponding to lead times of 3, 5, 7, and 9-days for the inflow peak of 20

March, were downloaded for the forecasting followed by VIC hydrological modeling. This

resulted in forecasted inflow into the dam over 16-day lead time as plotted in Figure 4.19 (three

lead times are shown for clarity). The resulting optimized elevations found using the optimization

strategy are shown in Figure 4.20.
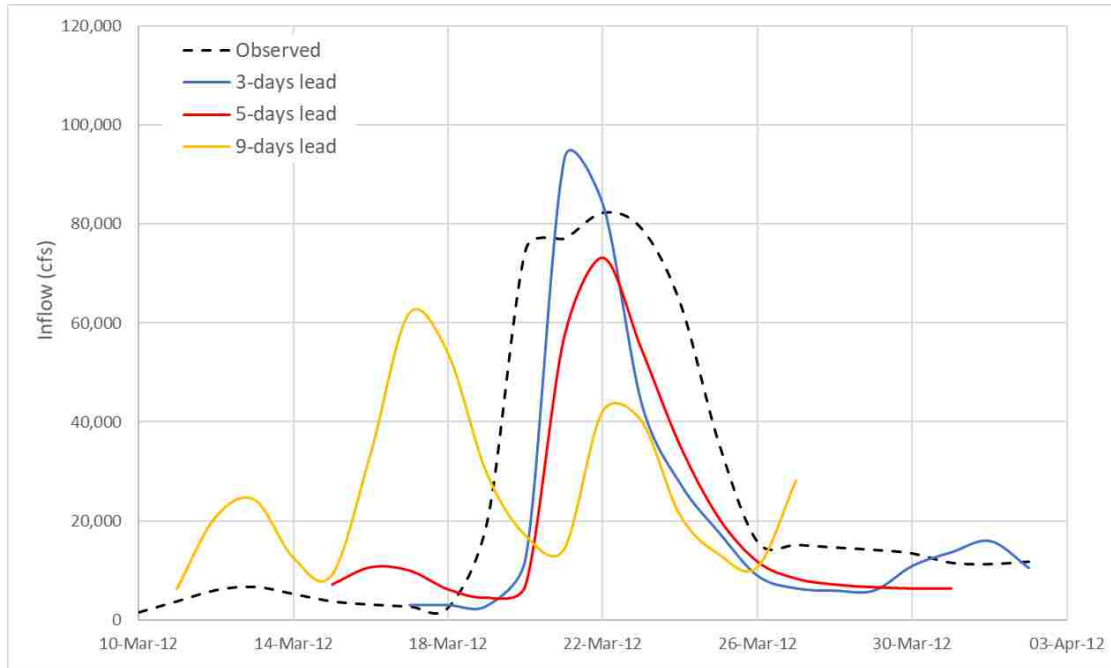
Figure 4.19. Forecasted inflow into dam over 16-day lead time using actual WRF-downscaled

forecasts produced on three different lead times from 11th to 17th March (Pensacola dam, OK)
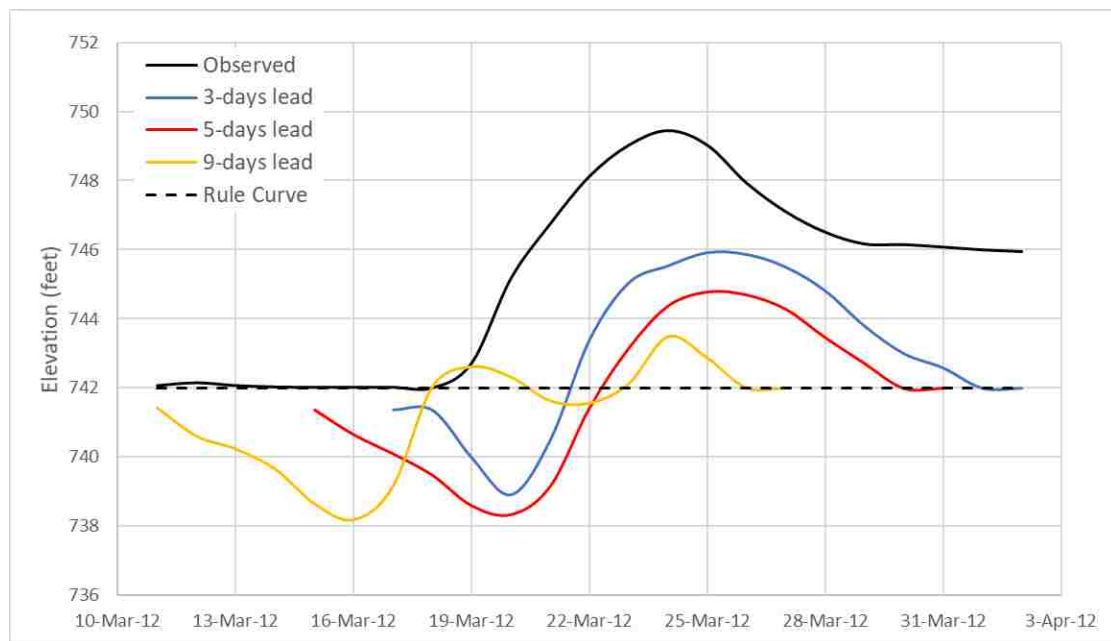
Figure 4.20. Optimized reservoir elevations for different lead times of forecast, using actual

WRF-downscaled forecasts (Pensacola dam, OK)

The plot above in Figure 4.20 shows that the optimization strategy results in an elevation closer to the rule curve at the end of peak event, and with increasing lead time of forecast, the rule curve-specified level is reached earlier.

The evaluation of the actual forecast run and control run was performed, similar to that for Detroit dam, using four different hydropower benefits as specified in Table 3.3. The respective benefits are shown in Figure 4.21.
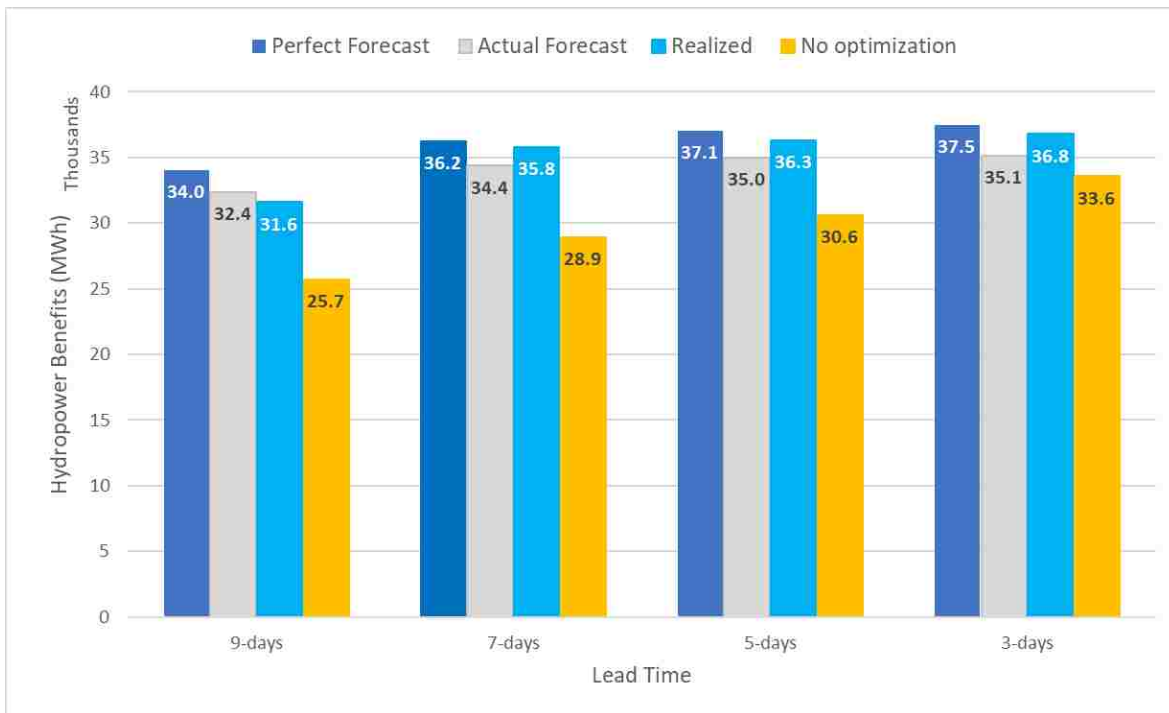
(a)
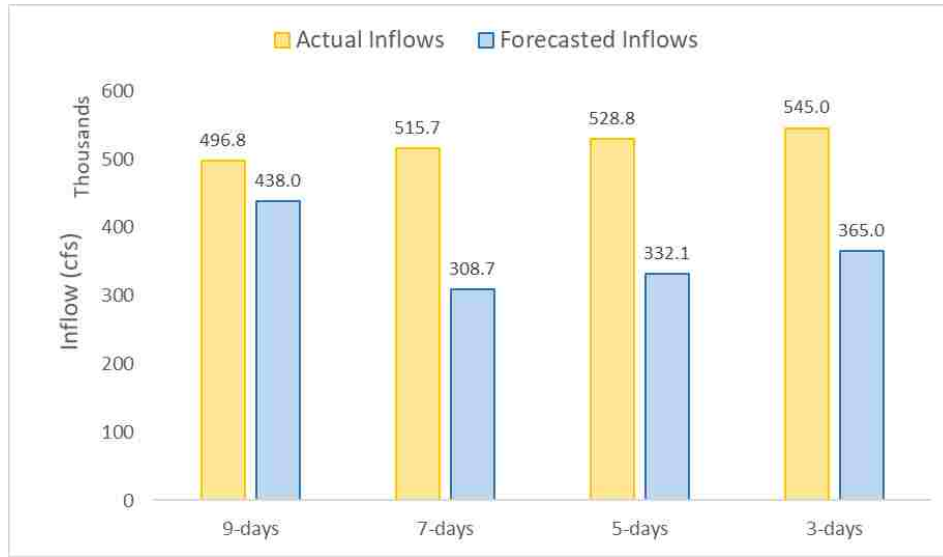
(b)

Figure 4.21. (a) Comparison of the various hydropower benefits obtained using control run and actual forecast run (one-time forecasts) along with those obtained from operations with no optimization (b) Total actual and forecasted inflow over the optimization period (Pensacola dam, OK).

In the plot above, the benchmark for the practically obtainable benefits is set by the benefits from the control run (*perfect forecast benefits*). While the *actual forecast benefits* do exceed this benchmark, owing to the overestimated inflow peak from WRF based forecasts, the more realistic evaluation of the benefits was performed by using the actual inflow instead of the forecasted one (*realized benefits*), which are limited by the benchmark of *perfect forecast benefits* for all the lead times. The difference between the perfect forecast and actual forecast benefits (first two bars) decreases with smaller lead times, signifying the corresponding increase in forecast skill. Also, the higher realized benefit relative to the actual forecast benefit is due to the total forecasted inflow being lower than the corresponding observed inflow thus generating higher power (and hence higher realized benefit) when the actual inflow is passed. The additional realized benefits

80

(difference between the *realized* and *no-optimization benefits*) are 5856, 6862, 5700, and 3212 MWh for lead times of 9, 7, 5, and 3 days, respectively. This decrease in benefits, like for Detroit dam, reflects the associated tradeoff of the higher forecast skill and reduced benefits with smaller lead time of forecasts. The daily optimization plots for Pensacola dam for observed and optimized release and elevations for each lead time using the control and actual forecast runs are shown in Appendix B.

When compared to Detroit dam, the WRF model's performance for Pensacola dam is better as the difference between the actual forecast and control forecast benefits in Figure 4.21 are smaller. This could be explained by the fact that the reservoirs with smaller storage capacity are more prone to forecast errors as found in the study by Zhao et al. [2011].

4.2.2.3   Real-time Sequential Run

Like Detroit dam, instead of doing multiple runs for different lead times, this scheme is sequentially implemented to update the inflow into reservoir with actual WRF forecasts every alternate day. For Pensacola dam, this is tested on the March 2014 event, as described above, with the optimization starting from 11 March for the peak inflow starting from 20 Mar (9-days lead). First, the reservoir release procedure is obtained using 11 March forecast data for 16-days lead time, optimizing the reservoir elevations for hydropower and flood control over 16 days using the corresponding sequentially updated WRF-based forecasts. This resulting procedure is followed for two days (i.e. 11 and 12 March), following which an update to the inflow forecasts is made by running the forecast model on 13 March. The optimization is again performed, this time the initial storage being that obtained from the optimized procedure of 11 March. Thus, the second optimization run is done based on new inflow forecasts of 13 March and subsequent changes to optimized release procedure are made accordingly.

81

The sequential updating of inflow forecasts is continued for every alternate day till 17 March (3-days lead) to result in the optimized release policy over the course of the event, as shown in Figure 4.22. The actual observed outflow and resulting reservoir elevations were compared with the respective optimized parameters. Observed inflow is also plotted to compare with the timing of peak inflow event.
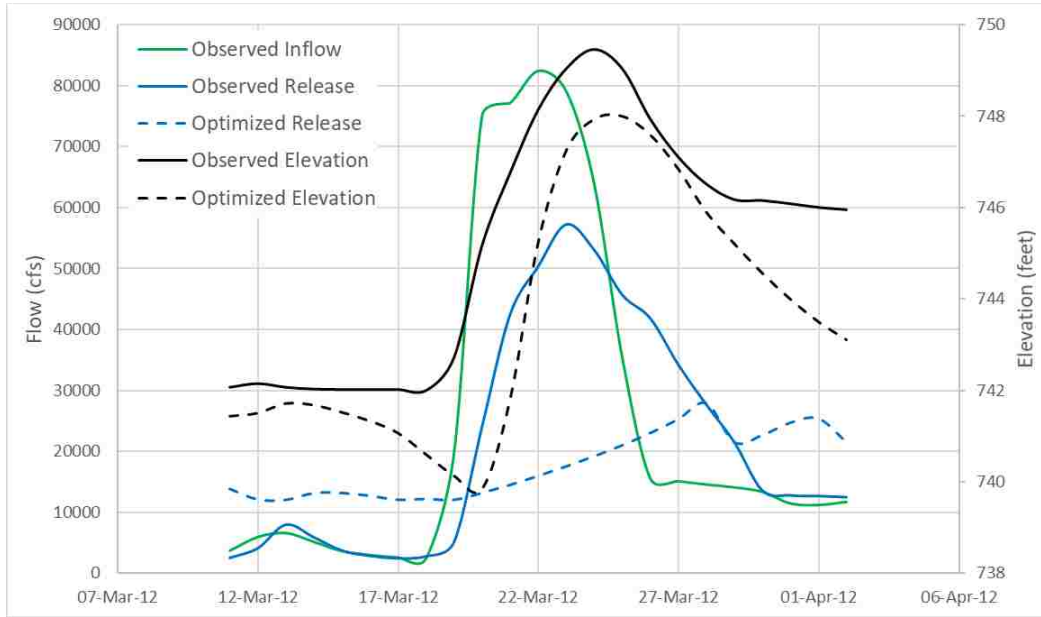
Figure 4.22. Observed inflow, releases, and elevation along with the respective optimized variables obtained using real-time sequential run, updating forecasts every alternate day from 11 March to 17 March, optimized over 16-day period (Pensacola dam, OK).

The plot in Figure 4.22 suggests, the optimized release starts to increase as soon as the peak inflow is forecasted from WRF-downscaled forecasted inflow on 11 March and keeping it to the maximum, satisfying the flood control bounds. The resulting elevation decreases due to this enhanced release until the peak inflow hits the reservoir, after which there is a sudden increase in reservoir elevation. Like the results for Detroit dam, the ending level at the end of optimization period was brought closer to the rule curve specified level, closer than what the observed

82

operations (without optimization) resulted in. Considering the daily hydropower benefits before and during the peak inflow event, total additional benefit *(net sequential benefit)* of 13,048 MWh was obtained from 11 to 24 March, where additional benefit refers to the difference in hydropower benefit obtained from sequentially optimized operations (passing actual inflow with optimized releases) and the corresponding observed operations. The daily hydropower benefits over this period are compared in Figure 4.23.
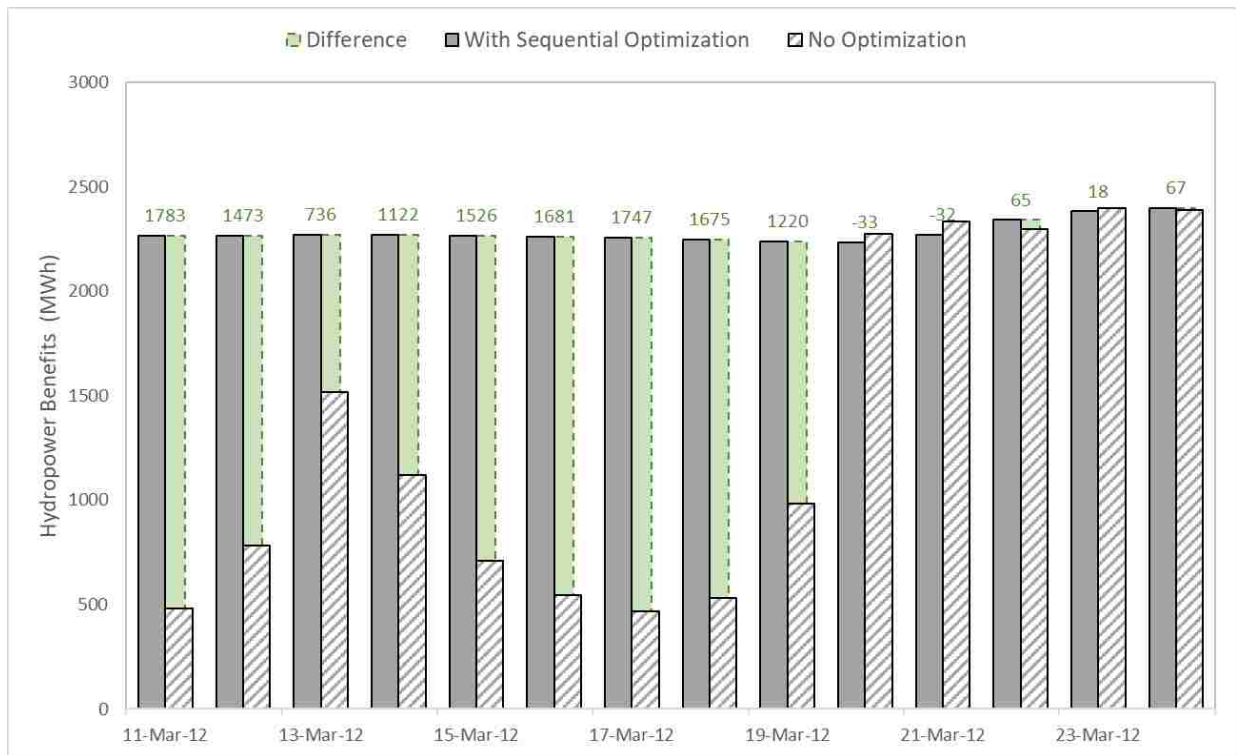
Figure 4.23. Daily comparison of hydropower benefits (MWh) obtained using observed operations (no-optimization) and from sequential optimization (Pensacola dam, OK). Green bars and the corresponding values show the difference in benefits from the two strategies.

4.3 PERFORMANCE ASSESSMENT - HYDROPOWER VERSUS FLOOD CONTROL BENEFITS

The two competing benefits of hydropower and flood control considered in the optimization need

to be satisfied simultaneously for the optimization strategy to be successful. For the Pensacola dam, during the Mar 2012 peak event, the most dynamic scheme of real-time sequential update (updating the forecasts every alternate day) results into an additional benefit (*net sequential benefit*) of 13,048 MWh over the pre-event and during event days, on top of what the operations without optimization result in. With an average retail price of 7.90 cents/kWh ["State Electricity Profiles - EIA"], the benefit amounts to $1,030,792. Also, at an average electricity consumption of 900 kWh per month per US household, this additional benefit could fulfill the demands of 14,500 households for one month. For the competing objective of flood control, the performance of optimization can be assessed from the extent to which the outflow peak is reduced during the event. For the selected event, a maximum release of 57,211 cfs was observed on Mar 23, 2012 in response to the peak event. After optimizing the operations, this maximum release was limited to 30,000 cfs as a safe threshold to prevent flooding downstream. Thus, a 47.5% reduction in the peak outflow was achieved compared to the operations without optimization. Moreover, after the peak event ends, the reservoir's forebay head was brought lower and closer to rule curve specified level, which leaves more pool for any following peak event in future and brings the reservoir back to normal operating state. Furthermore, using the one-time actual forecasts, which suffers from the uncertainties in WRF-based forecasts, additional *realized benefits* ranging from 3212 to 6862 MWh can be obtained on top of the observed benefits, depending on the lead time of forecasts. These figures translate to $253,748 to $542,098, supporting 3570 to 7624 households per month.

In case of Detroit dam, the sequential optimization resulted into an additional hydropower benefit (*net sequential benefit*) of 9,820 MWh from 11 Dec to 23 Dec (before and during the peak inflow event) over which the sequential updates to the inflow forecasts were performed. This additional energy amounts to $859,250 over 13 days of optimization, using an average retail price

of 8.75 cents/kWh for the state of Oregon ["State Electricity Profiles - EIA"]. This amount can light up to 10,911 US households for a single month considering the average electricity consumption rate same as for Pensacola dam. Further, the flood control objective was also satisfied, as the maximum total of 24,170 cfs was reduced by 63% to only 9,000 cfs, which was set as the threshold for downstream flood control. Furthermore, similar to the case of Pensacola dam, reservoir levels were brought closer to what the rule curve specifies, closer than the operations without optimization would have resulted into. The actual one-time forecast runs produce *realized benefits* ranging from 2132 to 7469 MWh ($186,550 to $653,540) depending on the forecast's lead time. Further, for the major flood event of 1996 (for which only the control run was performed due to absence of forecast data), the optimization using control run produced an additional benefit of 5,000 MWh to 10,000 MWh (depending on lead time of forecast), amounting to $437,500 to $875,000 over the flood event, and reducing the peak inflow of 48,300 cfs by 81% to only 9,000 cfs. Thus, the proposed optimization strategy is able to address both the competing objectives to a reasonable extent.

85

Chapter 5. DISCUSSION, CONCLUSION AND RECOMMENDATIONS

5.1 DISCUSSION AND CONCLUSION

In this present research, the potential of weather forecasts has been dynamically evaluated for the optimization of reservoir operations based on maximizing the hydropower production, without compromising other competing objectives. The short-term weather forecast model, hydrologic model, genetic algorithm optimization and reservoir operations model were synergistically employed to result into optimized reservoir operating policy over short-term forecast period. To demonstrate the concept, two dam sites of small to medium storage receiving unregulated inflow were selected. Short-term weather forecasts from the Global Forecast System (GFS) data, dynamically downscaled by Weather Research Forecasting (WRF) Model, were used to forecast the reservoir inflow. This resulting forecast inflow information was used to the optimize reservoir operations aimed at maximizing hydropower with flood control, environmental flow and dam safety as key constraints. One of the contributions of this study is recommendation of a new forecast evaluation framework for application to reservoir optimization. Typical measures that are used for forecast evaluation include correlation, RMSE, etc., while we propose the flood peak reduction and daily hydro power additional benefits, which are more effective in minimizing the flood damages and realizing higher hydropower benefits.

The study reveals that there indeed exists potential for optimizing the reservoir operations over short-term duration using weather forecasts. The critical factor that plays a key role in optimizing the operations is the lead time of forecasting the peak inflow. As the lead time increases, there is a higher uncertainty associated with forecasts [Zhao et al., 2011], leading to more uncertain operations that risk-averse dam operators will try to mitigate. For such high lead times, the dam

operator is likely to operate the dam based on the rule curves rather than just relying on the forecast inflow information. Thus, there exists a tradeoff between the benefits that can be extracted by predicting the reservoir inflow ahead of time and the confidence with which such a prediction can be made. The short-term optimization, being the focus of this study, relies on the downscaling of the coarser GFS forecasts, thus limited to a period of 16-days. For the actual forecast run strategy of optimization (when no updates are being made to the inflow forecasts), the 7-10 days' lead time of forecasts is the optimum, considering tradeoff between stakeholder benefits and loss in forecasting skill. While the control run and actual forecast run validate the tradeoff (forecast skill versus benefits) associated with the lead time of the forecasts, the sequential optimization tries to overcome the limitation of under/overestimation in forecasts by updating the forecasted inflow every alternate day, thus assimilating with the best available information at hand. For Pensacola dam, an additional revenue of $1,030,792 was obtained from sequential optimization, while for Detroit dam, the figure amounts to $859,250, which is significant as the optimization policy has been demonstrated over just a single peak inflow event and there are usually more than one such occurrences (although the magnitude of other peaks is smaller) over the late winter and spring season, during which the uncertainty of the events are high, more so with the climate change playing its part. The outflow peak has also been reduced significantly as compared to what resulted from the observed operations (without optimization). Further, the reservoir state at the end of peak event was brought closer to the rule-curve specified level, leaving out more pool for any future peaks hitting the reservoir and bringing the reservoir back to normal level of operation.

Further, the contrast in the shape of the drainage basins for Detroit and Pensacola dams (smaller for Detroit with fast response in contrast to the narrower and much larger for Pensacola with slow hydrologic response) reveal interesting insights into how the reservoir characteristics

87

affect the resulting operation policies from short-term forecast information. As Detroit dam lies at higher elevation and in mountainous region with steep slopes, the rainfall occurring over the basin quickly turns into runoff, with a lesser time of concentration. This leads to lower forecast horizon, with the accuracy of resulting forecast streamflow dictated mainly by the atmospheric forecast skill, and with lesser dependence on the performance of the hydrologic model. However, in case of Pensacola dam, due to its narrower drainage basin with longer rivers, the basin possesses higher time of concentration with slower hydrologic response, and the forecast skill is dictated by the shape of basin in addition to atmospheric forecast skill. With a longer forecast horizon and a good hydrologic model setup, the peak inflow is forecasted more accurately and the resulting optimized policy from the forecasts is closer to that obtained using the perfectly accurate forecasts scenario. Thus, the shape and size of drainage basin drives the performance of optimized operation procedures, which needs to be taken into account individually for each dam.

Although, the study considered only two dams, the characteristics associated with these can cover a wide range of dams spread over the US. Detroit dam has a small surface area, but its height is one of the highest, with a modest power generation capacity. On the other hand, Pensacola dam consists of a medium surface area but with smaller height as compared to Detroit dam. However, both the dams lie upstream enough to receive unregulated natural streamflow, thus presenting a suitable case for modeling the inflow into the reservoir and subsequently optimizing the operations. In a particular year, the peak inflow events happen to occur during the late winter and spring season, and this period is the most efficient to run the optimization scheme based on weather forecasts. For operational purposes, the WRF forecasts need to be updated every day over the event to update the optimized flow release with a new WRF run in the lead up to the event. This will result in a more dynamic and realistic strategy with frequent updating of forecasts,

88

minimizing the missed and false hydropower benefits.

Considering the scalability of this particular study, although the case study was performed considering only single peak event on both the dams, the procedure of short-term optimization using forecast information can be applied to any dam over the entire CONUS that satisfies the criteria of (a) powered dam, (b) reservoir surface area of $< 200km^2$, and (c) lying upstream in the dam network, receiving unregulated flow. A quick analysis over the dams in the US revealed 525 dams that satisfy these criteria, amongst the 2248 powered dams, as obtained from the National Hydropower Asset Assessment Program's (NHAAP) Existing Hydropower Assets (EHA) dataset of powered dams. The dams lying on rivers with stream order of $1 - 3$ were assumed to be located upstream and receiving unregulated flow, where the stream order data was obtained from NHDPlus version 2 national dataset [McKay et al., 2012]. The selected dams are shown in Figure 5.1.
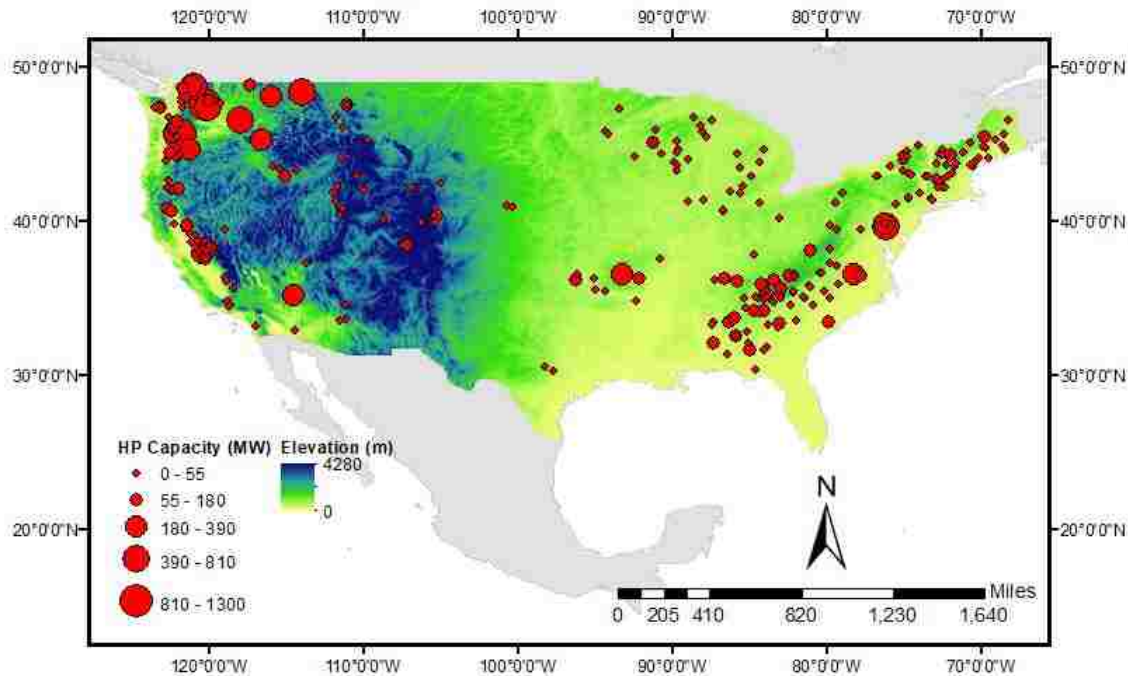
Figure 5.1. Distribution of the selected dams satisfying the necessary criteria for scalability of this study over the CONUS.

With a dynamic operational framework for the dams and reservoirs in place, a significant improvement in the hydropower production – both the firm energy and the variable non-firm energy supplied over and above it, can be obtained out of the same infrastructure that the US has built over the previous century. As most dams are used for more than just extracting hydropower, it also facilitates addressing other competing objectives of water security, flood control and pertinent environmental constraints. To increase management flexibility and efficiency, as Hamlet et al. [2002] notes, multiple energy distribution systems are frequently inter-linked. This feature is important to incorporate in case of, say, a surplus hydropower production in one state from the optimization over an extreme peak inflow event. This surplus can be supplied to other linked systems during a time of their peak demand, if not needed instantly. For instance, peak demand for electricity is seasonally reversed in the Pacific Northwest (PNW, peak demand in mid-winter) and the Southwest and California (peak demand in late summer). So, even if California does not receive enough inflow in summer, the surplus from PNW can supply the summer demand through the electric grid.

For the dams that operate with flood control as the primary purpose, there is certainly less flexibility and hydropower generation is more of an afterthought, being hardly considered during the flood events by the operating agencies. However, the current study makes an effort to persuade the agencies to be more inclusive and include the other competing benefits as well, without affecting the primary purpose of dam operation. Further, the long-term benefits of generating hydropower (every day) far outweigh the damages avoided through flood control (as floods do not happen every day). So, if the operations can extract the most out of any flood event by utilizing the additional amount of water poured in by the nature and minimizing the damages downstream,

then the operating policy can surely be considered to be efficient and sustainable, preventing the surplus water to get wasted by causing harm to the downstream lives.

Further, taking an example of the case of Pensacola dam's rule curve amendment (see section 4.2.1), even after the accepted change to operating policy, the organization is seeking a long-term solution to the lake level management issue to provide more operational control over the lake, while balancing all the other stakeholder concerns of hydroelectric generation, flood control and recreation. This is the need of hour, and is demanded by most of the operational/managing agencies of dams and reservoirs. Such manual amendments to the classically developed rule curve takes a significant amount of resource and time, making infeasible for the changes and amendments to be made in accordance with the changing climatic conditions and inflow patterns. This study provides a possible alternative, by putting forward the operations that are more dynamic and adjustable to the real-time weather patterns, and maximizing the advantages for the multiple stakeholders with competing benefits.

The far-reaching effects of this study also shed light on the more sophisticated techniques of electricity production. The recent concept of integrated hydro-powered wind mills, introduced by a German firm (as mentioned in Chapter 1), can benefit from the short-term optimization scheme. The integration of wind mill-produced electricity with the hydropower require a framework that can assimilate the information from multiple sources coming at frequent intervals and optimize the hydro- and wind-borne turbine operations accordingly. In future, the integration of electricity from multiple sources to create a synergistic framework, optimizing the operation of the sources involved therein can prove to be a landmark step towards revolutionizing the way renewable sources are utilized.

5.2 RECOMMENDATIONS AND FUTURE WORK

Through this study, a concept has been put forth for making the conventional operating policy of dam more dynamic and adjustable to the real-time and short-term forecast inflow information employing the weather forecasts. Such a dynamic operational policy could be of a great significance for the country, especially in the coming decades when environmental sustainability will play a key role in any nation's economic growth and development. A lot can be improved and built upon this demonstrated concepts from this study. Future work should include developing a better coupled hydropower-flood control optimization framework by integrating the present hydropower optimization strategy with more sophisticated flood forecasting techniques and then scaling it up for other hydropower dams that are part of regional energy infrastructure. By using real data on real dams with real-world constraints, we have demonstrated very clearly that the currently available weather forecasts from numerical weather prediction models have a lot to offer to address our nation's energy security. Because these weather forecasts are already available, the challenge now is to convert availability to accessibility so that dam operators have an additional basis of decision-making that builds on the rule curves and improves the state of the art.

The entire procedure starting from short-term weather forecasting to hydrologic modeling, optimization and reservoir operations modeling can be integrated and presented in the form of user friendly GUI as a Decision Support System (DSS). The DSS will compute every few days, the 'optimized' storage and release (power and non-powered) to maximize the stakeholder benefits for varying risk-averse constraints set by the dam operator. The future prospects of this study include developing such a DSS using Detroit dam as the starting point, and will later be generalized for 'any' small-medium dam receiving unregulated inflow in the US. Also, as deterministic forecasts were employed here for the purpose of demonstrating the utilization of forecasts,

uncertainty in forecasts is certainly a future step that needs to be considered in order for the dam operator to have a possible optimal range of operating the reservoir.

The optimization model considered here can be improved upon by including other major downstream stakeholder benefits, such as water supply, irrigation, recreational activities etc., considering the water-energy-food nexus. A year-round optimization framework could be developed, considering the different benefits pertinent to the time of year, season and weather scenario. The region of operation should also affect the optimization strategy, depending on what the downstream users are concerned with. Moreover, the forecast data can be modified in that the long-term seasonal forecasts can be included in the optimization along with the short-term GFS forecasts to produce the operating policy at the both the short and long-term temporal scales, providing the dam operator with enough insight into the future. Also, for operational purposes, the real-time sequential run demonstrated in this study is the way to go, as the dam operator would be interested in operating based on the most recently available forecast inflow information.

For dams with smaller drainage basins, other hydrologic models can be explored as the VIC model (being used in this research) is a mesoscale model, which sometimes might not give the best results when run over smaller domains. Also, the study used MS Excel's built-in Evolutionary GA solver, which could be expanded upon by using other heuristic optimization algorithms as the situation at hand demands. Possible alternatives could be Particle Swarm Optimization, Simulated Annealing, Ant Colony Optimization, Bee Algorithm etc. In recent years, heuristic search methods have gained significant attention from researchers, as they can produce many non-dominated, optimal solutions simultaneously in multi-objective optimization problems, as compared to the traditional gradient methods, such as linear and nonlinear programming, which can only produce a locally converged optimal solution. Multi-reservoir systems can also be

93

considered for investigating the efficiency of short-term weather forecasts, as the current study only considered a single dam for optimization without receiving no regulated inflow. Lastly, this procedure can be replicated globally, and especially over the dams in the developing world, where most of the future construction is going to be witnessed. These upcoming dams can embrace the dynamic dam operations instead of going for a conventional static rule curve, so as to increase the efficiency of the infrastructure that is to be built and optimize the benefits to multiple stakeholders.

The take-home messages that can be derived from this study are summarized as follows:

- The GFS-based forecasts dynamically downscaled using WRF model provide a basis for optimizing the reservoir operations over short-term peak inflow events and in dams with small to moderate storage receiving unregulated inflow.

- The short-term optimization can result in significant improvements in the hydropower generated over such events, without compromising the objectives of flood control, water security, dam safety and environmental regulations.

- Optimization using short-term forecasts can sometimes result into an additional hydropower than what is theoretically possible (control run), if the peak inflow is overestimated while opposite can occur in case of the underestimation of peak.

- Control and actual forecast runs validate the tradeoff in lead time of forecasts, while sequentially updating the forecasts tends to minimize the under/overestimations, resulting in a more dynamic and close to real-time scheme to be followed by a dam operator.

- As any 'green' energy technology succeeds or fails based on the price of power it generates, the current study adds a factor in favor of hydropower by harnessing the most out of the current infrastructure, generating an increased revenue and minimizing downstream losses that can occur in case of a peak inflow event.

94

REFERENCES

Ahmad, S. K. (2017). GRanD Interactive Visualizer. Retrieved October 17, 2017, from http://students.washington.edu/skahmad/GRanD_map/

Ahmadi, M., O. Bozorg Haddad, and M.A. Mariño (2014). Extraction of Flexible Multi-Objective Real-Time Reservoir Operation Rules. Water Resour Manag, 28: 131, https://doi.org/10.1007/s11269-013-0476-z

Anghileri, D., N. Voisin, A. Castelletti, F. Pianosi, B. Nijssen, and D.P. Lettenmaier (2016). Value of long-term streamflow forecasts to reservoir operations for water supply in snow-dominated river catchments. Water Resources Research, 52(6), 4209-4225.

Barros, M. T. L., F. T-C. Tsai, S. Yang, J. E. G. Lopes, and W. W.G. Yeh (2003). Optimization of Large-Scale Hydropower System Operations. Journal of Water Resources Planning and Management, 129 (June), 11, https://doi.org/10.1061/(ASCE)0733-9496(2003)129:3(178)

Bauer, P., A. Thorpe, and G. Brunet (2015). The quiet revolution of numerical weather prediction. Nature, 525(7567), 47-55.

Block, P. (2011). Tailoring seasonal climate forecasts for hydropower operations. Hydrology and Earth System Sciences, 15(4), pp. 1355–1368, https://doi.org/10.5194/hess-15-1355-2011

BP Statistical Review of World Energy 2017. British Petroleum, (66), 1-52. https://www.bp.com/content/dam/bp/en/corporate/pdf/energy-economics/statistical-review-2017/bp-statistical-review-of-world-energy-2017-full-report.pdf

Chen, X. and F. Hossain (2016). Revisiting extreme storms of the past 100 years for future safety of large water management infrastructures. Earth's Future, 4, https://doi:10.1002/2016EF000368.

Christensen, N. S., A.W. Wood, N. Voisin, and R.N. Palmer (2004). The Effects of Climate Change on the Hydrology and Water Resources of the Colorado River Basin. Climatic Change, 62, pp. 337–363, https://doi.org/10.1023/B:CLIM.0000013684.13621.1f

Coren, M. J. (2016). Germany had so much renewable energy on Sunday that it had to pay people to use electricity — Quartz. Retrieved October 10, 2017, from https://qz.com/680661/germany-had-so-much-renewable-energy-on-sunday-that-it-had-to-pay-people-to-use-electricity/

"Dataquery 2.0: Query Timeseries from USACE Northwestern Division" (2017). Retrieved October 17, 2017, from http://www.nwd-wc.usace.army.mil/dd/common/dataquery/www/

Denaro S., D. Anghileri, M. Giuliani, and A. Castelletti (2017). Informing the operations of water reservoirs over multiple temporal scales by direct use of hydro-meteorological data. Advances in Water Resources, 103:51-63.

Ding, W., C. Zhang, Y. Peng, R. Zeng, H. Zhou, and X. Cai (2015). An analytical framework for flood water conservation considering forecast uncertainty and acceptable risk. Water Resources Res., 51, 4702–4726, https://doi:10.1002/2015WR017127.

DOE Report (2016). "Hydropower Vision: A New Chapter for America's 1st Renewable Electricity Source." U.S. Department of Energy. Retrieved 20 Nov, 2016, from https://energy.gov/eere/water/articles/hydropower-vision-new-chapter-america-s-1st-renewable-electricity-source

Duncan, J. and T. Carlson (2011). Characterization of Fish Passage Conditions through a Francis Turbine and Regulating Outlet at Cougar Dam, Oregon, Using Sensor Fish, 2009–2010. Pacific Northwest National Laboratory, (May), 2009–2010.

"Excel Solver - Change Options for Evolutionary Solving Method | solver" (2017). Retrieved October 17, 2017, from https://www.solver.com/excel-solver-change-options-evolutionary-solving-method

Fan, F. M., D. Schwanenberg, R. Alvarado, A. A. dos Reis, W. Collischonn, and S. Naumman (2016). Performance of deterministic and probabilistic hydrological forecasts for the short-term optimization of a tropical hydropower reservoir. Water Resources Management, 30(10), 3609-3625.

Fan, F. M., D. Schwanenberg, W. Collischonn, and A. Weerts (2015). Verification of inflow into hydropower reservoirs using ensemble forecasts of the TIGGE database for large scale basins in Brazil. Journal of Hydr.: Regional Studies, 4, 196-227.

Ficchì, A., L. Raso, D. Dorchies, F. Pianosi, P. O. Malaterre, P. J. Van Overloop, and M. Jay-Allemand (2015). Optimal operation of the multireservoir system in the Seine river basin using deterministic and ensemble forecasts. Journal of Water Resources Planning and Management, 142(1), 05015005.

"FIRO Overview, Forecast Informed Reservoir Operations" (2017), Center for Western Weather and Water Extremes. Retrieved 29 July, 2017, from http://cw3e.ucsd.edu/firo_executive-summary/#TOP

Gebremichael, M. and W. W.G. Yeh (2014). Optimizing Reservoir Operations for Hydropower Production in Africa through the use of Remote Sensing Data and Seasonal Climate Forecasts. Retrieved February 2, 2017, from http://ral.ucar.edu/~hopson/NCAR_DA_Postdoc_Prog/UCLA_ROSES_NASA_Proposal2014Final_text.pdf

Georgakakos, K. P., H. Yao, M. Kistenmacher, K.P. Georgakakos, and T.M. Modrick (2015). Integrated Forecast and Reservoir Management (INFORM) For Northern California. Retrieved February 10, 2017, from http://www.gwri.gatech.edu/sites/default/files/files/miscdocs/inform2015forecastoutlookwat

erresassessessmentmarch1st.pdf

"Global Forecast System (GFS) | National Centers for Environmental Information (NCEI)" (2017). Retrieved October 12, 2017, from https://www.ncdc.noaa.gov/data-access/model-data/model-datasets/global-forcast-system-gfs

Goldberg, D. E. and K. Deb (1989). A Comparative analysis of selection schemes used in genetic algorithms. Foundations of genetic algorithms, Morgan Kaufman, San Mateo, Calif., 69–93.

"GRDA - FERC grants GRDA Pensacola license variance". (2017). Retrieved October 18, 2017, from http://www.grda.com/ferc-grants-grda-pensacola-license-variance/

Grumet, T. (2017). "This Unique Combo of Wind and Hydropower Could Revolutionize Renewable Energy - GE Reports". Retrieved July 29, 2017, from http://www.ge.com/reports/unique-combo-wind-hydro-power-revolutionize-renewable-energy/

"GSOD Global Surface Summary of the Day - NOAA Data Catalog" (2017). Retrieved August 30, 2017, from https://data.noaa.gov/dataset/global-surface-summary-of-the-day-gsod

Hamlet, A. F., D. Huppert, and D.P. Lettenmaier (2002). Economic value of long-lead streamflow forecasts for Columbia River hydropower. J. Water Resources Planning and Management ASCE, 128(2), pp.91–101.

Hamlet, A. F. and D.P. Lettenmaier (1999). Effects of Climate Change on Hydrology and Water Resources of the Columbia River Basin. J. Amer. Water Resour. Assoc. 35, pp. 1597–1623.

Holland, J. H. (1975). Adaptation in natural and artificial systems. MIT Press, Cambridge, Mass.

Hossain, F., A. M. Degu, W. Yigzaw, D. Niyogi, S. Burian, J.M. Shepherd, and R. Pielke Sr. (2012). Climate Feedback-based Considerations to Dam Design, Operations and Water Management in the 21st Century. ASCE J. Hydrologic Engineering, 17(8), pp. 837-850, https://doi:10.1061/(ASCE)HE.1943-5584.0000541.

Hossain, F., S. Sikder, N. Biswas, H. Lee, N.D Luong, N.H. Hiep, B. D. Duong, and D. Long (2017). Predicting Water Availability of the Regulated Mekong River Basin Using Satellite Observations and a Physical Model. Asian Journal of Water and Environmental Pollution, 14(3), 39-48.

HRC-GWRI (2013). Integrated Forecast and Reservoir Management (INFORM): Enhancements and Demonstration Results for Northern California (2008-2012). California Energy Commission. Publication number: CEC-500-2014-019. Retrieved July 29, 2017, from http://www.energy.ca.gov/2014publications/CEC-500-2014-019/CEC-500-2014-019.pdf

Hsu, N. S. and C. C. Wei (2007). A multipurpose reservoir real-time operation model for flood control during typhoon invasion. Journal of Hydrology, 336(3–4), pp. 282–293,

https://doi.org/10.1016/j.jhydrol.2007.01.001

"ICOLD: Definition of a Large Dam". Retrieved August 27, 2017, from http://www.icold-cigb.net/GB/dams/definition_of_a_large_dam.asp

Ji, Y., X. Lei, S. Cai, and X. Wang (2016). Hedging Rules for Water Supply Reservoir Based on the Model of Simulation and Optimization. Water, 8(6), pp. 249.

Jordan, F. M., J-L Boillat, and A. J. Schleiss (2012). Optimization of the flood protection effect of a hydropower multi-reservoir system. International Journal of River Basin Management, 10:1, 65-72, https://doi: 10.1080/15715124.2011.650868

Jothiprakash, V. and R. Arunkumar. (2014). Multi-reservoir optimization for hydropower production using NLP technique. KSCE Journal of Civil Engineering, 18(1), pp. 344–354, https://doi.org/10.1007/s12205-014-0352-2

Knudby, A., S. K. Ahmad, and C. Ilori (2016). The Potential for Landsat-Based Bathymetry in Canada. Canadian Journal of Remote Sensing, 42(4), 367-378.

Kottek, M., J. C. Grieser, C. Beck, B. Rudolf, and F. Rubel (2006). World Map of the Köppen-Geiger climate classification updated. Meteorol. Z., 15, pp. 259-263, https://doi: 10.1127/0941-2948/2006/0130.

Labadie, J. W. (2004). Optimal Operation of Multireservoir Systems: State-of-the-Art Review. Journal of Water Resources Planning and Management, 130(2), pp. 93–111, https://doi.org/10.1061/(ASCE)0733-9496(2004)130:2(93)

Lee S-Y., A. Hamlet, C. Fitzgerald, and S. J. Burges (2009). Optimized flood control in the Columbia River basin for a global warming scenario. J Water Resour Plan Manag 135(6):440–450

Lehner, B., C.R. Liermann, C. Revenge, C. Vörösmarty, B. Fekete, P. Crouzet, P. Döll, M. Endejan, K. Frenken, J. Magome, and C. Nilsson (2011). Global Reservoir and Dam (GRanD) database. Technical Documentation, Version, 1.

Lessard, J. L. and D. B. Hayes (2003). Effects of elevated water temperature on fish and macroinvertebrate communities below small dams. River Res. Applic., 19: 721–732, https://doi:10.1002/rra.713

Liang, X., D.P. Lettenmaier, E.F. Wood, and S. J. Burges (1994). A Simple Hydrologically Based Model of Land Surface Water and Energy Fluxes for General Circulation Models. J. Geophys. Res. 99 (D7), pp. 14415–14428.

Liang, X., E.F. Wood, and D.P.Lettenmaier (1996). Surface Soil Moisture Parameterization of the VIC-2L Model: Evaluation and Modifications. Glob. Plan. Change 13, pp. 195–206.

Lin, Y. (2011). GCIP/EOP Surface: Precipitation NCEP/EMC 4KM Gridded Data (GRIB) Stage IV Data. Version 1.0. UCAR/NCAR - Earth Observing Laboratory, https://doi.org/10.5065/D6PG1QDD. Accessed 19 Oct 2017.

Livneh B., E.A. Rosenberg, C. Lin, B. Nijssen, V. Mishra, K.M. Andreadis, E.P. Maurer, and D.P. Lettenmaier (2013). A Long-Term Hydrologically Based Dataset of Land Surface Fluxes and States for the Conterminous United States: Update and Extensions. Journal of Climate, 26, 9384–9392.

Lohmann, D., R. Nolte-Holube, and E. Raschke (1996). A large-scale horizontal routing model to be coupled to land surface parametrization schemes. Tellus, 48(A), pp. 708-721.

Lohmann, D., E. Raschke, B. Nijssen, and D.P. Lettenmaier (1998). Regional scale hydrology: I. Formulation of the VIC-2L model coupled to a routing model. Hydrol. Sci. J., 43(1), pp. 131-141.

Loucks, D. P., E. Van Beek, J. R. Stedinger, J. P. Dijkman, and M.T. Villars (2005). Water Resources Systems Planning and Management: An Introduction to Methods, Models and Applications. Paris: UNESCO.

Mao, J.,P. Zhang, L. Dai, L., H. Dai, and T. Hu (2016). Optimal operation of a multi-reservoir system for environmental water demand of a river-connected lake. Hydrology Research, 47(S1), 206 -224.

McKay, L., T. Bondelid, T. Dewald, J. Johnston, R. Moore, and A. Rea (2012). "NHDPlus Version 2: User Guide".

Miao, Y., X. Chen, and F. Hossain (2016). Maximizing hydropower generation with observations and numerical modeling of the atmosphere. Journal of Hydrologic Engineering, 21(6), 02516002.

Michalewicz, Z. (1992). Genetic algorithms + data structures = evolution programs. Springer, New York.

"Monthly Charts for Grand Lake O' The Cherokees, Pensacola Dam". USACE. Retrieved August 21, 2017, from http://www.swt-wc.usace.army.mil/PENScharts.html

Murphy, J. (2000). Predictions of climate change over Europe using statistical and dynamical downscaling techniques. International Journal of Climatology, 20(5), pp. 489-501.

Nash, J. E. and J.V. Sutcliffe (1970). River flow forecasting through conceptual models part I— A discussion of principles. Journal of hydrology, 10(3), 282-290.

Neelakantan, T. R. and N.V. Pundarikanthan (1999). Hedging Rule Optimisation for Water Supply Reservoirs System. Water Resources Management, 13(6), pp. 409–426, https://doi.org/10.1023/A:1008157316584

Nijssen, B., D. P. Lettenmaier, X. Liang, S. W. Wetzel, and E. F. Wood (1997). Streamflow simulation for continental-scale river basins, Water Resour. Res., 33(4), 711–724, https://doi:10.1029/96WR03517.

"Order Data - NCDC | Archive Information Request System | National Climatic Data Center (NCDC)". (2017). Retrieved October 13, 2017, from https://www.ncdc.noaa.gov/has/HAS.FileAppRouter?datasetname=GFSGRB24&subqueryby=STATION&applname=&outdest=FILE

"Pacific Northwest Mesoscale Model Numerical Forecast Information" (2016). Retrieved September 8, 2017, from https://www.atmos.washington.edu/mm5rt/info.html

"Pensacola project - FERC No. 1494. Grand River Dam Authority" (2008). Retrieved from http://www.grda.com/wp-content/uploads/2014/04/SMP_FINAL_FERC-w_Maps.pdf

ReVelle, C. (1997). Chapter 1: Water resources: Surface water systems. Design and operation of civil and environmental engineering systems. C. ReVelle and A. E. McGarity, eds., Wiley, New York, 1–39.

Risley, J. C., J.R. Wallick, J.F. Mangano, and K.L. Jones (2012). An Environmental Streamflow Assessment for the Santiam River Basin, Oregon. U.S. Geological Survey.

Sale, M. J., E.D. Brill and E.E. Herricks (1982). An approach to optimizing reservoir operation for downstream aquatic resources. Water Resources Research, 18(4), pp. 705-712, https://doi:10.1029/WR018i004p00705.

Samu N. M., S.-C. Kao, and P.W. O'Connor (2017). National Hydropower Plant Dataset, Version 1, Update FY17Q4. Existing Hydropower Assets [series] FY17Q4. National Hydropower Asset Assessment Program. Oak Ridge National Laboratory, Oak Ridge, TN, Retrieved from: http://nhaap.ornl.gov, https://dx.doi.org/10.21951/1326801

Schwanenberg, D., F. M. Fan, S. Naumann, J. I. Kuwajima, R. A. Montero, and A. A. Dos Reis (2015). Short-term reservoir optimization for flood mitigation under meteorological and hydrological forecast uncertainty. Water Resources Management, 29(5), 1635-1651.

Séguin, S., C. Audet, and P. Côté (2017). Scenario-Tree Modeling for Stochastic Short-Term Hydropower Operations Planning. Journal of Water Resources Planning and Management, 143(12), 04017073.

Sikder, S. and F. Hossain (2016). Assessment of the Weather Research and Forecasting Model Generalized Parameterization Schemes for Advancement of Precipitation Forecasting in Monsoon-Driven River Basins. Journal of Advances in Modeling Earth Systems (AGU), vol. 8, https://doi:10.1002/2016MS000678.

Skamarock, W., J. Klemp, J. Dudhia, D. Gill, and D. Barker (2005). A description of the advanced research WRF Version 3, NCAR technical note.

"State Electricity Profiles - Energy Information Administration". Retrieved September 4, 2017, from https://www.eia.gov/electricity/state/

Stedinger, J. R. (1993). Frequency analysis of extreme events. Handbook of hydrology, 18.

Stedinger, J. R., S. N. Tan, C. A. Shoemaker, J. R. Lamontagne, and S.B. Barton (2014). Short-Term Optimization Model With ESP Forecasts For Columbia Hydropower System With Optimized Multi-Turbine Powerhouses. CUNY Academic Works. Retrieved November 10, 2017, from https://academicworks.cuny.edu/cc_conf_hic/333

Stensrud, D. J. (2007). Parameterization Schemes: Keys to Understanding Numerical Weather Prediction Models. Cambridge Univ. Press.

"U.S. Army Corps of Engineers. Water Control Manuals". Retrieved July 17, 2017, from http://www.lrp.usace.army.mil/Missions/Planning-Programs-Project-Management/Key-Projects/Water-Control-Manuals/

Voisin, N., M. Kintner-Meyer, D. Wu, R. Skaggs, T. Fu, T. Zhou, T. NGuyen, and I. Kraucunas (2017). Opportunities for joint water-energy management: sensitivity of the 2010 Western U.S. electricity grid operations to climate oscillations. Bull. Amer. Meteor. Soc., https://doi:10.1175/BAMS-D-16-0253.1

Wang, F., L. Wang, H. Zhou, S. Valeriano, C. Oliver, T. Koike, and W. Li (2012). Ensemble hydrological prediction-based real-time optimization of a multiobjective reservoir during flood season in a semiarid basin with global numerical weather predictions. Water Resources Research, 48(7).

"Willamette River Basin small-scale water supply allocation process | Oregon State Library". (2011). Retrieved October 17, 2017, from https://digital.osl.state.or.us/islandora/object/osl:14841

Windsor, J. S. (1973). Optimization model for the operation of flood control systems. Water Resources Research, 9(5), 1219–1226, https://doi.org/10.1029/WR009i005p01219

Woldemichael, A.T., F. Hossain, R.A. Pielke Sr., and A. Beltrán-Przekurat (2012). Understanding the Impact of Dam-triggered Land-Use/Land-Cover Change on the Modification of Extreme Precipitation. Water Resources Research, https://doi:10.1029/2011WR011684

World Energy Council (2016). "The Road to Resilience Managing the Risks of the Energy-Water-Food Nexus". Retrieved July 17, 2017, from https://www.worldenergy.org/publications/2016/world-energy-resources-2016/

Xu, B., P. A. Zhong, R. C. Zambon, Y. Zhao, and W. W. G. Yeh (2015). Scenario tree reduction in stochastic programming with recourse for hydropower operations. Water Resources Research, 51(8), 6359-6380.

Yao, H. and A. Georgakakos (2001). Assessment of Folsom Lake response to historical and potential future climate scenarios: 2. Reservoir management. Journal of Hydrology, 249(1), 176-196.

Yasar, M. (2016). Optimization of reservoir operation using cuckoo search algorithm: Example of adiguzel dam, Denizli, Turkey. Mathematical Problems in Engineering, https://doi.org/10.1155/2016/1316038

Yeh, W. W. G. (1985). Reservoir management and operations models: A State-of-the-Art Review. Water resources research, 21(12), 1797-1818.

Zarfl, C., A. E. Lumsdon, J. Berlekamp, L. Tydecks, and K. Tockner (2014). A global boom in hydropower dam construction. Aquatic Sciences, 77(1), 161–170, https://doi.org/10.1007/s00027-014-0377-0

Zhao, T., X. Cai, and D. Yang (2011). Effect of streamflow forecast uncertainty on real-time reservoir operation. Advances in water resources, 34(4), 495-504.

APPENDIX A. DAM AND RESERVOIR DETAILS
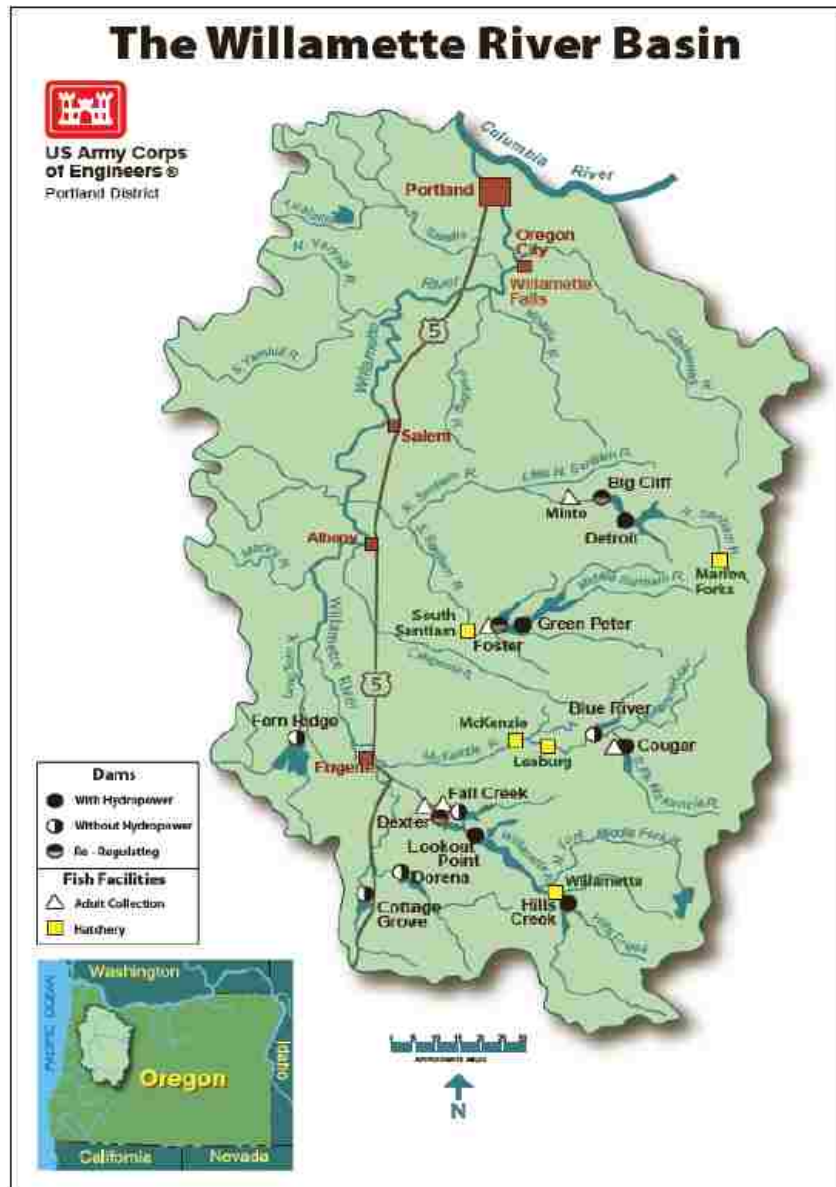
Figure A.1. Major river streams and dams thereupon in Willamette Basin. Also mapped are the fish facilities available at the river streams. Detroit dam lies upstream in the network of dams, receiving unregulated inflow (Source: "Willamette River Basin", 2011).
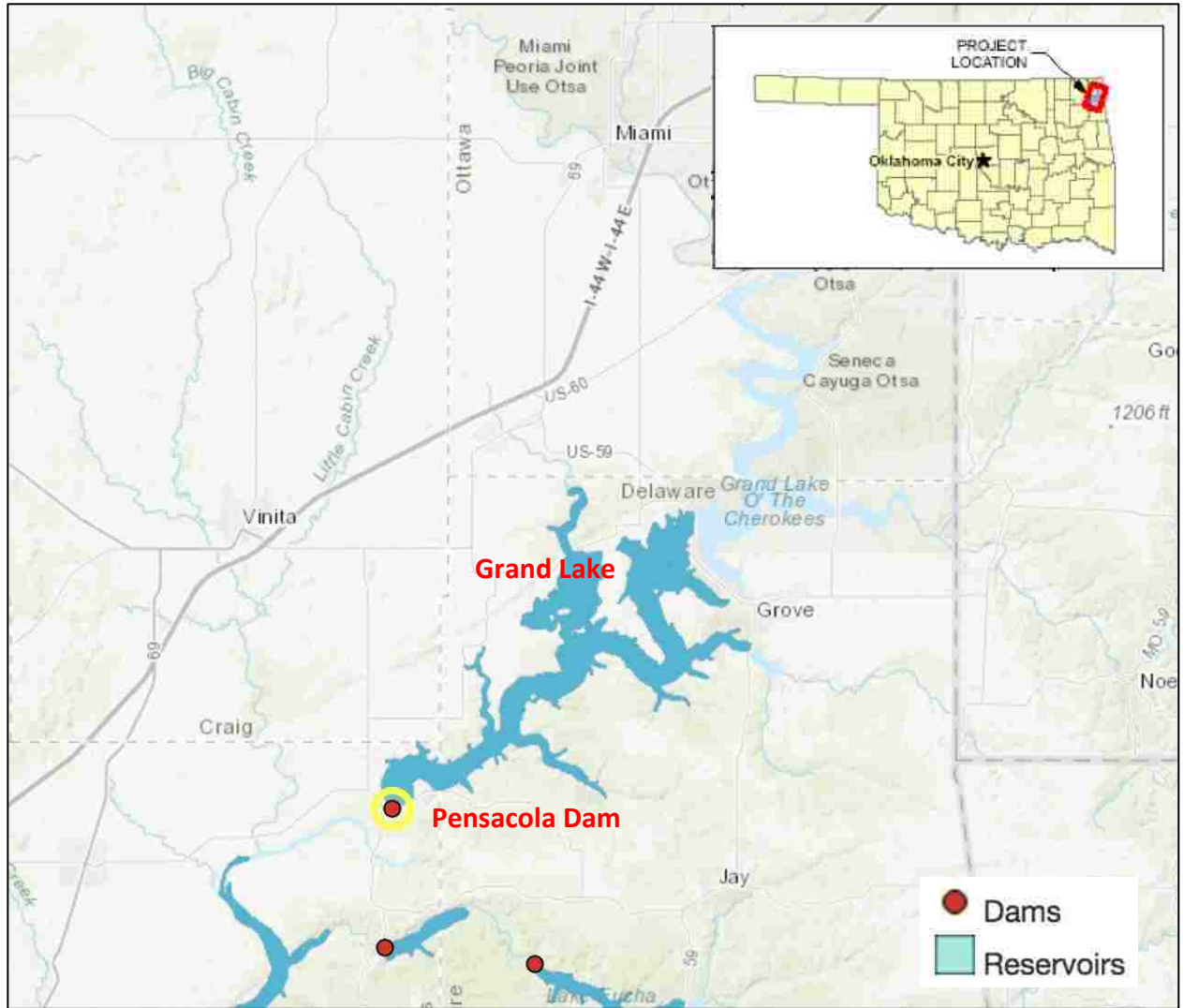
Figure A.2. Location of Pensacola Dam along with the formed reservoir, Grand Lake. No major dams lie upstream of the dam. (Visualization from Ahmad S. K. (2017). GRanD Interactive Visualizer)

Table A.1. Data for Storage-Area Relationship of Detroit Dam, OR

Storage (ac-feet)	Reservoir Elevation (feet)	Storage (ac-feet)	Reservoir Elevation (feet)	Storage (ac-feet)	Reservoir Elevation (feet)	Storage (ac-feet)	Reservoir Elevation (feet)
336233.455	1531.62	436805.9	1563.76	304048.167	1519.74	193898.194	1471.25
336317.542	1531.65	436805.9	1563.76	304023.122	1519.73	193858.294	1471.23
336429.688	1531.69	436872.023	1563.78	303998.079	1519.72	193858.294	1471.23
336513.82	1531.72	436838.96	1563.77	303998.079	1519.72	193838.347	1471.22
336626.027	1531.76	436872.023	1563.78	303948	1519.7	193818.401	1471.21
341117.454	1533.4	436872.023	1563.78	303948	1519.7	193818.401	1471.21
341173.415	1533.42	436872.023	1563.78	303922.963	1519.69	193818.401	1471.21
341369.348	1533.49	436872.023	1563.78	303922.963	1519.69	193818.401	1471.21
341453.351	1533.52	436905.089	1563.79	303872.895	1519.67	193798.458	1471.2
341621.414	1533.58	436971.226	1563.81	303847.864	1519.66	164531.84	1455.63
341705.475	1533.61	436971.226	1563.81	303847.864	1519.66	164531.84	1455.63
341733.499	1533.62	437004.298	1563.82	303822.834	1519.65	164531.84	1455.63
341733.499	1533.62	436971.226	1563.81	303797.807	1519.64	164531.84	1455.63
341761.525	1533.63	437004.298	1563.82	303772.781	1519.63	164513.817	1455.62
342069.955	1533.74	437004.298	1563.82	303722.736	1519.61	164513.817	1455.62
342547.123	1533.91	437004.298	1563.82	303697.716	1519.6	164513.817	1455.62
342603.301	1533.93	437070.449	1563.84	303547.637	1519.54	164513.817	1455.62
345619.307	1534.94	437070.449	1563.84	219222.795	1483.88	164513.817	1455.62
345649.414	1534.95	437070.449	1563.84	219222.795	1483.88	164513.817	1455.62
345739.752	1534.98	437070.449	1563.84	219222.795	1483.88	164513.817	1455.62
345799.989	1535	437136.609	1563.86	219222.795	1483.88	164495.796	1455.61
345859.755	1535.02	437169.692	1563.87	219199.709	1483.87	164495.796	1455.61
345889.641	1535.03	437202.778	1563.88	219199.709	1483.87	164495.796	1455.61
345919.53	1535.04	437235.866	1563.89	219199.709	1483.87	154160.932	1449.86
345949.421	1535.05	371417.219	1543.54	219176.627	1483.86	154160.932	1449.86
345949.421	1535.05	371387.212	1543.53	219176.627	1483.86	154160.932	1449.86
345949.421	1535.05	371357.206	1543.52	219176.627	1483.86	154160.932	1449.86
345949.421	1535.05	371297.202	1543.5	219176.627	1483.86	154160.932	1449.86
345979.315	1535.06	371267.203	1543.49	219153.546	1483.85	154160.932	1449.86
345979.315	1535.06	371267.203	1543.49	219130.468	1483.84	154160.932	1449.86
346069.009	1535.09	371237.206	1543.48	219130.468	1483.84	154160.932	1449.86
346128.818	1535.11	371147.23	1543.45	219130.468	1483.84	154143.869	1449.85
436706.732	1563.73	371117.242	1543.44	219130.468	1483.84	154143.869	1449.85
436739.786	1563.74	371087.257	1543.43	219107.392	1483.83	154143.869	1449.85
436772.842	1563.75	371057.274	1543.42	219107.392	1483.83	154143.869	1449.85
436772.842	1563.75	371027.293	1543.41	219222.795	1483.88	154143.869	1449.85
436772.842	1563.75	370967.337	1543.39	219222.795	1483.88	154143.869	1449.85
436805.9	1563.76	370967.337	1543.39	193898.194	1471.25	154143.869	1449.85

105

Storage (ac-feet)	Reservoir Elevation (feet)	Storage (ac-feet)	Reservoir Elevation (feet)	Storage (ac-feet)	Reservoir Elevation (feet)	Storage (ac-feet)	Reservoir Elevation (feet)
154937.936	1450.3	220311.61	1484.37	350747.288	1536.65	191479.897	1469.99
154937.936	1450.3	220311.61	1484.37	350717.254	1536.64	191479.897	1469.99
154937.936	1450.3	220311.61	1484.37	350657.192	1536.62	191479.897	1469.99
154937.936	1450.3	220311.61	1484.37	350657.192	1536.62	191479.897	1469.99
154937.936	1450.3	220311.61	1484.37	350597.14	1536.6	191479.897	1469.99
154937.936	1450.3	220311.61	1484.37	350567.117	1536.59	191479.897	1469.99
154937.936	1450.3	220311.61	1484.37	350537.097	1536.58	191459.801	1469.98
154937.936	1450.3	220311.61	1484.37	350477.064	1536.56	191459.801	1469.98
154919.977	1450.29	220289.637	1484.36	350477.064	1536.56	191459.801	1469.98
154919.977	1450.29	220289.637	1484.36	350447.051	1536.55	191459.801	1469.98
154919.977	1450.29	220289.637	1484.36	350417.041	1536.54	191439.708	1469.97
154919.977	1450.29	220289.637	1484.36	350387.032	1536.53	191439.708	1469.97
154919.977	1450.29	220289.637	1484.36	350327.023	1536.51	191439.708	1469.97
154919.977	1450.29	220289.637	1484.36	350297.022	1536.5	191439.708	1469.97
154919.977	1450.29	220289.637	1484.36	350297.022	1536.5	191439.708	1469.97
154919.977	1450.29	220289.637	1484.36	350267.023	1536.49	191439.708	1469.97
154919.977	1450.29	220267.667	1484.35	419578.064	1558.57	191479.897	1469.99
154919.977	1450.29	292348.808	1515.14	419578.064	1558.57	267307.317	1505.35
174217.909	1461.01	292298.954	1515.12	419578.064	1558.57	267255.392	1505.33
174217.909	1461.01	292298.954	1515.12	419578.064	1558.57	267229.434	1505.32
174199.995	1461	292298.954	1515.12	419545.048	1558.56	267177.523	1505.3
174199.995	1461	292274.029	1515.11	419545.048	1558.56	267177.523	1505.3
174199.995	1461	292224.187	1515.09	419545.048	1558.56	267125.622	1505.28
174199.995	1461	292124.525	1515.05	419545.048	1558.56	267099.675	1505.27
174181.908	1460.99	292074.705	1515.03	419545.048	1558.56	267073.73	1505.26
174181.908	1460.99	291999.991	1515	419545.048	1558.56	267047.788	1505.25
174181.908	1460.99	291947.78	1514.98	419545.048	1558.56	267047.788	1505.25
174163.823	1460.98	291843.383	1514.94	419545.048	1558.56	267021.848	1505.24
174163.823	1460.98	291765.108	1514.91	419545.048	1558.56	266995.91	1505.23
174163.823	1460.98	291686.853	1514.88	426971.974	1560.78	266995.91	1505.23
174145.74	1460.97	291634.693	1514.86	426971.974	1560.78	281855.367	1511.06
174145.74	1460.97	291556.47	1514.83	426971.974	1560.78	281803.566	1511.04
174145.74	1460.97	291556.47	1514.83	426971.974	1560.78	281803.566	1511.04
174145.74	1460.97	291556.47	1514.83	426971.974	1560.78	281777.669	1511.03
174127.659	1460.96	291530.4	1514.82	426938.91	1560.77	281751.774	1511.02
174127.659	1460.96	292348.808	1515.14	426938.91	1560.77	281699.991	1511
174127.659	1460.96	292298.954	1515.12	426938.91	1560.77	281649.789	1510.98
174217.909	1461.01	291426.142	1514.78	426938.91	1560.77	281933.085	1511.09

[Source: US Army Corps of Engineers (USACE), Northwestern Division]

Table A.2. Data for Storage-Area Relationship of Pensacola Dam, OK

Storage (ac-feet)	Reservoir Elevation (feet)	Storage (ac-feet)	Reservoir Elevation (feet)	Storage (ac-feet)	Reservoir Elevation (feet)	Storage (ac-feet)	Reservoir Elevation (feet)
2010562	754.81	1667859	744.91	1538759	742.04	1500891	744.65
2008878	751.72	1667859	744.91	1538759	742.04	1500879	741.16
2005294	754.72	1667401	744.9	1538759	742.04	1500476	744.64
2000030	754.63	1666466	748.37	1538759	742.04	1500451	741.15
1995934	754.56	1665559	744.86	1538759	742.04	1500060	744.63
1984581	751.27	1665505	748.35	1538759	742.04	1499645	744.62
1978966	754.27	1665099	744.85	1538759	742.04	1499590	741.13
1976038	754.22	1664641	744.84	1538759	742.04	1499590	741.13
1958619	753.92	1663720	744.82	1538321	742.03	1499590	741.13
1958050	753.91	1662800	744.8	1538321	742.03	1499230	744.61
1956347	753.88	1661881	744.78	1538321	742.03	1499160	741.12
1950390	750.63	1661881	744.78	1538321	742.03	1498814	744.6
1942970	750.49	1659579	744.73	1538321	742.03	1498814	744.6
1942706	753.64	1659579	744.73	1538321	742.03	1498814	744.6
1935885	753.52	1659119	744.72	1538321	742.03	1498729	741.11
1929065	753.4	1658661	744.71	1538321	742.03	1498729	741.11
1919969	753.24	1658661	744.71	1538321	742.03	1498729	741.11
1909169	753.05	1658201	744.7	1538321	742.03	1497986	744.58
1907310	749.81	1657280	744.68	1535037	745.46	1497871	741.09
1899169	752.87	1608449	743.61	1534420	741.94	1497871	741.09
1896416	752.82	1608052	747.12	1534183	745.44	1497571	744.57
1895314	752.8	1607589	747.11	1533559	741.92	1497571	744.57
1893032	749.53	1607127	747.1	1533559	741.92	1497571	744.57
1722066	749.51	1607101	743.58	1533129	741.91	1497571	744.57
1719481	746.01	1606204	747.08	1533129	741.91	1497441	741.08
1719081	749.45	1606200	743.56	1532478	745.4	1497441	741.08
1717089	749.41	1605750	743.55	1532050	745.39	1497155	744.56
1714769	745.91	1604851	743.53	1532050	745.39	1497010	741.07
1714301	745.9	1604401	743.52	1532050	745.39	1497010	741.07
1712115	749.31	1604401	743.52	1531196	745.37	1496740	744.55
1711949	745.85	1604401	743.52	1531196	745.37	1496580	741.06
1711011	745.83	1604354	747.04	1530979	741.86	1496580	741.06
1710540	745.82	1603895	747.03	1530769	745.36	1496325	744.54
1710070	745.81	1603500	743.5	1530549	741.85	1496325	744.54
1707250	745.75	1601701	743.46	1530342	745.35	1496325	744.54
1707250	745.75	1601701	743.46	1530342	745.35	1496325	744.54
1706780	745.74	1601701	743.46	1530342	745.35	1496150	741.05
1703960	745.68	1601618	746.98	1529918	745.34	1496150	741.05

107

Storage (ac-feet)	Reservoir Elevation (feet)	Storage (ac-feet)	Reservoir Elevation (feet)	Storage (ac-feet)	Reservoir Elevation (feet)	Storage (ac-feet)	Reservoir Elevation (feet)
1476409	744.06	1393890	742.03	1485124	744.27	1896416	752.82
1475994	744.05	1393890	742.03	1485124	744.27	1895314	752.8
1475994	744.05	1393890	742.03	1484708	744.26	1893032	749.53
1475994	744.05	1393890	742.03	1484708	744.26	1888155	752.67
1475994	744.05	1393890	742.03	1484293	744.25	1882098	752.56
1475994	744.05	1393890	742.03	1483878	744.24	1880996	752.54
1475994	744.05	1393890	742.03	1483878	744.24	1880448	752.53
1475994	744.05	1393890	742.03	1483047	744.22	1876593	752.46
1475994	744.05	1393890	742.03	1483047	744.22	1870533	752.35
1475994	744.05	1393890	742.03	1482634	744.21	1865028	752.25
1475579	744.04	1393486	742.02	1482219	744.2	1864999	748.98
1475579	744.04	1393486	742.02	1482219	744.2	1860622	752.17
1475579	744.04	1393486	742.02	1481804	744.19	1857318	752.11
1475579	744.04	1393486	742.02	1481388	744.18	1854565	752.06
1475579	744.04	1393486	742.02	1481388	744.18	1851812	752.01
1475579	744.04	1393486	742.02	1481388	744.18	1851261	752
1475579	744.04	1393486	742.02	1481388	744.18	1842001	748.52
1475579	744.04	1393486	742.02	1480973	744.17	1842001	748.52
1475166	744.03	1393486	742.02	1480973	744.17	1590509	746.73
1475166	744.03	1351950	740.97	1604354	747.04	1590451	743.21
1439977	743.17	1351950	740.97	1603895	747.03	1590451	743.21
1439567	743.16	1351950	740.97	1603500	743.5	1589100	743.18
1439160	743.15	1351950	740.97	1601701	743.46	1588199	743.16
1439160	743.15	1351950	740.97	1601701	743.46	1587398	746.66
1439160	743.15	1351950	740.97	1601701	743.46	1586850	743.13
1438751	743.14	1351568	740.96	1601618	746.98	1586850	743.13
1438342	743.13	1351568	740.96	1600800	743.44	1586400	743.12
1437932	743.12	1351568	740.96	1600800	743.44	1586400	743.12
1437932	743.12	1351568	740.96	1600350	743.43	1586400	743.12
1437932	743.12	1351185	740.95	1600350	743.43	1585622	746.62
1437114	743.1	1351185	740.95	1599899	743.42	1585051	743.09
1437114	743.1	1351185	740.95	1599899	743.42	1583700	743.06
1437114	743.1	1351185	740.95	1599899	743.42	1583700	743.06
1436707	743.09	1351185	740.95	1599449	743.41	1582799	743.04
1436707	743.09	1350801	740.94	1599001	743.4	1582799	743.04
1436297	743.08	1350801	740.94	1598551	743.39	1582799	743.04
1436297	743.08	1350801	740.94	1598100	743.38	1582511	746.55
1435888	743.07	1350033	740.92	1596749	743.35	1581901	743.02

[Source: US Army Corps of Engineers (USACE), Southwestern Division]

APPENDIX B. DAILY OPTIMIZATION DETAILS

PENSACOLA DAM – CONTROL & ACTUAL FORECAST RUN

Figure B.1. Actual/Optimized release and elevations for lead time – 3 days (17 March 2012) (Pensacola dam, OK)

Figure B.3. Actual/Optimized release and elevations for lead time – 5 days (15 March 2012)

(Pensacola dam, OK)

Figure B.4. Actual/Optimized release and elevations for lead time – 7 days (13 March 2012)
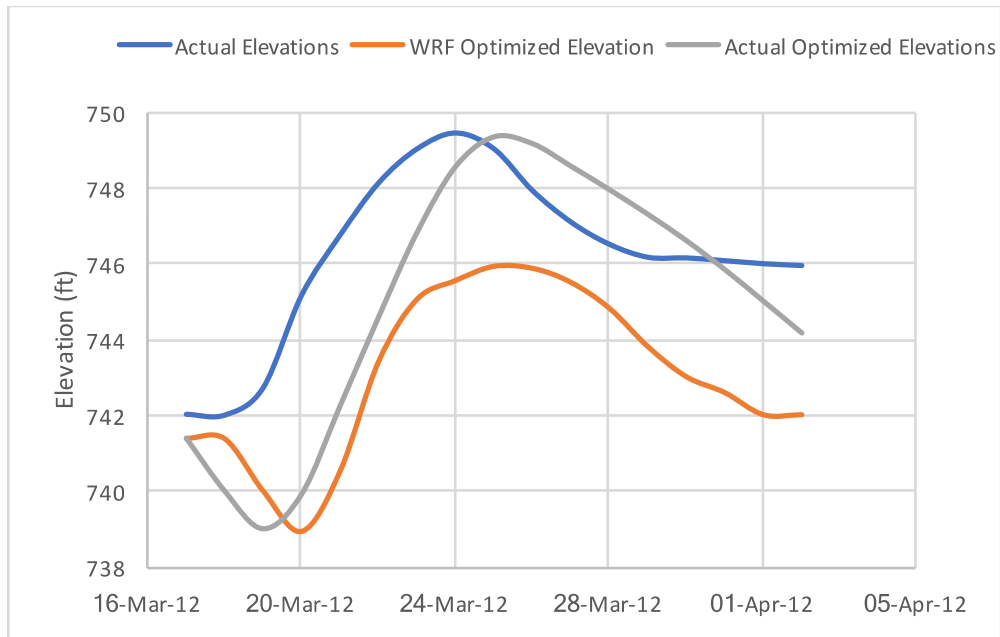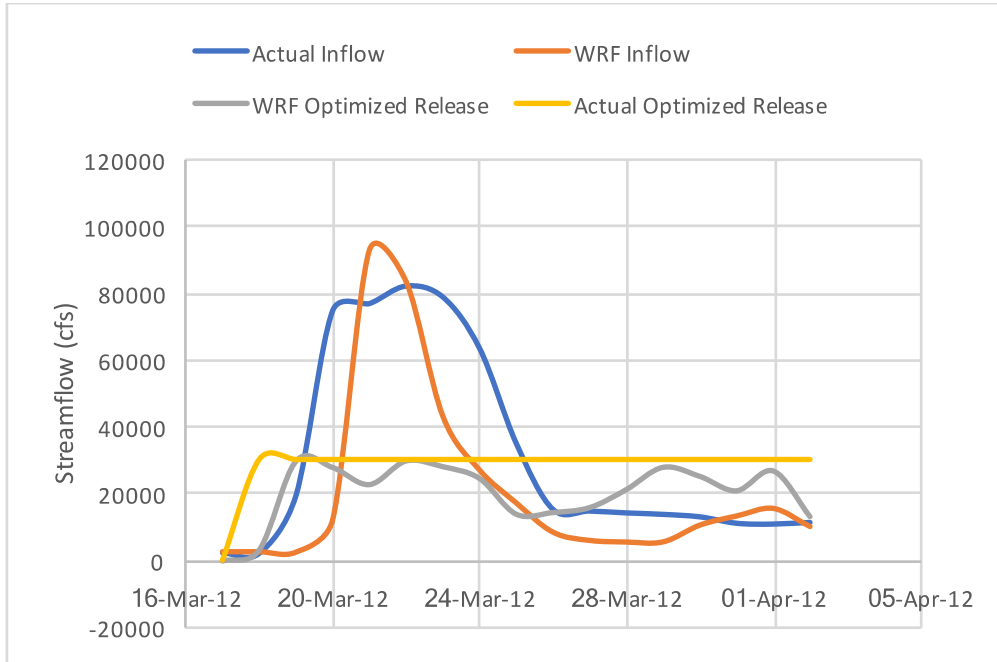(Pensacola dam, OK)
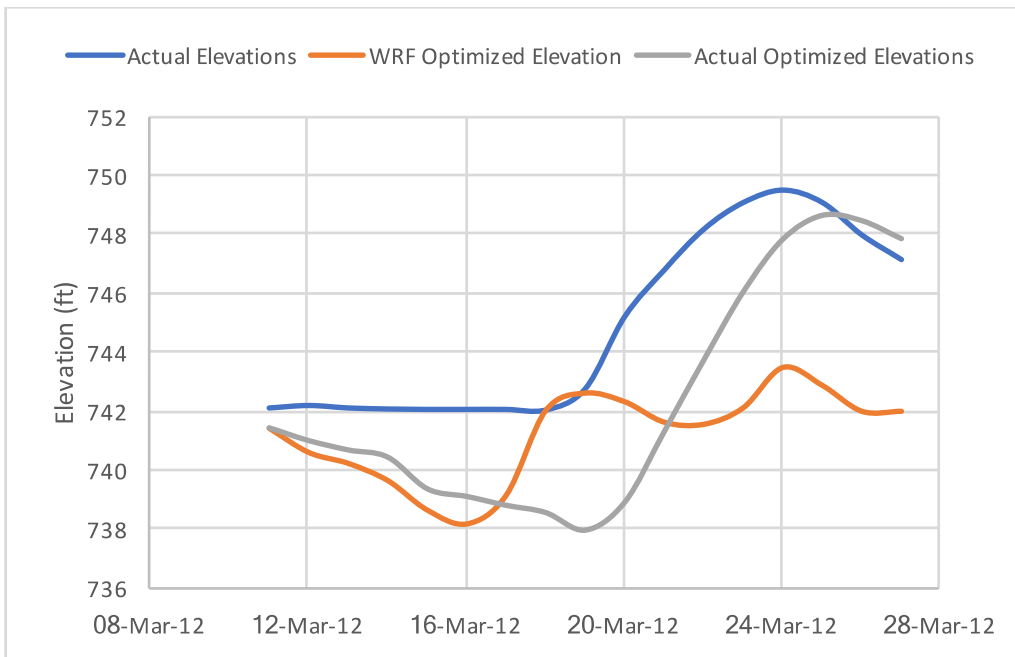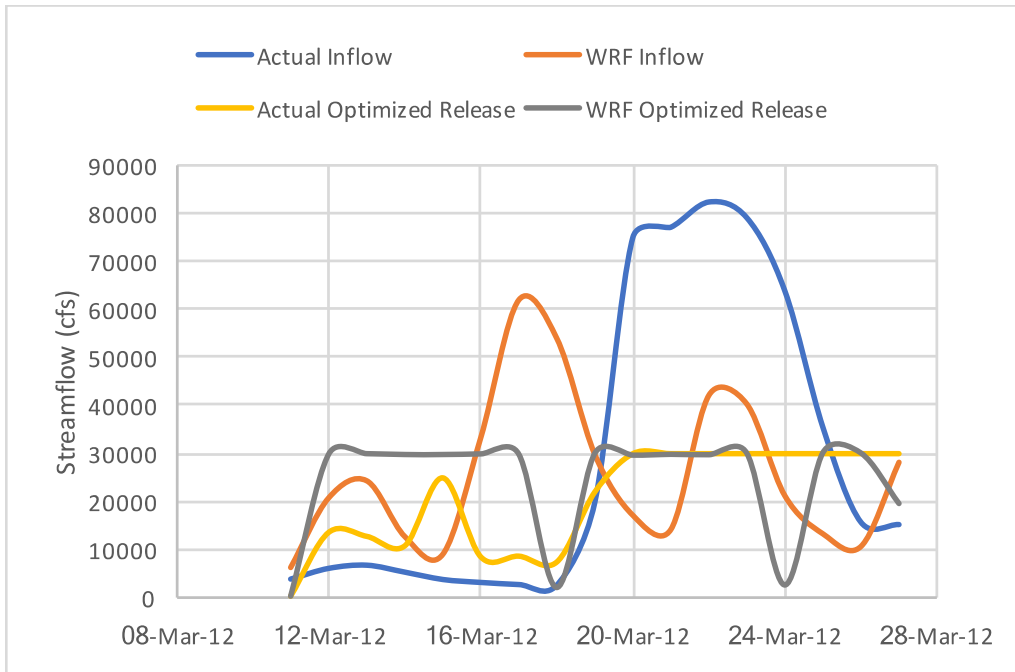
Figure B.5. Actual/Optimized release and elevations for lead time – 9 days (11 March 2012)
(Pensacola dam, OK)

DETROIT DAM – CONTROL & ACTUAL FORECAST RUN

Figure B.6. Actual/Optimized release and elevations for lead time – 3 days (19 Dec 2014)

(Detroit dam, OR)

Figure B.7. Actual/Optimized release and elevations for lead time – 5 days (17 Dec 2014)
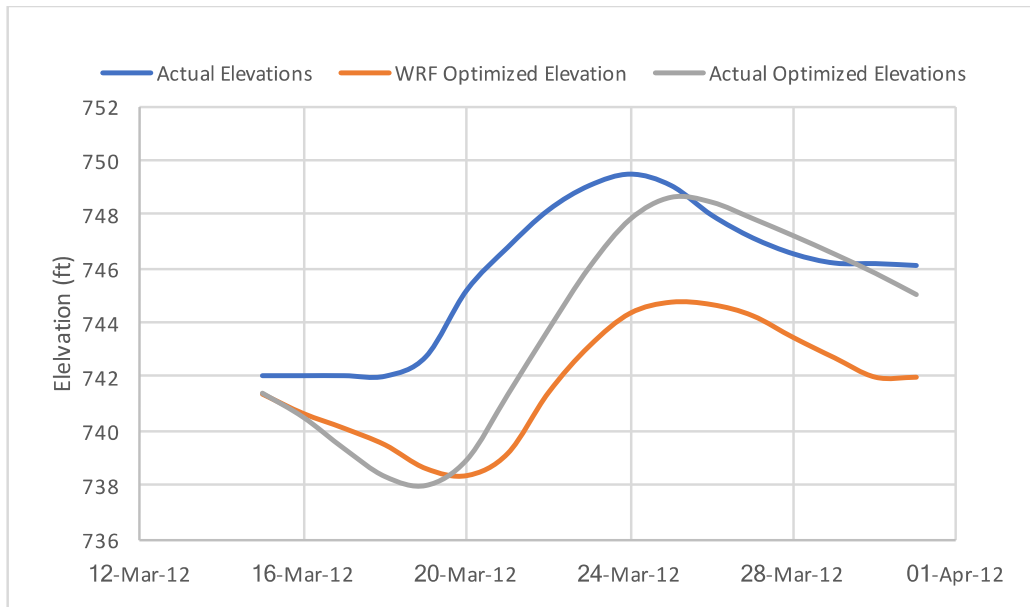(Detroit dam, OR)

115

Figure B.8. Actual/Optimized release and elevations for lead time – 7 days (15 Dec 2014)
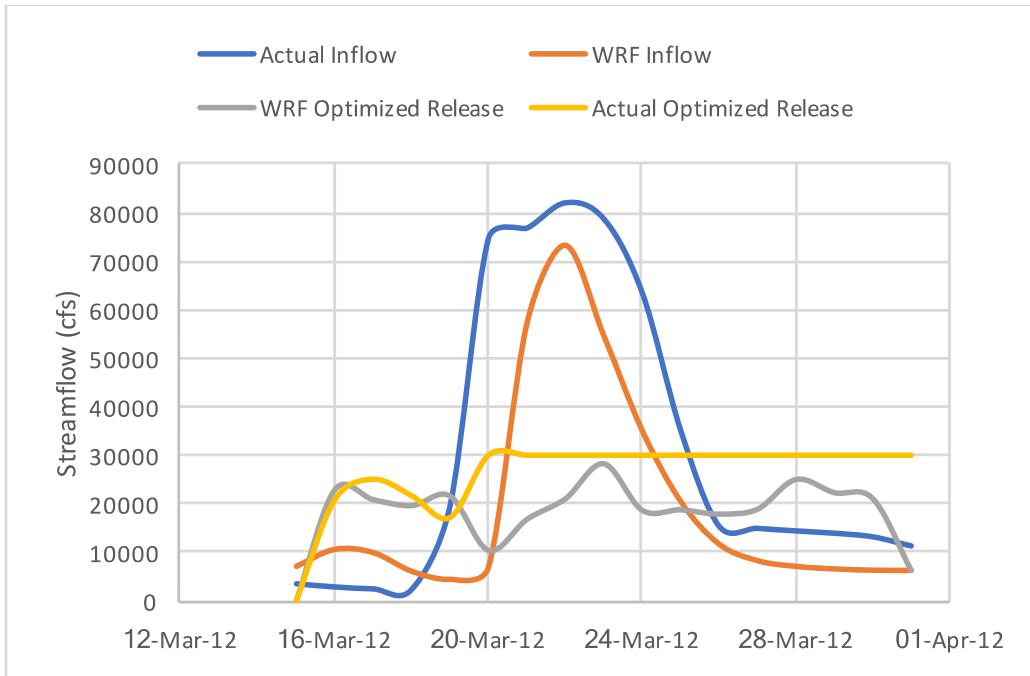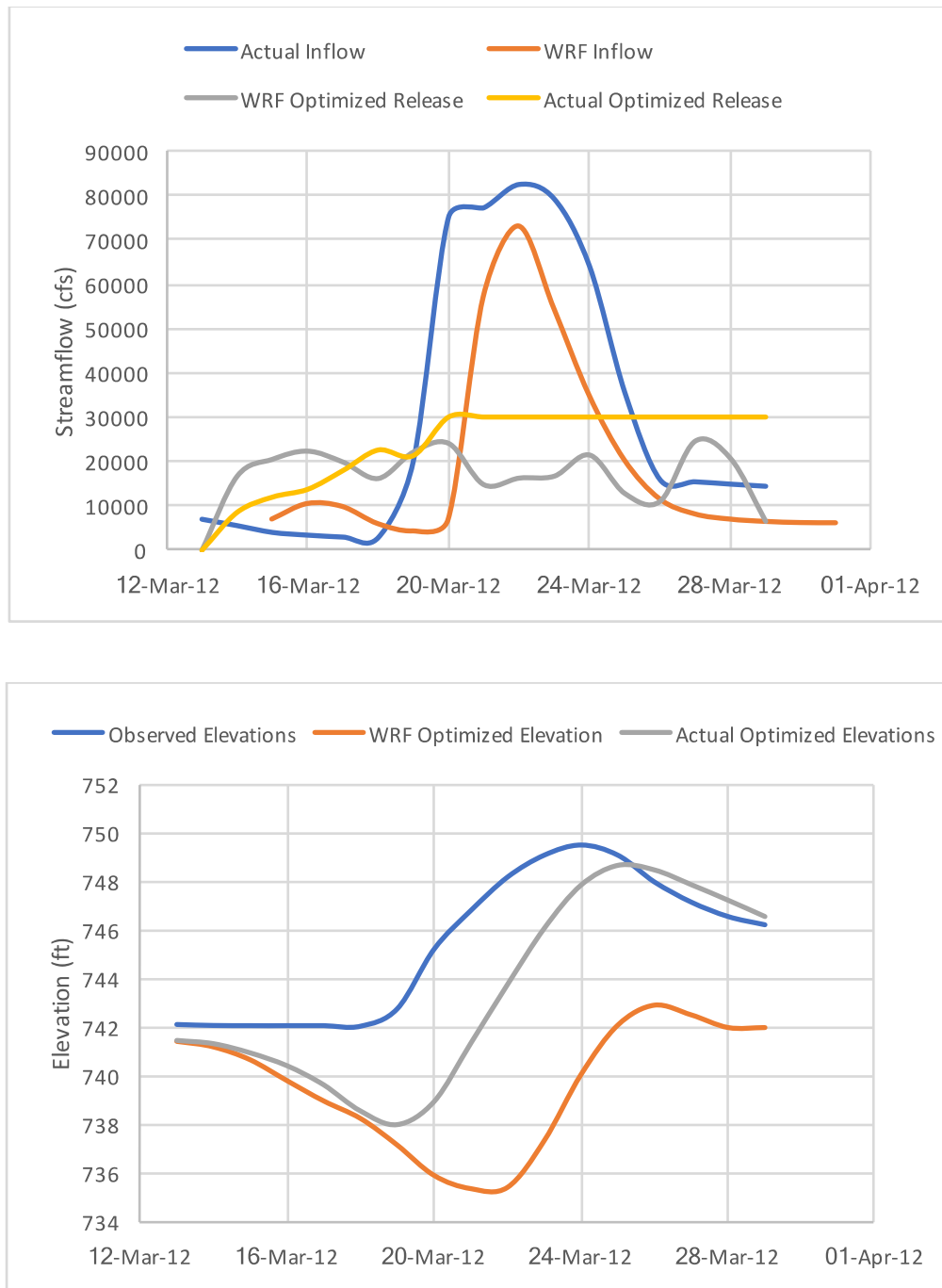
(Detroit dam, OR)
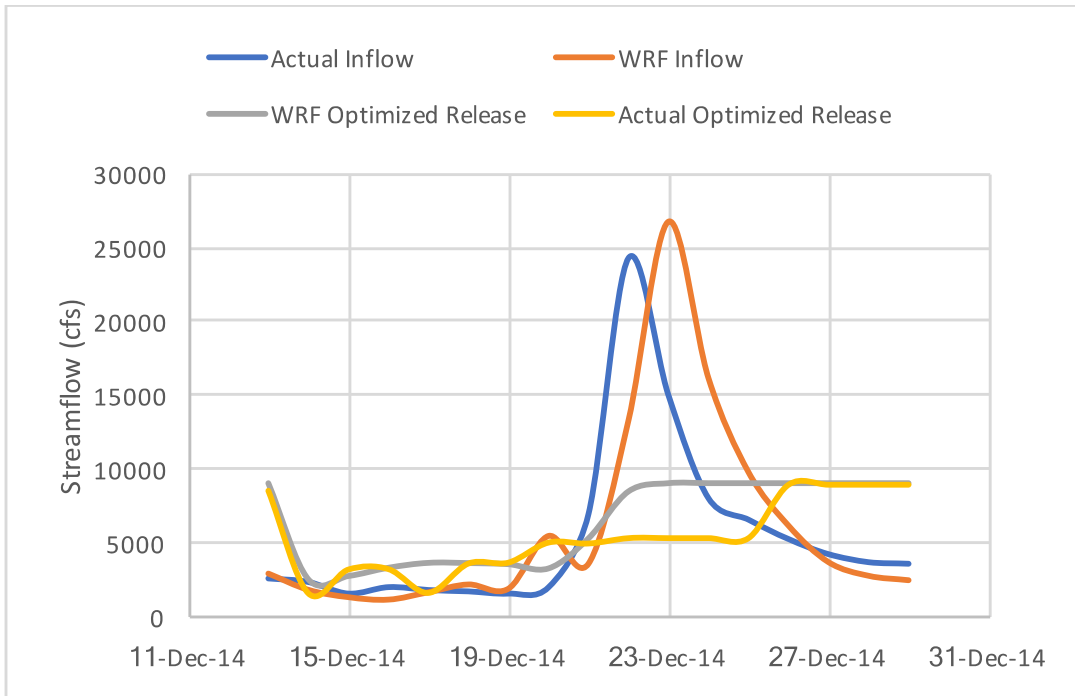
Figure B.9. Actual/Optimized release and elevations for lead time – 9 days (13 Dec 2014)

(Detroit dam, OR)
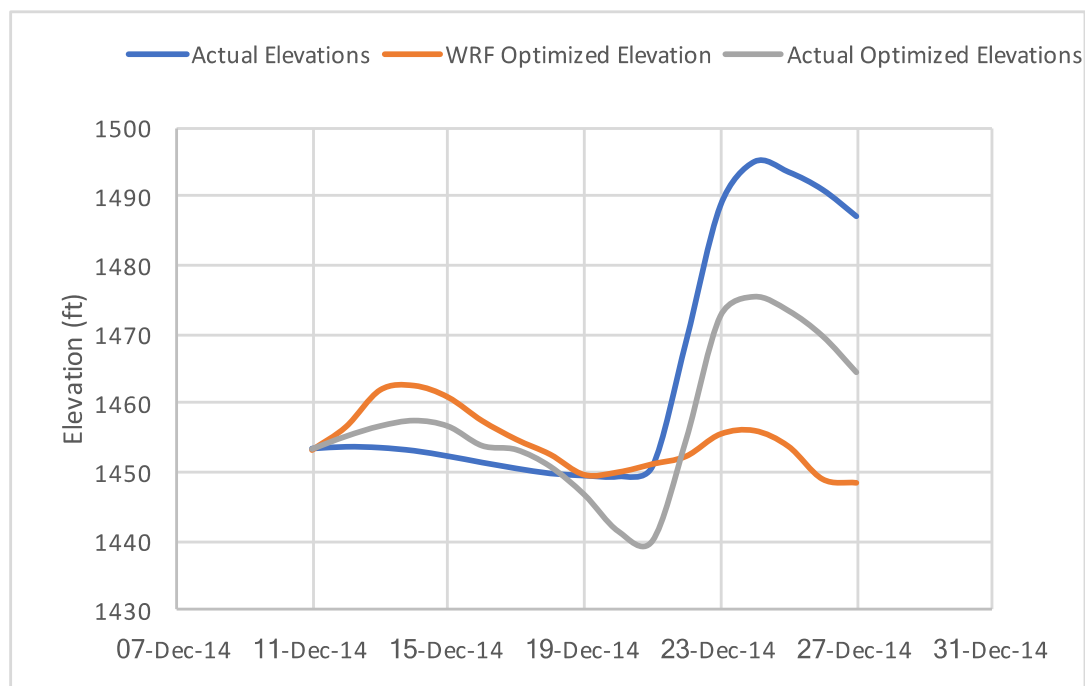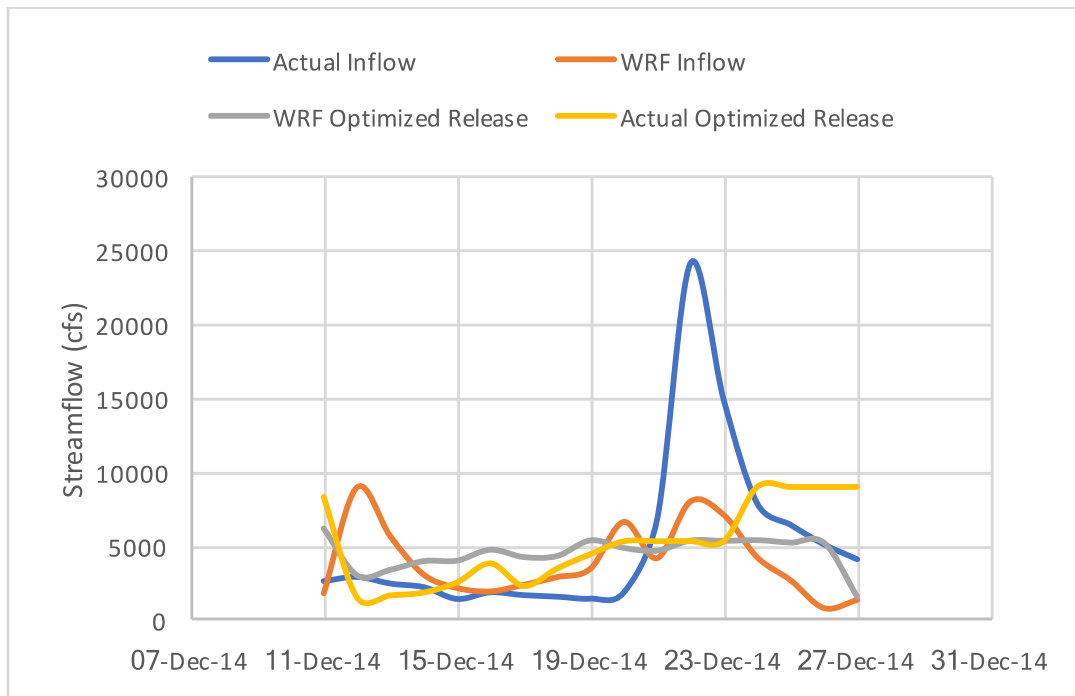
Figure B.10. Actual/Optimized release and elevations for lead time – 11 days (11 Dec 2014)
(Detroit dam, OR)

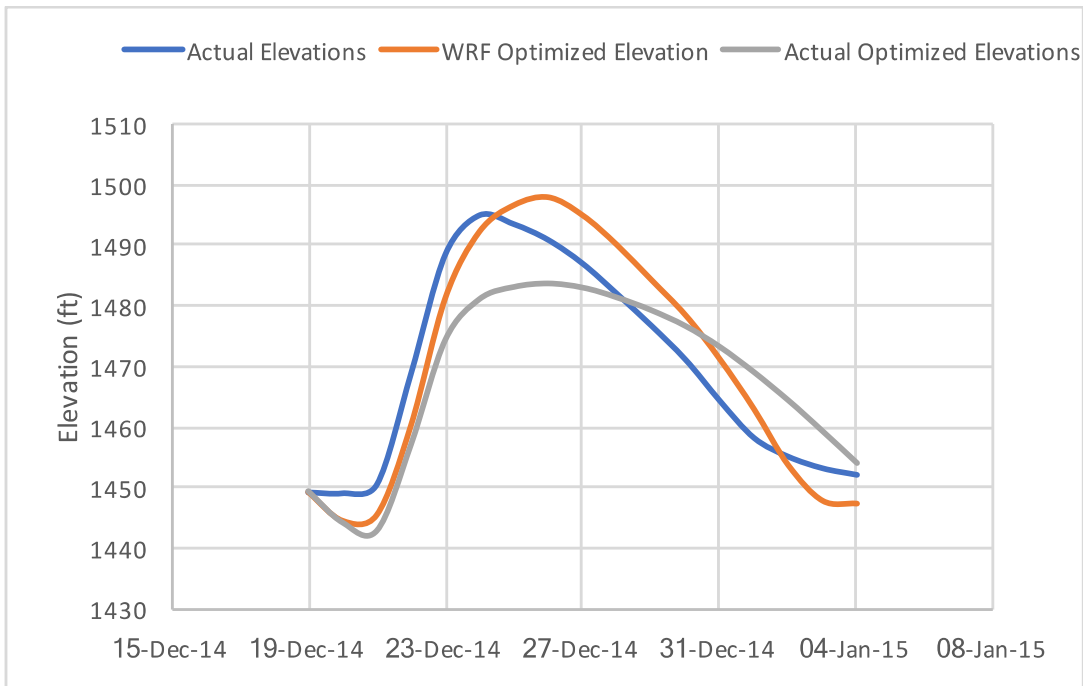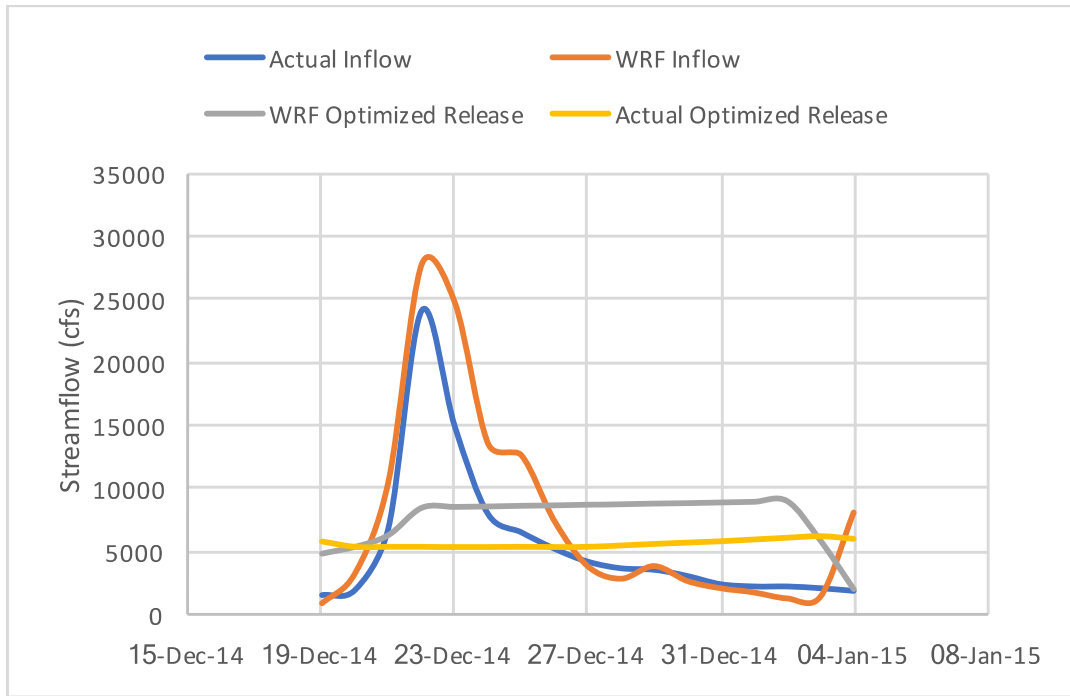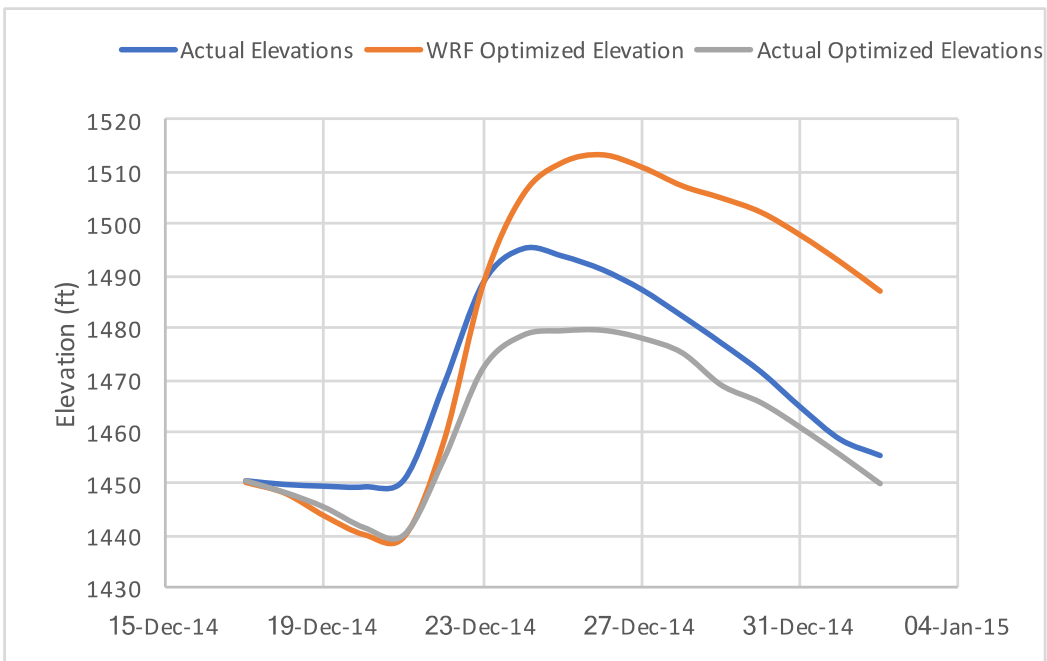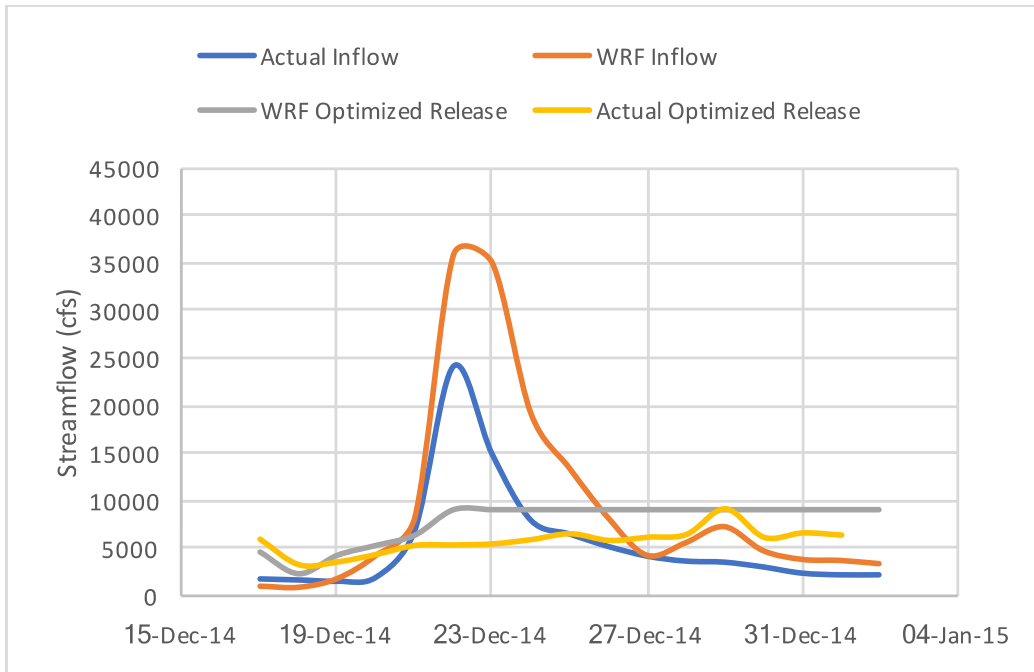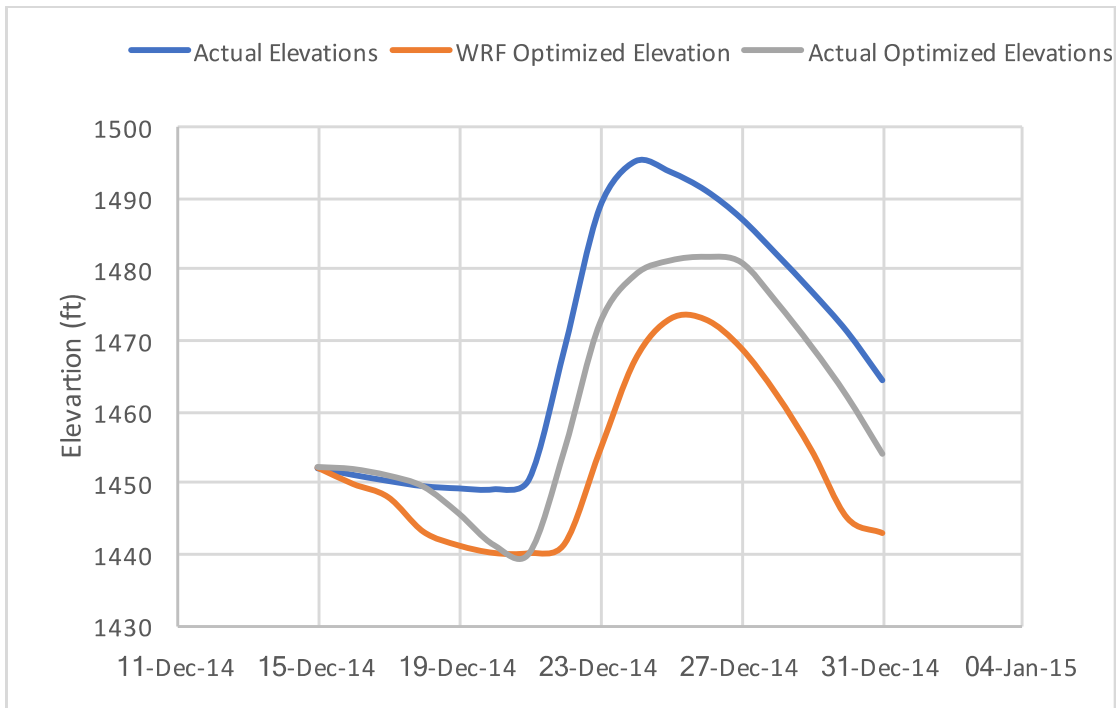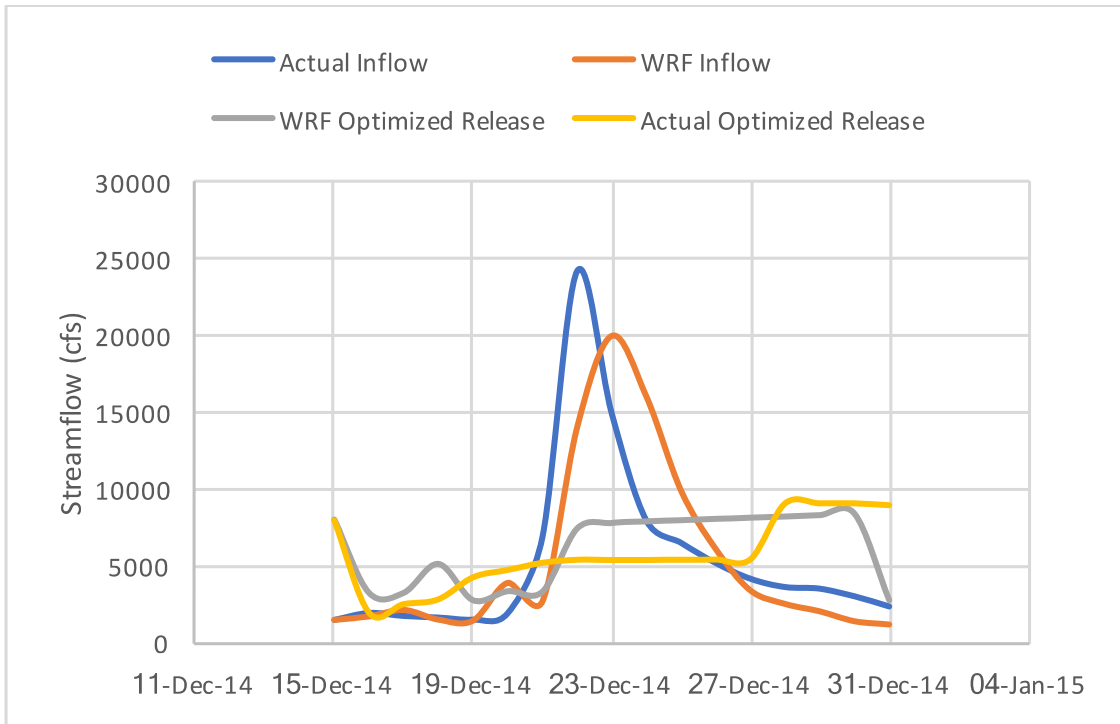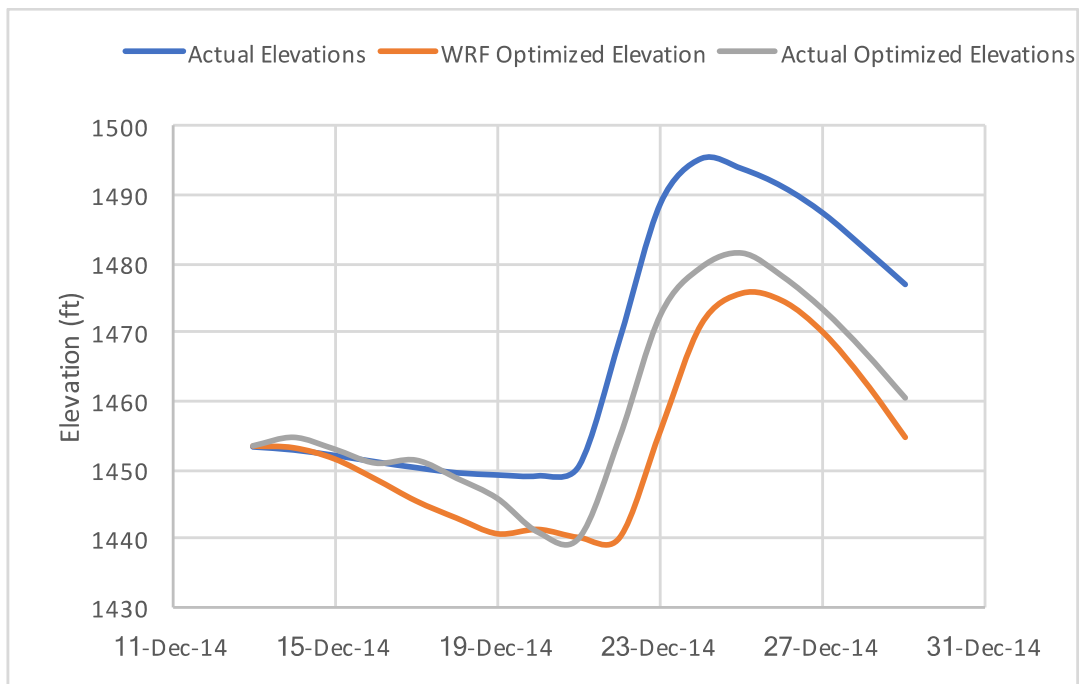# APPENDIX C. WRF MODEL CONFIGURATIONS

namelist.input – DETROIT DAM

```
&time_control
 run_days                          = 0,
 run_hours                         = 384,
 run_minutes                       = 0,
 run_seconds                       = 0,
 start_year                        = 2014, 2014,
 start_month                       = 12,   12,
 start_day                         = 19,   19,
 start_hour                        = 00,   00,
 start_minute                      = 00,   00,
 start_second                      = 00,   00,
 end_year                          = 2015, 2015,
 end_month                         = 01,   01,
 end_day                           = 04,   04,
 end_hour                          = 00,   00,
 end_minute                        = 00,   00,
 end_second                        = 00,   00,
 interval_seconds                  = 43200
 input_from_file                   = .true.,.true.,
 history_interval                  = 60,   60,
 frames_per_outfile                = 24, 24,
 restart                           = .false.,
 restart_interval                  = 5000,
 io_form_history                   = 2
 io_form_restart                   = 2
 io_form_input                     = 2
 io_form_boundary                  = 2
 debug_level                       = 0
 /

 &domains
 time_step                         = 180,
 time_step_fract_num               = 0,
 time_step_fract_den               = 1,
 max_dom                           = 2,
 e_we                              = 90,     112,
 e_sn                              = 90,     97,
 e_vert                            = 38,     38,
 p_top_requested                   = 5000,
 num_metgrid_levels                = 27,
 num_metgrid_soil_levels           = 4,
 dx                                = 30000,10000,
 dy                                = 30000,10000,
 grid_id                           = 1,2,
 parent_id                         = 1,1,
 i_parent_start                    = 1,48,
 j_parent_start                    = 1,31,
 parent_grid_ratio                 = 1,3,
 parent_time_step_ratio            = 1,3,
 feedback                          = 0,
 smooth_option                     = 0
 /

 &physics
 mp_physics                        = 8,     8,
 ra_lw_physics                     = 1,     1,
```

119

```
ra_sw_physics                       = 1,       1,
radt                                = 30,      30,
sf_sfclay_physics                   = 1,       1,
sf_surface_physics                  = 4,       4,
bl_pbl_physics                      = 1,       1,
bldt                                = 0,       0,
cu_physics                          = 3,       3,
cudt                                = 5,       5,
isfflx                              = 1,
ifsnow                              = 1,
icloud                              = 1,
surface_input_source                = 1,
num_soil_layers                     = 4,
num_land_cat                        = 21,
sf_urban_physics                    = 0,       0,
/

&fdda
/

&dynamics
w_damping                           = 0,
diff_opt                            = 1,       1,       1,
km_opt                              = 4,       4,       4,
diff_6th_opt                        = 0,       0,       0,
diff_6th_factor                     = 0.12,   0.12,    0.12,
base_temp                           = 290.
damp_opt                            = 0,
zdamp                               = 5000.,  5000.,   5000.,
dampcoef                            = 0.2,    0.2,     0.2
khdif                               = 0,       0,       0,
kvdif                               = 0,       0,       0,
non_hydrostatic                     = .true., .true., .true.,
moist_adv_opt                       = 1,       1,       1,
scalar_adv_opt                      = 1,       1,       1,
/

&bdy_control
spec_bdy_width                      = 5,
spec_zone                           = 1,
relax_zone                          = 4,
specified                           = .true., .false.,.false.,
nested                              = .false., .true., .true.,
/

&grib2
/

&namelist_quilt
nio_tasks_per_group = 0,
nio_groups = 1,
/
```

120

namelist.input – PENSACOLA DAM

```
&time_control
 run_days                            = 0,
 run_hours                           = 384,
 run_minutes                         = 0,
 run_seconds                         = 0,
 start_year                          = 2012, 2012,
 start_month                         = 03,   03,
 start_day                           = 11,   11,
 start_hour                          = 00,   00,
 start_minute                        = 00,   00,
 start_second                        = 00,   00,
 end_year                            = 2012, 2012,
 end_month                           = 03,   03,
 end_day                             = 27,   27,
 end_hour                            = 00,   00,
 end_minute                          = 00,   00,
 end_second                          = 00,   00,
 interval_seconds                    = 43200
 input_from_file                     = .true.,.true.,
 history_interval                    = 60,  60,
 frames_per_outfile                  = 24, 24,
 restart                             = .false.,
 restart_interval                    = 5000,
 io_form_history                     = 2
 io_form_restart                     = 2
 io_form_input                       = 2
 io_form_boundary                    = 2
 debug_level                         = 0
 /

 &domains
time_step               = 180,
time_step_fract_num     = 0,
time_step_fract_den     = 1,
max_dom                 = 2,
e_we                    = 90,       124,
e_sn                    = 90,       130,
e_vert                  = 35,       35,
p_top_requested         = 5000,
num_metgrid_levels      = 27,
num_metgrid_soil_levels = 4,
dx                      = 30000,    10000,
dy                      = 30000,    10000,
grid_id                 = 1,        2,
parent_id               = 1,        1,
i_parent_start          = 1,        14,
j_parent_start          = 1,        18,
parent_grid_ratio       = 1,        3,
parent_time_step_ratio  = 1,        3,
feedback                = 1,
smooth_option           = 0,
 /

 &physics
 mp_physics                          = 10,     10,
 ra_lw_physics                       = 1,     1,
 ra_sw_physics                       = 1,     1,
 radt                                = 30,    30,
 sf_sfclay_physics                   = 1,     1,
 sf_surface_physics                  = 4,     4,
 bl_pbl_physics                      = 1,     1,
```

121

```
bldt                              = 0,      0,
cu_physics                        = 3,      3,
cudt                              = 5,      5,
isfflx                            = 1,
ifsnow                            = 1,
icloud                            = 1,
surface_input_source              = 1,
num_soil_layers                   = 4,
num_land_cat                      = 21,
sf_urban_physics                  = 0,      0,
/

&fdda
/

&dynamics
w_damping                         = 0,
diff_opt                          = 1,        1,      1,
km_opt                            = 4,        4,      4,
diff_6th_opt                      = 0,        0,      0,
diff_6th_factor                   = 0.12,   0.12,   0.12,
base_temp                         = 290.
damp_opt                          = 0,
zdamp                             = 5000.,  5000.,  5000.,
dampcoef                          = 0.2,    0.2,    0.2
khdif                             = 0,        0,      0,
kvdif                             = 0,        0,      0,
non_hydrostatic                   = .true., .true., .true.,
moist_adv_opt                     = 1,        1,      1,
scalar_adv_opt                    = 1,        1,      1,
/

&bdy_control
spec_bdy_width                    = 5,
spec_zone                         = 1,
relax_zone                        = 4,
specified                         = .true., .false.,.false.,
nested                            = .false., .true., .true.,
/

&grib2
/

&namelist_quilt
nio_tasks_per_group = 0,
nio_groups = 1,
/
```